HiPTI - High Performance Thermal Insulation
IEA/ECBCS Annex 39

Vacuum Insulation Panels

Study on VIP-components and Panels for Service Life Prediction of VIP in Building Applications (Subtask A)

Institutions and Authors

EMPA - Switzerland
Hans Simmler
Samuel Brunner

ZAE-Bayern - Germany
Ulrich Heinemann
Hubert Schwab

NRC - Canada
Kumar Kumaran
Phalguni Mukhopadhyaya

CSTB - France
Daniel Quénard
Hébert Sallée

Fraunhofer IVV - Germany
Klaus Noller
Esra Kücükpinar-Niarchos
Cornelia Stramm

TU Delft - Netherlands
Martin Tenpierik
Hans Cauberg

Dr.Eicher+Pauli AG - Switzerland
Markus Erb (Operating Agent)

September 2005

Impressum

IEA/ECBCS Annex 39

The work presented here is a contribution to Annex 39 of IEA/ECBCS-Implementing Agreement.

Title

Vacuum Insulation Panels - Study on VIP-components and Panels for Service Life Prediction of VIP in Building Applications (Subtask A)

Institutions & Authors

EMPA: Swiss Federal Laboratories for Materials Testing and Research (Switzerland)
Hans Simmler, Samuel Brunner

ZAE-Bayern: Bavarian Centre for Applied Energy Research (Germany)
Ulrich Heinemann, Hubert Schwab

NRC-IRC: National Research Council - Institute for Research in Construction (Canada)
Kumar Kumaran, Phalguni Mukhopadhyaya

CSTB: Scientific and Technical Centre for Construction (France)
Daniel Quénard, Hébert Sallée

Fraunhofer IVV: Institute for Process Engineering and Packaging (Germany)
Klaus Noller, Esra Kücükpinar-Niarchos, Cornelia Stramm

TU Delft Technical University of Delft (Netherlands)
Martin Tenpierik, Hans Cauberg

Dr.Eicher+Pauli AG (Switzerland)
Markus Erb - Operating Agent

September 2005

Summary

In accordance with the aims of the Kyoto protocol, a great energy-saving potential and therefore potential for reducing CO_2 emissions has been found in the building sector. In 1997, about 25% of the energy consumption in the EU came from room heating. Increasingly restrictive building regulations focus on using better thermal insulation, which means insulation layers of up to 30 to 50 cm, if conventional insulation material is used. The motivation for examining the applicability of high performance thermal insulation in buildings (i.e. evacuated insulation in the form of vacuum insulation panels) came from the difficulties involved in renovation – namely severe space limitations and therefore technical constraints, as well as from aesthetic considerations. The thermal resistance of evacuated insulation is a factor of five to ten better than conventional insulation of the same thickness. Vacuum insulation panels (VIP) in general are flat elements consisting of an open porous (and therefore evacuation-capable) core material which has to withstand the external load caused by atmospheric pressure, as well as a sufficiently gas-tight envelope to maintain the required quality of the vacuum.

Nano-structured materials have been found to require the least quality of vacuum, which has to be achieved and to be maintained. In panels basically made of pressed fumed silica, the contribution of the gas to the total heat transfer is virtually eliminated even at an internal gas pressure of a few hundred Pascals. The requirements on the gas-tightness of the envelope are also relatively moderate for these extremely fine-structured core materials – the largest pores are in the order of 100 nanometres. Thin laminated metal foils and special high-barrier metallized laminates consisting mainly of polymers are therefore used for the envelope. This report focuses especially on this type of VIP, which combines relatively simple and flexible production methods (and is therefore currently the least expensive alternative) with an acceptable service life of 30 to 50 years before the thermal barrier is impaired in any way due to air permeation into the panels. Even if the vacuum failed completely, the thermal resistivity of this filler material is twice as efficient as that of any standard insulation material.

Investigations have been performed individually on the core materials and laminates designed for the envelope as well as manufactured VIP.

All the core materials investigated in this study are fumed silica products with minor differences, particularly in the nature of the fibres used for reinforcement. The densities are in the range of 160 kg/m³ to 190 kg/m³. The porosity is higher than 90%, the specific surface area is higher than 200 m²/g. High sorption capability results from the huge specific surface area; at 75% relative humidity, 0.05 kg of water per kg material is typically adsorbed. Thus fumed silica may act as a desiccant.

At a low gas pressure (100 Pa) and at room temperature the total thermal conductivity of the core material is about 0.004 W/(m·K) - 0.001 W/(m·K) from infrared radiative heat transfer and 0.003 W/(m·K) due to heat conduction via the solid skeleton. The thermal conductivity increases with the internal gas pressure to about 0.020 W/(m·K) at ambient pressure. At 10°C the impact of water content on the thermal conductivity was found to be linear with an increase of about 0.0005 W/(m·K) per mass% of adsorbed water.

Laminates with the highest grade barrier properties had to be determined to fulfil the requirements of long-term application in buildings. As with all polymeric films, the transmission rate for water vapour for these laminates was found to be several orders of magnitude greater than those for oxygen or nitrogen. Measuring extremely low permeation rates is challenging and very time-consuming. A fast measurement tool was developed to derive

water vapour transmission rates from helium transmission measurements. The effects of corners and edges on water vapour and on oxygen transmission rates were also determined.

The thermal performance of VIP is impaired in two ways: increasing internal gas pressure and increase in the internal water content. Measurements on panels stored in different climatic conditions gave detailed information on permeation rates for air and water vapour as a function of temperature and humidity including all the effects of edges, corners and processing. The laminate with only one metallized layer was clearly proved not to fulfil the requirements. Acceptable pressure increases of about 100 Pa per year can be expected for VIP with an Al-foil and for laminates with three metallized layers. The significant contribution of air permeation through the edges of the VIP postulates that panels may not be too small in size, (i.e. larger than 50 cm x 50 cm).

Water vapour uptake in the threefold metallized film was found to be basically proportional to the size of the panel surface, whereas the panels with Al-film absorbed water vapour at a much lower rate, and this occurred mostly through the edges and seams.

The dependence of air transmission rates on temperature can be described by the Arrhenius law with activation energies that are in the range of 25 to 40 kJ/mol. Water vapour transmission rates are proportional to the differences in the partial pressures inside and outside, a significant explicit dependence on temperature could not be observed.

From the thermal point of view, metallized films are more favourable than laminated aluminium foils. A significant thermal bridge effect at the edge of Al-foil panels has to be taken into account in the overall U-value.

Since the VIP's inherent aging is caused by the intrusion of gases, it thus also depends on climatic conditions and the size of the panels. Several more or less detailed models have been developed to predict the aging effects. To check the aging of VIP sufficiently slowly under practical conditions, VIP were integrated into five different building constructions in Germany and Switzerland. Temperature and humidity were monitored for more than a year and the panels dismantled for testing several times. The measured pressure increases were quite close to the calculated data, and the water uptake was even smaller than expected - presumably due to transient behaviour in the laminate. Typical pressure increases are less than 200 Pa/yr. The initial moisture accumulation rate (typically less than 0.2 mass%/yr) diminishes with time as the internal and external (mean) humidity is equalized.

The VIP technique is therefore principally applicable even in the building industry. Special attention has to be paid to climatic conditions. As for other polymers, exposure to UV-radiation should be limited unless shown otherwise by testing.

Since VIP covered with laminates are highly sensitive to mechanical impact, cautious handling during transport and installation as well as mechanical protection in the construction are imperative.

Content

1 Introduction

1.1 Vacuum Insulation for buildings

1.1.1 Development of insulation standards

Most insulation materials have been developed before 1950 but the extensive use of thermal insulation started only after the oil crisis in 1973. Since the oil crisis, the thermal insulation of buildings became the key element to prevent heat losses and to improve energy efficiency. For a long time for regions with an extended annual heating period, 10 cm of standard insulation such as expanded or extruded polystyrene, foamed polyurethane (PU), fibreglass, etc, were considered as good insulation. But energy specialists calculated that the economically optimised thickness should be 30-50 cm depending on the specific climatic conditions. Today, many existing building regulations and standards demand U-value that is approximately equal to 0.2 W/(m^2·K) for roofs and walls, which means about 20 cm thick insulation layers. Many architects have a problem with such regulations. They want to create spaces, not insulated bunkers. The problem of thick insulation layers is especially critical in the case of renovated buildings where there are severe limitations on space and also many other technical constraints.

1.1.2 Energy in buildings

The effect of a major adoption of the VIP (Vacuum Insulation Panel) technology by the construction industry on environment is expected to be absolutely huge. The official numbers for the EU given below show that using VIP in buildings could account for most of the very challenging target of 8% reduction in emission of greenhouse gases (Kyoto Protocol).

The total final energy consumption in the EU in 1997 was about 930 Mtoe (Million tons oil equivalent). A simplified breakdown of this demand shows the importance of buildings in this context: 40.7% of total energy demand is used in the residential and commercial sectors, most of it for building-related energy services (Table 1). It should also be pointed out that approximately 10% of the consumed energy in buildings comes from renewable energy sources. Space heating is by far the largest energy end-use of households in EU Member States (57%), followed by water heating (25%). Electrical appliances and lighting make up 11% of the sector's total energy consumption. For the commercial sector the importance of space heating is somewhat lower (52%), while energy consumption for lighting, office equipment and "other" (water heating, cooking and cooling) are 14%, 16% and 18%, respectively.

Table 1: Energy consumption of buildings in Europe. (Source: Directive of the European Parliament And The Council on the energy performance of buildings.)

Residential Sector	[%]	Commercial	[%]
Space Heating	57	Space Heating	52
Water Heating	25	Water Heating	9
Electric Appliances	11	Lighting	14
Cooking	7	Office Equipment	16
		Cooking	5
		Cooling	4

From these numbers it can be derived that more than 25% of EU energy consumption and also CO_2 emissions are caused by heat transfer processes in buildings, which directly depend on insulation standards. It has to be kept in mind that these heat transfer processes not only do occur in the building envelope but also in boilers, refrigerators and freezers and cold storage rooms.

1.1.3 Potential impact of VIP for building insulation

In 1995, there were roughly 150 million dwellings in the EU-15; 32% of this stock was built prior to 1945, 40% between 1945 and 1975 and 28% between 1975 and 1995. The ratio, housing starts vs. housing stocks, varies between 1 to 2%. Therefore the reduction in CO_2 emissions by using VIP technology depends largely on how well the new technology is adopted in retrofitting the old building stock, which to a large extent (around 50%) is not insulated at all. This success depends not only on the technical solutions but also on regulations and energy prices. However, it can be assumed that the energy consumption of the dominating old buildings can be reduced by a factor of three. This means that the EU CO_2 emissions would be reduced by about 8%, which is the reduction the EU agreed on in the Kyoto Protocol. Since VIP-based systems are thinner and their recycling economically attractive, the resource intensity will be lower than for conventional solutions. Additional important impacts are reduction in adverse environmental effects of transporting fuel (sea and land) to and inside Europe and also reduction in the rate at which the global energy reservoirs is depleted. Furthermore, if one takes into account that use of the VIP technology is not limited to Europe only, the numbers can be much more impressive.

1.1.4 Vacuum Insulation today

Currently VIP have only limited use, mainly in top models home refrigerators/freezers and cold shipping boxes. Japan controls more than 50% of the small global VIP market with several million panels per year. The VIP market in Japan is fast growing. The common core materials are fumed and precipitated silica, open-cell PU and several types of fibreglass. Both metallized-film and aluminium-foil laminates are being used to seal the vacuum.

For buildings, most of the VIP activity is still in the R&D phase with some demonstration projects. Germany and Switzerland are the only countries where a market in its early stage has been established. Fumed silica boards are being used almost exclusively. Fumed silica is the best core material due to the small size of the pores and the low heat conductivity of

the powder (Figure 4). There are only three producers of fumed silica in the world, and two of them are large EU companies: Wacker (Germany), Cabot (USA) and Degussa (Germany).

1.2 Physics and core materials

1.2.1 Physics

The physics of heat transfer through conventional insulation materials is well known. A short description of the most important phenomena is given below.

In conventional insulation materials like mineral wool, glass wool or organic foams the total heat transfer is dominated by the contribution of the (non-convective) gas within the hollow spaces or pores (Figure 1).

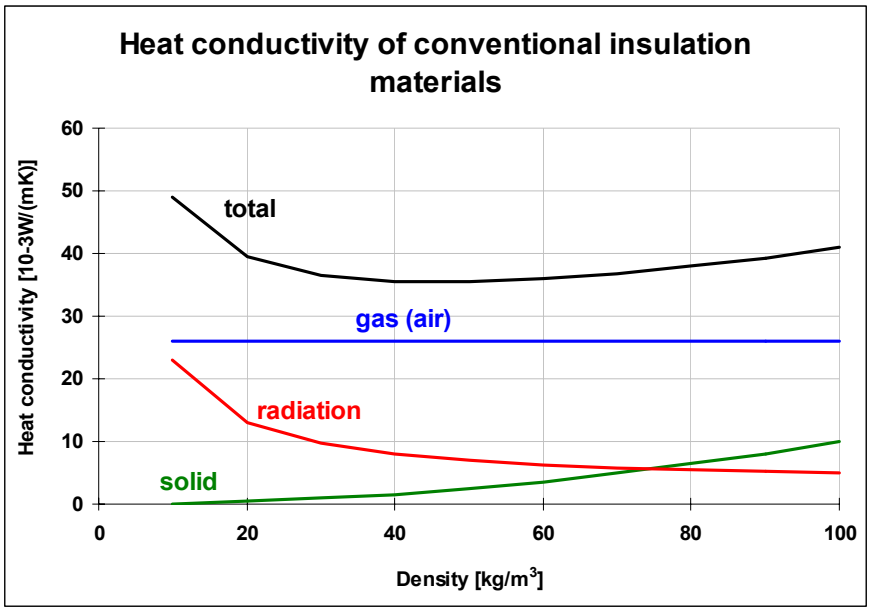

Figure 1: Heat conductivity of conventional insulations (fibres and foams) is dominated by the gas conductivity.

Thus a large potential for improvement of the insulation properties can be realised by reducing or even completely eliminating the gas conductivity. The gas conductivity in a porous medium is determined by the number of gas molecules as transfer medium as well as by the number of "walls" on the way from the hot to the cold side. At a high pressure, when the mean free path of the gas molecules is much smaller than the size of the pores, collision between the gas particles is the limiting mechanism for an efficient heat transfer. Here an increase in the gas pressure with an increase in the number of gas particles is correlated with a decrease in the mean free path. As the two effects, number of gas particles and frequency of collisions, compensate each other the thermal conductivity of a gas is nearly independent on the gas pressure, at higher pressures.

At atmospheric gas pressure the above behaviour holds for most conventional insulation materials. Also, gaseous conductivity is determined by the thermal conductivity of the non-convective gas. Reducing the gas pressure by "evacuation", the gaseous conductivity remains almost unaffected until the mean free path attains values that are in the order of the

size of the (largest) pores or higher. An extraordinary material in this regard is pressed powder boards made of fumed silica with the largest pores in the same order of magnitude as the mean free path of air molecules at atmospheric pressure (about 70 nm). For this material even at atmospheric pressure gaseous conductivity already is affected by the fine structure. It may be considered as "partially evacuated" and thus seems to be a favourite material for "evacuated" insulations.

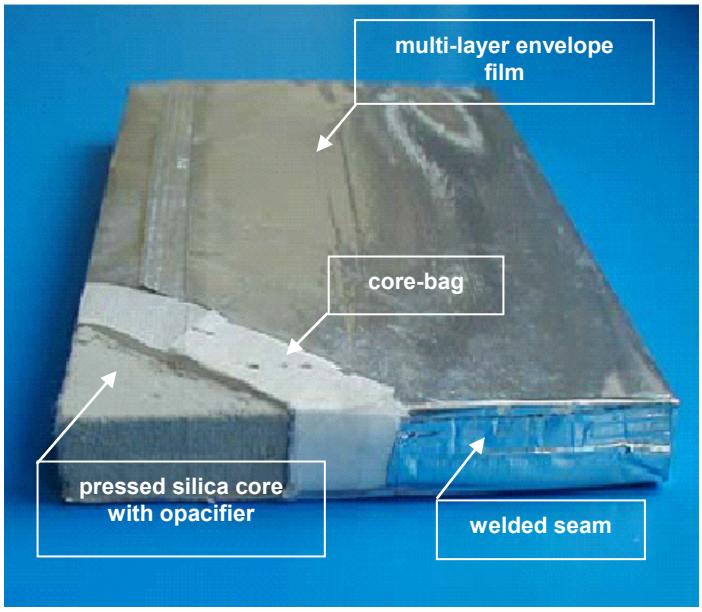

Figure 2: Components of a VIP. The core-bag provides mechanical stability for handling and protects the welding area from being polluted by core-powder.
(foto: va-Q-tec).

Current VIP-technology uses especially this material with the least requirements to the quality of the vacuum, that has to be achieved and maintained in combination with special high barrier films and foils, which fulfil the requirements for long term applications as in buildings (Figure 2).

1.2.2 Core materials

The core material suitable for VIP production has to fulfil different requirements: very small pore diameter, open cell structure, resistance to compression (atmospheric pressure) and almost impermeable to infrared radiation.

Pore diameter

To reduce the gas conductivity in normal insulation materials the pressure has to be very low (Figure 3) which is difficult to maintain by an envelope mainly made of organic materials. That is why for VIP a combination of a nano-structured core material and pressure reduction is used.

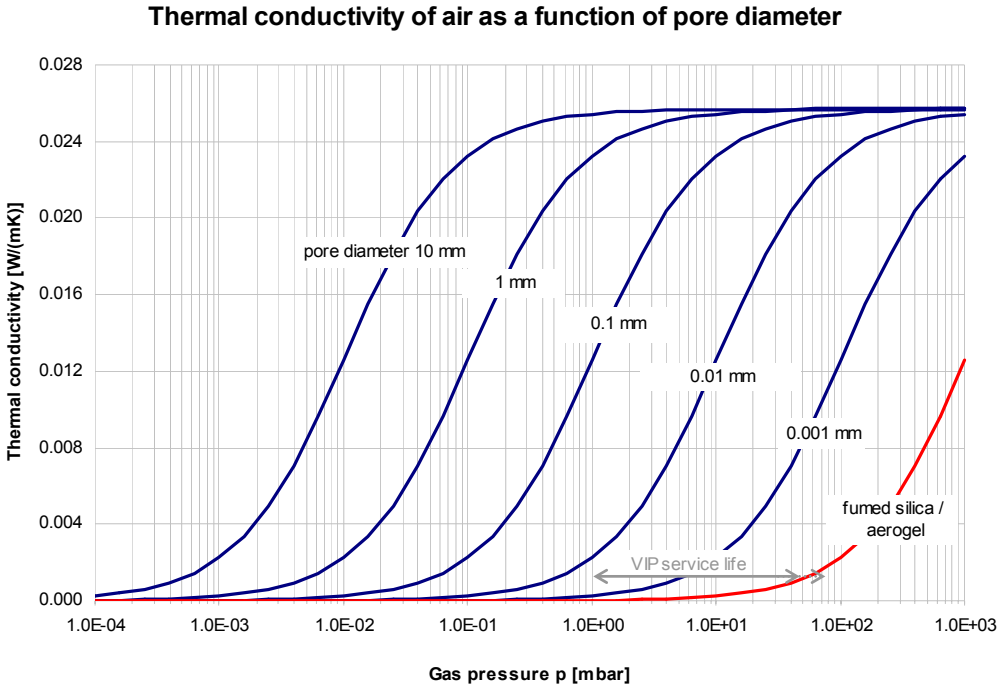

Figure 3: The small pore size of fumed silica or aerogels do reduce gas conductivity even at ambient pressure [1]. Today produced VIP (fumed silica core) start with in internal pressure in the range of 1 to 3 mbar. The VIP's end of service life is reached when the gas conductivity is starting to rise (50-100 mbar).

Cell structure

To be able to evacuate the core material it has to be 100% open-celled, so that the gas (air) can be quickly removed out of the material.

Stability

The internal pressure of a VIP is only few mbar. Consequently the pressure load on the panel is close to 1 bar or 10 tons/m^2. The core material therefore has to be stable enough so that the pores do not collapse when evacuated.

Radiation

Besides gas conductivity, radiation has also to be reduced to reach very low conductivity values. This is done by adding opacifiers to the core material.

Heat conductivity

Today different organic and inorganic insulation materials with open-cell structure are available for the use as core for VIP-production. Corresponding to the pore size distribution, the solid conductivity and the radiation properties of a material, a specific heat conductivity results, depending on the gas pressure (Figure 4). The figure shows clearly the advantages of fumed silica: low conductivity up to a pressure of more than 50 mbar and a conductivity at ambient pressure of half that of a conventional insulation material.

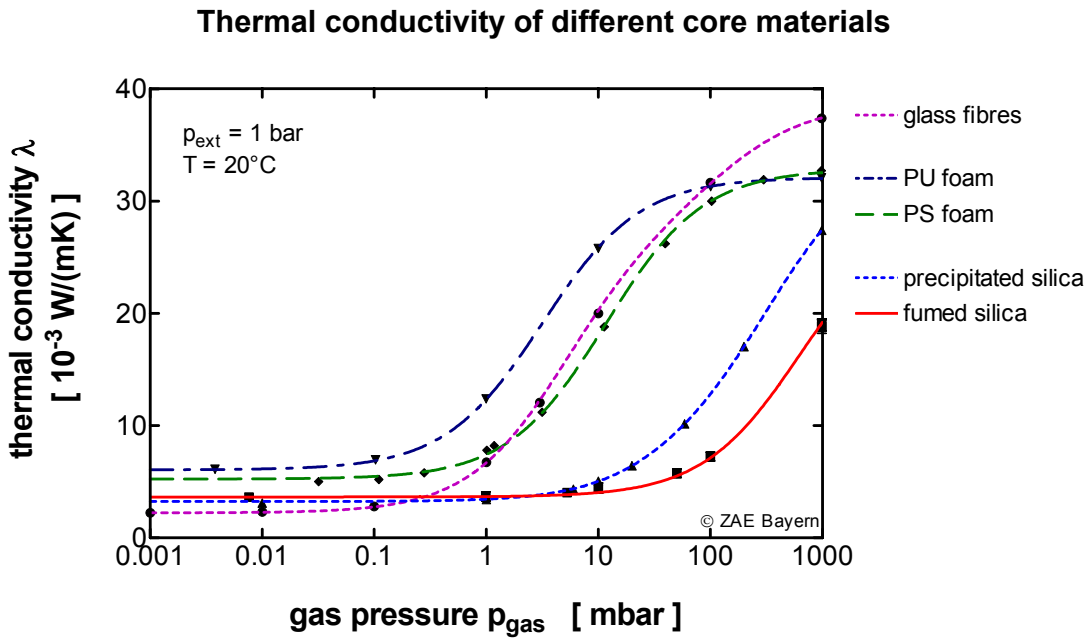

Figure 4: The heat conductivity of fumed silica starts to rise only above a gas pressure of more than 50 mbar.

1.3 IEA/ECBCS Annex 39

Germany and Switzerland were the first two countries supporting R&D activities with the aim of introducing VIP-technology to the building industry. In 2000 Switzerland decided to launch the topic on an international level. This happened in the frame of the IEA (International Energy Agency) Implementing Agreement called ECBCS (Energy Conservation in Buildings and Community Systems). Implementing Agreements are a kind of international networks of national representatives with the aim of coordinating applied research in the field of energy.

Annex 39 is the 39th research program of ECBCS. It was officially adopted by the Executive Committee of ECBCS in November 2000 and started with an international conference in January 2001.

Since the topic was new to the research community, it was quite difficult to set up a work plan with the participating institutes. One problem for instance was the lack of standard methods to study VIP. But finally a work plan with two main fields of activity was developed:

Subtask A: Panels

- Existing products, mainly VIP, will be analysed and their properties optimised in the way, that they meet the requirements of the systems in which they will be applied.
- Measurement standards concerning product declaration and quality monitoring procedures will be developed.

Subtask B: Applications

Part 1: Application and system development

Support companies which want to develop VIP-systems for the building envelope and HVAC components. The support will consist in informing potential companies about VIP, form

suitable groups for each development project, provide theoretical and practical information (simulation and testing of systems).

Part 2: Demonstration and information dissemination

- Realize demonstration projects together with well-known architects and important building owners.
- Lessons learned from the demonstration projects will be collected and used for further improvement of the materials and systems.
- Information material will be distributed to increase the interest of construction companies and clients.

1.4 Participating institutes

Annex 39	Name	e-mail	Contribution
Dr.Eicher+Pauli AG Switzerland	Markus Erb	markus.erb@eicher-pauli.ch	*Operating Agent* Introduction
Subtask A			
ZAE-Bayern Germany	Ulrich Heinemann	heinemann.ulrich@zae.uni-wuerzburg.de	*Leader Subtask A*
	Hubert Schwab	schwab@zae.uni-wuerzburg.de	Core material, Panel, Quality assurance , Outlook
EMPA Switzerland	Hans Simmler	hans.simmler@empa.ch	Panel
	Samuel Brunner	samuel.brunner@empa.ch	
NRC/IRC Canada	Kumar Kumaran	kumar.kumaran@nrc.ca	Core material, Envelope
	Phalguni Mukhopadhyaya	phalguni.mukhopadhyaya@nrc-cnrc.gc.ca	
CSTB* France	Daniel Quénard	quenard@cstb.fr	Core material
	Hébert Sallée	sallee@cstb.fr	
Fraunhofer IVV Germany	Klaus Noller	klaus.noller@ivv.fraunhofer.de	Envelope
	Esra Kücükpinar-Niarchos	esra.kucukpinar@ivv.fraunhofer.de	
	Cornelia Stramm	cornelia.stramm@ivv.fraunhofer.de	
TU Delft Netherlands	Martin Tenpierik	m.j.tenpierik@bk.tudelft.nl	Panel
	Hans Cauberg	h.cauberg@chri.nl	

Subtask B	Name	e-mail	Contribution
FHBB Switzerland	Armin Binz André Moosmann Gregor Steinke	a.binz@fhbb.ch andre.moosmann@fhbb.ch gregor.steinke@fhbb.ch	*Leader Subtask B* Report editor, Practice Report I, Recommendations, Economics
EMPA Switzerland	Karim Ghazi Reto Bundi	karim.ghazi@empa.ch reto.bundi@empa.ch	Thermal bridges
ZAE-Bayern Germany	Ulrich Heinemann Hubert Schwab	heinemann.ulrich@zae.uni-wuerzburg.de schwab@zae.uni-wuerzburg.de	Practice Report II
TU Delft Netherlands	Hans Cauberg Martin Tenpierik	h.cauberg@chri.nl m.j.tenpierik@bk.tudelft.nl	Case studies
KTH Stockholm Sweden	Gudni Johannesson Thomas Thorsell	gudni@bim.kth.se thomas.thorsell@byv.kth.se	Edge effect (stainless steel)

** Work of CSTB partially funded by the French Energy Agency (ADEME - www.ademe.fr) and the French Electricity Company (EDF - www.edf.fr)*

2 Core Material

In this chapter the hygro-thermo-mechanical properties of two porous fumed silica based materials used as core materials for VIP applications are presented. They are named SIL1 (silica 1) and SIL2 (silica 2)

2.1 Physical Properties

2.1.1 Density

This test was carried out by weighing boards of sizes 300 mm x 300 mm x 25 mm according to the standard EN 1602 “Thermal insulating products for building applications - Determination of the apparent density” (see Appendix)

The mean values are listed in Table 2.

Table 2: Density.

Material	Density
	kg/m^3
SIL1	192
SIL2	162

It’s important to note that the densities of both materials are nearly one order of magnitude higher than that of traditional insulating materials.

2.1.2 Porosity

The porosity was measured using a Helium pycnometer with samples of sizes: 60 mm x 40 mm x 25 mm. With this method, it is also possible to evaluate the bulk and skeleton density.

The results are presented in Table 3.

Table 3: Porosity & Densities

Material Reference	Total Porosity	Bulk Density	Skeleton Density
	%	kg/m^3	kg/m^3
SIL1	93 ± 1	191	2’578
SIL2	94 ± 1	161	2’454

The bulk densities obtained with the pycnometer are in good agreement with the apparent densities given by the previous method. The skeleton density is almost the same as the density of silica.

In spite of the high density of both materials, their porosity is still higher than 90%. It means that the specific area is also very large, about several hundred m²/g.

2.1.3 Specific Area

The specific area was measured using the BET (Brunauer-Emmet-Teller) method [2] according to the ISO Standard 9277 “Determination of the specific surface area of solids by gas adsorption using the BET method”. MICROMERITICS 2100E2 apparatus was used for this purpose.

The BET method is based on the adsorption of Nitrogen molecules considered as a probe to cover the surface and then to estimate the specific surface (m^2/g).

The measurement has been performed using a small sample (about 0.3 g) dried at 300°C.

For both materials, the experimental curves, presented in Figure 23 are very similar.

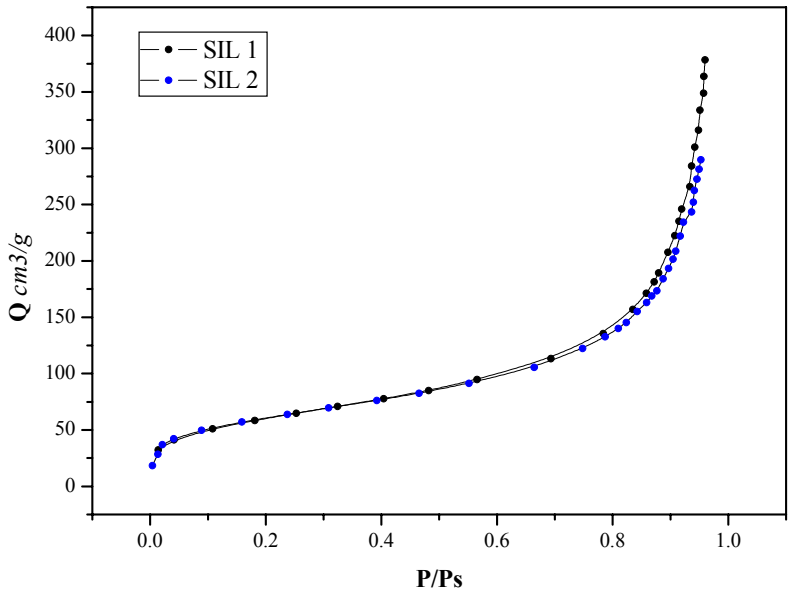

Figure 5: BET Nitrogen sorption isotherm.

The computed values are summarized in Table 4.

Table 4: BET Specific Area

Material	Specific Area
	m^2/g
SIL1	213
SIL2	208

The specific surfaces of both materials are about 200 m²/g, in agreement with data given for commercialized products (between 100 & 400 m²/g). In comparison to carbon black (50-100 m²/g) or gypsum (~ 2 m²/g), it's a high value.

2.1.4 Pore Size Distribution

The Pore Size Distribution (PSD) was investigated using the Mercury Intrusion Porosimetry (MIP) method. The basic principle consists in putting a small sample (about 0.2 g) in a glass bulb filled with mercury. Then the pressure is increased gradually and the volume intruded by mercury is measured (Figure 6). The pore radius is related to the applied pressure as:

$$r = \frac{2 \cdot \gamma \cdot \cos\theta}{P} \qquad (1)$$

r: pore radius
P: mercury applied pressure
γ: surface tension - 0.485 N/m
θ: contact angle - 130°

The test has been done with a MICROMERITICS AutoPore III 9410. The range of the PSD lies from 360 µm to 0.003 µm. The intruded volume is plotted against the pore radius.

The PSD is computed from the derivative of this curve.

With material such as compressed silica powder with a weak cohesion and thus a low elastic modulus, the high pressure (400 MPa) needed to reach tiny pores (< 10 nm) could significantly deform the material [3].

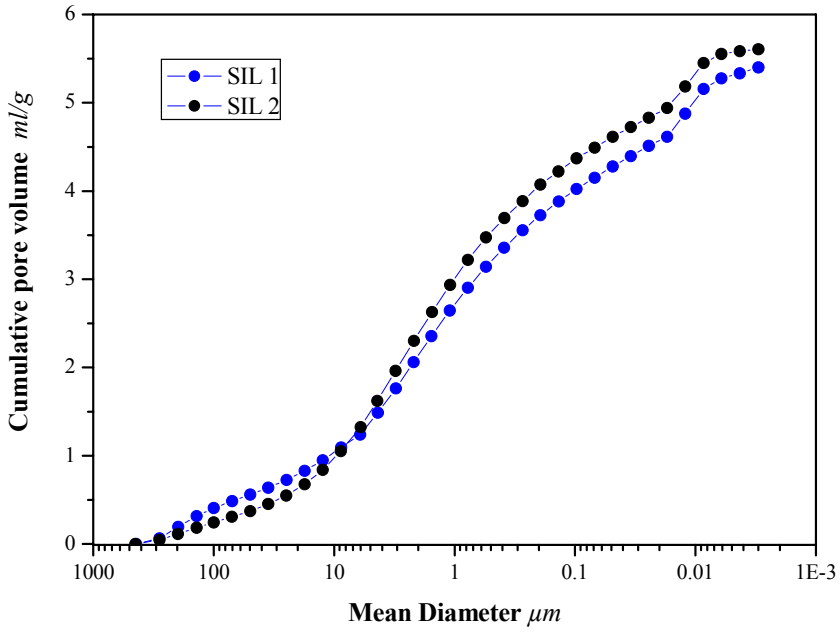

Figure 6: MIP: Intruded volume versus pore diameter.

The density and porosity obtained from MIP curves are presented in Table 5.

Table 5: Density & Porosity from MIP.

Material	Density kg/m^3	Porosity %
SIL 1	175	95
SIL 2	162	91

The four methods applied (gravimetry, pycnometer, BET, MIP) confirm the high porosity (> 90%) and the high specific area (> 200 m²/g) of silica core materials. As for the density, it ranges between 161 and 192 kg/m^3. The discrepancy between the three methods are due to several reasons:

- the size of the sample: 300 mm x 300 mm x 20 mm for the weighting, 60 mm x 40 mm x 25 mm for the pycnometer and less than 10 mm x10 mm x 10 mm for the MIP.
- the friability or low cohesion of the materials which can lead to structural changes during the MIP test at high pressure.

2.1.5 Scanning Electron Microscopy - SEM

Even at low magnification (x30, x300), the fibres appear very clearly and one notices that each manufacturer does not use the same type of fibres. One type seems to be very stiff (SIL 1) whereas the other one is softer (SIL 2).

x30 – SIL 1

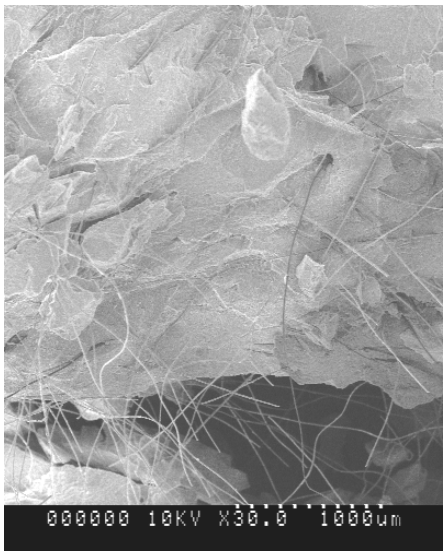

x30 – SIL 2

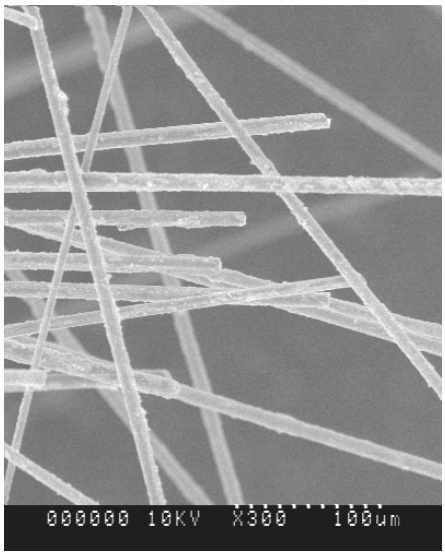

x300 – SIL 1

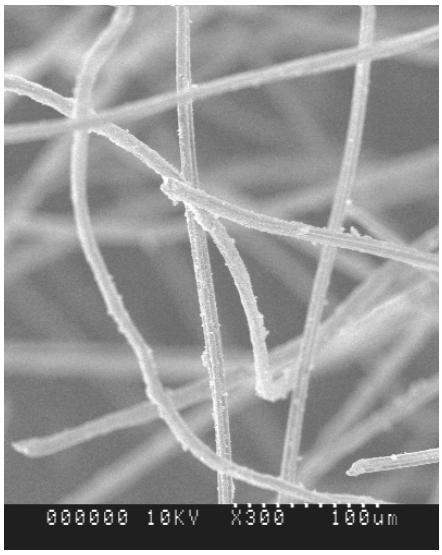

x300 - SIL 2

Figure 7: Fibres in silica matrix.

The next set of images obtained with a higher magnification (x1’000, x5’000) emphasises the interface between the fibres and the silica matrix. The granular structure starts to appear.

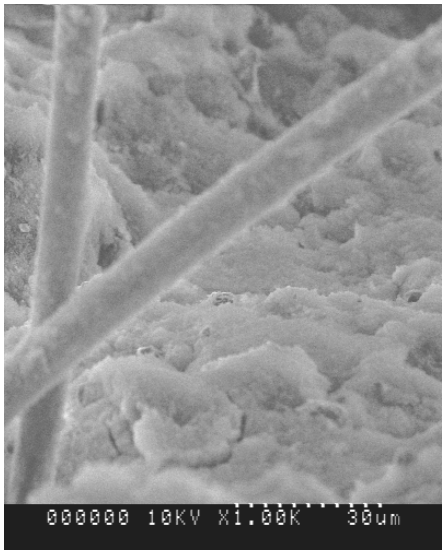

x1’000 - SIL 1

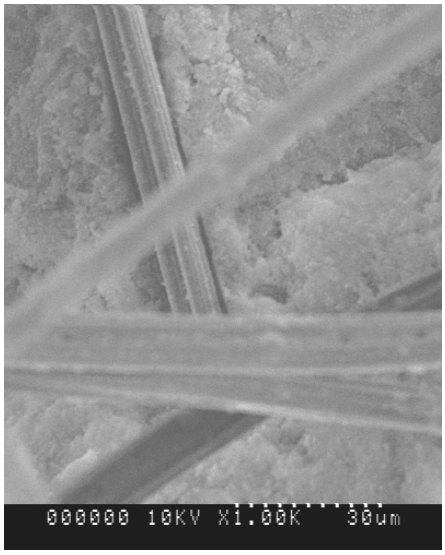

x1’000 - SIL 2

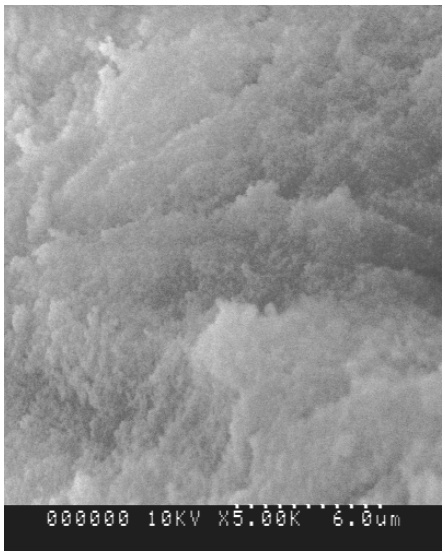

x5’000 - SIL 1

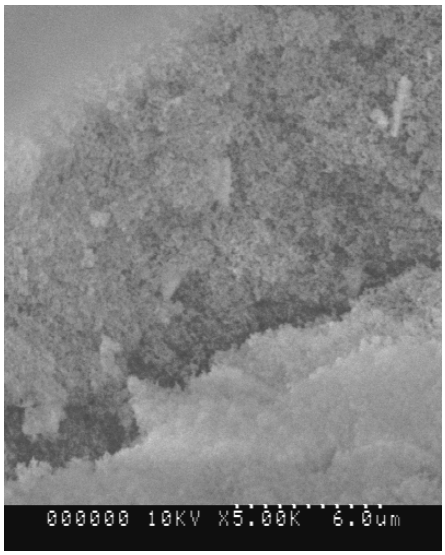

x5’000 - SIL 2

Figure 8: Interface fibres, silica matrix & granular porous structure.

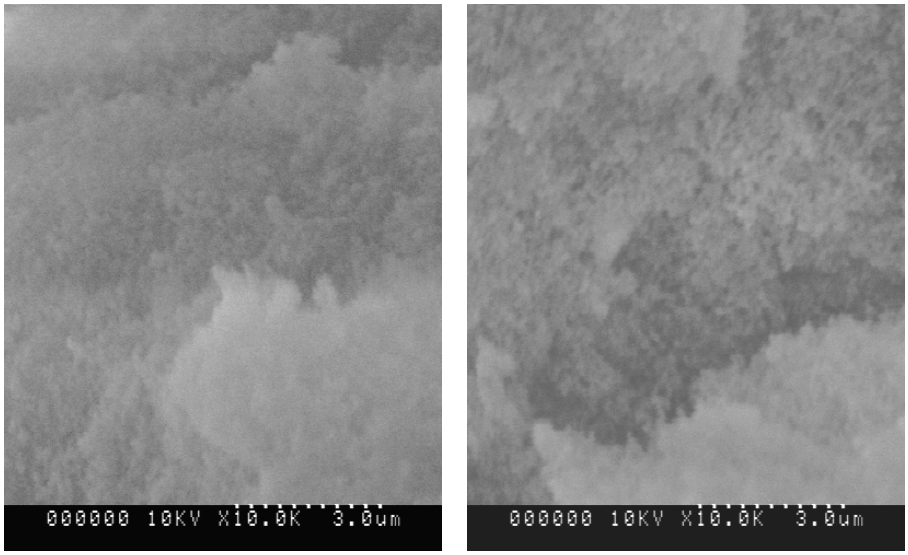

x10'000 - SIL 1 *x10'000 - SIL 2*

Figure 9: Microporous silica matrix.

In Figure 8 and Figure 9, the porosity with a characteristic size of 2 µm mainly due to interfaces fibres/matrix and the cracking of the skeleton are shown.

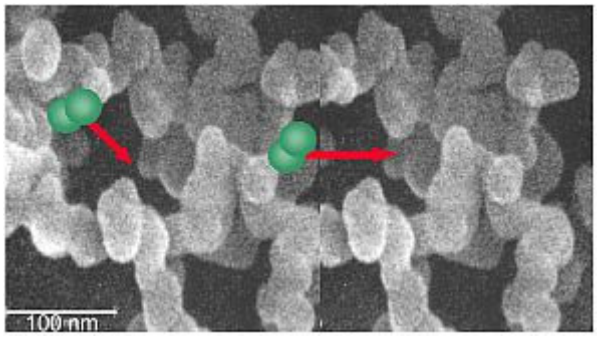

Figure 10: SEM image - Pore Size Distribution.
(Source: ZAE/Wacker)

The SEM image presented in Figure 10 illustrates the net-like structure of fumed silica grains.

At this scale, the fine porosity is clearly shown.

The artist's depiction of the gas molecules simulates the 70nm (mean free path of air) sized pores in the material.

2.2 Mechanical Properties

2.2.1 Curing

The samples have been tested according to the following curing conditions.

- First, as for easier handling, only VIP samples (cores wrapped in the film) have been sent from the manufacturers, the mechanical tests were performed one day after the opening of the film and the cutting samples of size 50 mm x 60 mm. This condition is defined as the “initial condition” or condition 1.
- For the second condition, samples are stored in stable laboratory conditions: 23°C & 50% of Relative Humidity (RH) for 13 days and then tested. This curing defines the condition 2.

2.2.2 Compression tests

The tests were performed according to the French standard NF T 56 101 “Alveolar Products made with elastomer or polymer: compression test of rigid material”.

The parameters of the test are as follows:

- Speed: 10 mm/min
- Sample geometry L x l x e: 60 mm x 50 mm x 20 mm
- Number of samples: 4

The compression stress was measured at 10, 25 and 40% of deformation.

The results are summarised in Table 6 and Table 7.

Table 6: Results at 23°C – Initial Conditions or Condition 1.

Material	**Compression Stress** *kPa*		
	10%	**25%**	**40%**
SIL 1	142	408	835
SIL 2	108	325	630

In dry conditions, the silica core materials fulfil the requirement for main building applications such as sub-floor heating.

Table 7: Results at 23°C and 50% RH or Condition 2.

Référence	**Compression Stress** *kPa*		
	10%	**25%**	**40%**
SIL 1	92	264	555
SIL 2	90	274	521

By comparing results in Table 6 and Table 7, the effect of moisture on compression stress is clearly shown, the reduction is about 35% for SIL 1 and 20% for SIL 2.

2.2.3 Three Point Flexion Test

The tests were performed according to the French standard NF T 56 102 “Alveolar Products made with elastomer or polymer: flexion test of rigid materials”.

The parameters of the test are as follows:

- distance between points: 230 mm
- speed: 5 mm/min
- geometry of sample L x l x e: 300 mm x 110 mm x 20 mm
- number of samples: 4

Results are presented in Table 8 and Table 9.

Table 8: Results at 23°C - Condition 1.

Material	**Breaking Stress**	**Flexion Modulus**	**Deformation**
	kPa	*MPa*	*%*
SIL 1	28.7	8.93	0.59
SIL 2	38.6	2.34	3.24

Table 9: Results at 23°C and 50% RH - Condition 2.

Reference	**Breaking Stress**	**Flexion Modulus**	**Deformation**
	kPa	*MPa*	*%*
SIL 1	13.29	2.94	0.8
SIL 2	20.66	*not measured*	*not measured*

Table 9 clearly shows the extremely low cohesion of the material but as soon as it is compressed under vacuum inside the envelope; this weakness is no more critical.

As for compression, the moisture has an important effect on flexion properties, a reduction of 50% is found for the SIL 1 product.

2.2.4 Thermal Dilation

The dimension of the sample is as follows: 250 mm x 30 mm x 25 mm. Two glass beads are glued on the sample with a distance, L_0, of 200 mm. Then, the sample is hung in a climatic chamber with regulated temperature. An optical extensometer was used to measure the distance L between both glass beads.

Temperature steps of 30°C each are applied between -20°C and 190°C. For each step, about one hour, the distance L is measured.

Due to the weakness of samples, the uncertainty in the results is very high.

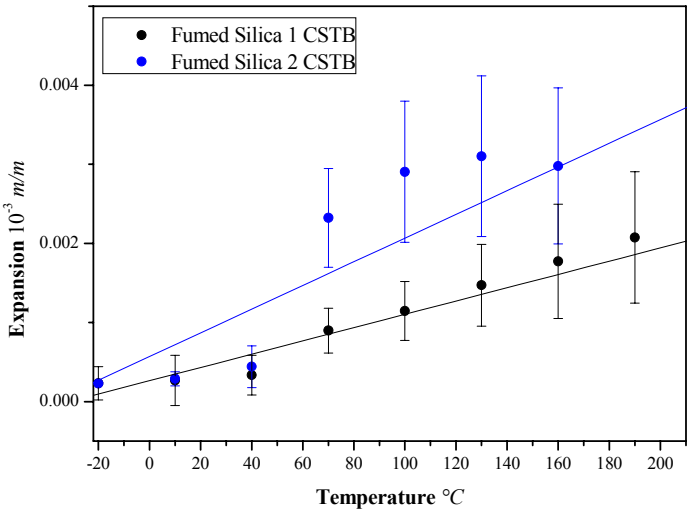

Figure 11: Thermal Dilation.

Table 10: Thermal Dilation.

Material	Thermal dilation $°C^{-1}$
Fumed Silica 1 CSTB	10.10^{-6}
Fumed Silica 2 CSTB	15.10^{-6}

2.3 Hygro-Thermal Properties

2.3.1 Water Vapour Adsorption

This test was performed according to the standard EN ISO 12571 “Hygrothermal performance of building materials and products – Determination of hygroscopic sorption properties”. Before testing in the laboratory at controlled temperature of 23°C, samples have been dried at 105°C to constant weight in order to define the reference dry mass. Then, the samples were stored and regularly weighed in climatic chamber at respectively: 30, 50, 75 and 95% of relative humidity.

The increase in the sample weight at each step allows the calculation of water content by mass (kg/kg).

The results are summarized in Table 11 & Table 12 and plotted in Figure 12. In this figure, the experimental points are fitted with the equation (2), presented in [4]:

$$u = \frac{RH}{A \cdot RH^2 + B \cdot RH + C} \quad (2)$$

u: mass water content (kg/kg)
A, B, C: fitting coefficients,
RH: Relative Humidity 0<RH<1

Table 11: Adsorption Isotherms – Experimental results.

Relative Humidity	**Mass Water Content**	
RH	*kg/kg*	
	SIL 1	**SIL 2**
0.00	0.000	0.000
0.30	0.013	0.017
0.50	0.030	0.032
0.75	0.055	0.057
0.95	0.198	0.172

Table 12: Desorption Isotherms – Experimental Results.

Relative Humidity	**Mass Water Content**	
RH	*kg/kg*	
	SIL 1	**SIL 2**
0.95	0.198	0.172
0.75	0.112	0.103
0.50	0.035	0.039
0.30	0.017	0.020
0.00	0.000	0.000

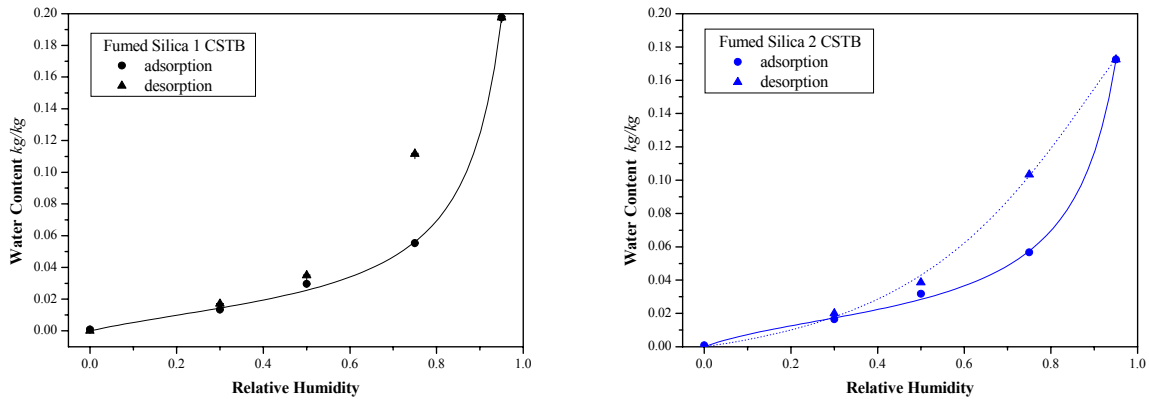

Figure 12: Adsorption & Desorption Isotherms at 23°C and fitted curves.

Table 13: Fitting parameters for SIL 1 & SIL 2 adsorption-desorption Isotherms.

Adsorption	***A***	***B***	***C***
SIL 1 CSTB	-40.1	25.42	16.86
SIL 2 CSTB	-43.2	35.8	10.51

Desorption	***A***	***B***	***C***
SIL 1 CSTB	32.23	-64.55	37.03
SIL 2 CSTB	18.26	-40.15	27.15

For comparison, adsorption data form NRC and ZAE-Bayern have been added in Figure 13 and a new fitting curve is suggested to plot the moisture content versus relative humidity:

$$u = \frac{t_1 \cdot RH}{t_2 + RH} \; e^{g \cdot RH^{\,f}} \qquad (3)$$

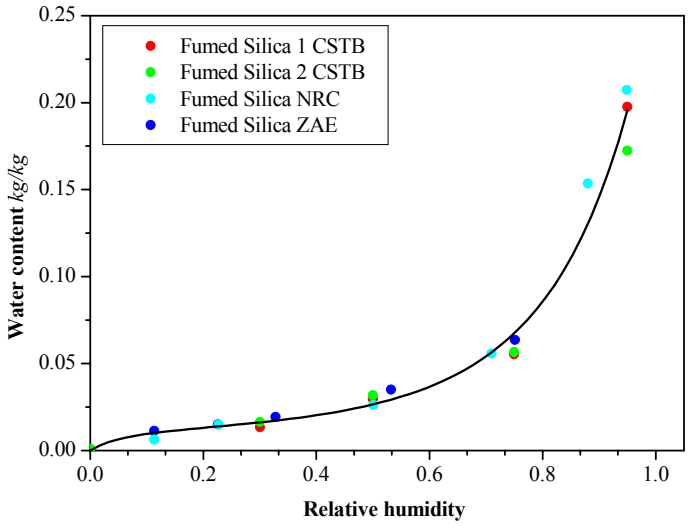

Figure 13: Comparison of experimental results from CSTB, NRC and ZAE-Bayern and the new fitting curve.

Table 14: Fitting parameters for SIL 1 adsorption Isotherms.

t_1	t_2	g	f
0.01721	0.08356	2.82429	2.26663

Figure 13 shows that SIL 1 & SIL 2 samples are very similar and results from the three laboratories are very close to one another.

On one hand, for low humidity (RH < 60%), the amount of adsorbed water is low (u < 5%) and the sorption isotherm can be approximated by a linear relationship. In this range, water molecules (average size ~ 0.3 nm) only cover the surface of the silica grains by adsorption [2] [5] (Figure 10).

On the other hand, for high humidity, from 60 up to 95%, there is an exponential increase mainly due to the capillary condensation in the small pores. Indeed, according to the Kelvin-Laplace law, at 95%, all the pores with a size smaller than 20 nm are filled with water.

2.3.2 Thermal Conductivity and Radiative Properties

In porous and cellular materials, heat is transferred through four distinct mechanisms: convection (λ_c), conduction through solid (λ_s) and gas phases (λ_g) and radiation (λ_r) [6].

The three modes should be considered simultaneously. However, in order to simplify the treatment, the standard approach is to assume that all the three mechanisms act in parallel, and the equivalent overall thermal conductivity λe is considered to be the sum of the four distinct modes:

- gas convection: λ_c
- solid conduction: λ_s
- gas conduction: λ_g
- radiation: λr

$$\lambda_e = \lambda_c + \lambda_s + \lambda_g + \lambda_r \quad (4)$$

With regard to cell or pore size, generally smaller than 1 µm, and temperature occurring in building, the Grashof number indicates that convection is nonexistent.

Consequently, at ambient pressure, in porous silica materials, the main contributions are:

- the solid conduction
- the gas conduction (air: 0.025 W/(m·K) in molecular regime)
- and the radiation.

2.3.2.1 Dependence on Pressure

The thermal conductivity versus pressure and temperature was measured using the hot-wire probe method [7] described in the European Standard EN 993-15: Methods of test for dense shaped refractory products - Part 15: Determination of thermal conductivity by the hot-wire (parallel) method.

The thin hot-wire probe is placed between two samples of size 80 mm x 150 mm. Then, the "sandwich" is put in a climatic chamber with a controlled temperature at 30°C. The pressure in the chamber was measured using a Baratron Gauge and the climatic chamber was installed in a laboratory at 23°C and 50% relative humidity.

The results are shown in Table 15 & Table 16 for both samples.

Table 15: Sample SIL 1.

Pressure	**Thermal Conductivity**
hPa	*10^{-3} W/(m·K)*
0.015	4.4
0.036	4.7
0.890	5.7
6.900	6.5
110.000	9.4
204.000	11.2
500.000	15.2
990.000	19.1

Table 16: Sample SIL 2.

Pressure	***Thermal Conductivity***
hPa	*10^{-3} W/(m·K)*
0.014	4.3
0.030	4.6
0.160	4.7
0.950	5.2
9.800	6.0
51.000	7.3
107.000	8.7
403.000	12.8
1000.000	20.8

In Figure 14, the experimental data obtained by CSTB for the fumed silica samples SIL 1 and SIL 2 are compared with the results published by ZAE-Bayern [8] [9] for a fumed silica sample provided by the manufacturer of SIL 2. At ZAE, the measurement was performed at 10°C instead of 23°C at CSTB, which yield slightly smaller values (see temperature dependence in Figure 15). Additional results for PU foam and precipitated silica are plotted only for comparison.

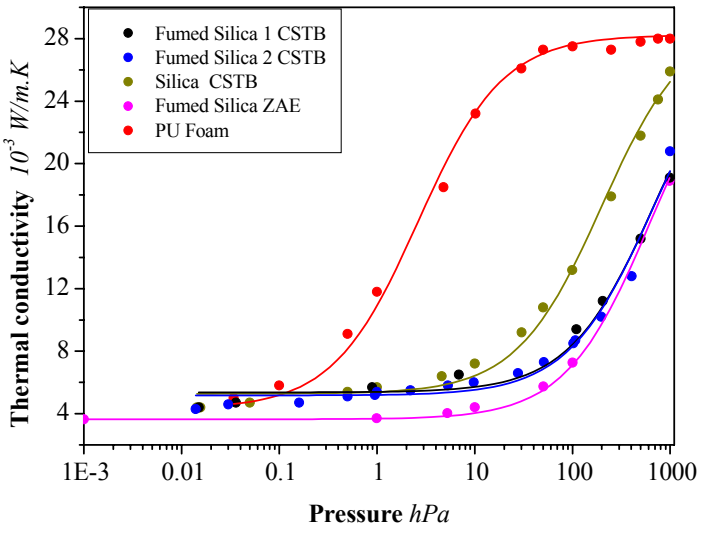

Figure 14: Thermal Conductivity versus pressure.

The gas conduction in a porous media can be written as follows [10] [11]:

$$\lambda_g = \frac{\lambda_{g0}}{1 + 2A \cdot K_n} \tag{5}$$

$K_n = \frac{l_m}{\delta}$ is the Knudsen number and A, a constant close to 1.5.

The Knudsen number is the ratio between lm , the mean free path of air molecules and δ, the characteristic size of pores.

On one hand, as the porosity of silica core is very high (> 90%), the gas contribution will play an important role at ambient pressure.

On the other hand, considering the narrow pore size in porous silica, the free air conduction $\lambda g0$ is reduced due to the Knudsen effect (interaction between gas molecules and pore walls). The gas conduction in such confined media can be written as follows [10] [11]:

The mean free path can be estimated using the following equation [12]:

$$l_m = \frac{k \cdot T}{\sqrt{2} \cdot \pi \cdot d_g^{\,2} \cdot P_g} \tag{6}$$

T is the temperature (K), Pg the gas pressure (Pa), dg the diameter of the gas molecule (3,53·10-10 m) and *k* the Boltzman's constant ($1{,}38066 \cdot 10^{-23}$ J/K).

In normal conditions, (23°C, 1 atm.), the mean free path of air is about 70 nm. A fit according equation (5) to the measured data yields for the fumed silica boards a characteristic pore size δ of about 300 nm. Both values are in the same order of magnitude. Thus even at ambient pressure the air conductivity will be strongly influenced by Knudsen effect.

From equations (5) and (6) the thermal conductivity of air in confined porous media can be written as follows:

$$\lambda_g = \frac{\lambda_{g0}(T)}{1 + C.\frac{T}{\delta \cdot P_g}} \tag{7}$$

This formula emphasizes the three main parameters, which play a great role for heat transfer in porous media:

- the gas pressure P_g
- the characteristic size δ
- the temperature T.

According to the equation (7), the gas conduction depends strongly on the product δ x Pg. It means, that if micro or nano-structured materials with a small pore size δ are used as VIP cores, only a weak vacuum is required to reach a low thermal conductivity.

From equations (5), (6) and (7) the equivalent thermal conductivity of the core in practice is often described by the simplified formula:

$$\lambda = \lambda_{evac} + \frac{\lambda_{g0}}{1 + \frac{P_{1/2}}{P_g}} \qquad (8)$$

λ_{evac}: *the thermal conductivity in the evacuated state,*
$P_{1/2}$: *a fitting pressure.*

Applying this formula for the investigated samples (Figure 14), we obtain the fitting parameters presented in Table 17.

Table 17: Sample SIL 2.

	λ 10^{-3} W/(m·K)$_0$	$P_{1/2}$ hPa
Fumed silica 1 CSTB	5.36	686.0
Fumed silica 2 CSTB	5.17	665.0
Precipitated silica CSTB	5.27	198.0
Fumed silica ZAE-Bayern	3.64	630.0
PU Foam	4.30	2.6

2.3.2.2 Dependence on temperature

The measurements were performed at a pressure of 0.01 hPa. At this low pressure, we can consider that the sample is dried and the thermal conductivity of the remaining gas molecules is negligible.

The effect of temperature on thermal conductivity is generally described using the following equation:

$$\lambda(T) = \lambda_s + \frac{16}{3}\frac{n^2\sigma T^3}{E} \qquad (9)$$

E (m^{-1}) is called the extinction coefficient and it can be estimated by fitting the experimental data, λ_s is the solid conductivity (W/(m·K)), σ the Stefan-Boltzman constant $5.6696 \cdot 10^{-8}$ W/(m^2K^4) and n the index of refraction.

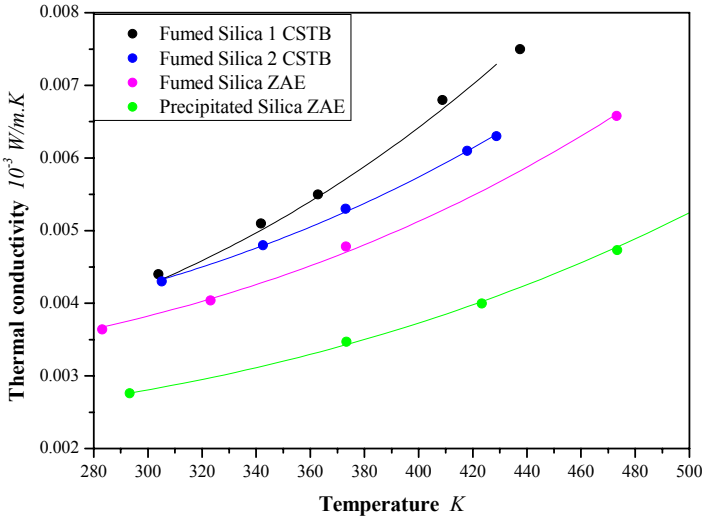

Figure 15: Thermal conductivity versus temperature.

In Figure 15 the experimental points and the fitted curves obtained for SIL 1 & SIL 2 samples are plotted and compared with results from ZAE-Bayern obtained for fumed silica similar to SIL 2 sample and a precipitated silica [13] [14].

For the comparable samples SIL 2 and the similar fumed silica samples characterised by ZAE-Bayern one can notice the same behaviour with a small constant difference of 0.0005 W/(m·K).

The fitting coefficients are listed in Table 18:

Table 18: Solid thermal conductivity and extinction coefficient.

	λ_s 10^{-3} W/(m·K)	E m^{-1}
Fumed Silica 1 CSTB	0.0027	5154
Fumed Silica 2 CSTB	0.0032	7632
Fumed Silica ZAE-Bayern	0.0029	8589
Precipitated Silica ZAE-Bayern	0.0021	12153

The solid thermal conductivity of fumed silica appears to be close to $3 \cdot 10^{-3}$ W/(m·K). The extinction coefficient, which depends on the density, varies from 5000 up to 12000 for the precipitated silica.

2.3.2.3 Dependence on water content

At ZAE-Bayern two sets of measurements were performed to study the influence of water vapour and adsorbed water on the thermal performance of vacuum insulation panels as well as on the thermal conductivity of the core material. The material investigated is assumed to be quite similar to SIL 2. In the first set, special VIP have been produced with additional water, sprayed on the core material. The amount of water was determined by repeated measurement of the panels mass. The second set of measurements was performed with a

vacuum guarded hot plate apparatus. Water vapour in different portions was let into this device. The water content is given by the partial pressure of the water vapour (see Figure 13) and in these tests this partial pressure is the same as the total gas pressure. Thermal conductivity was measured as a function of the relative humidity for different temperatures. For both sets of tests, thermal conductivity was determined at steady state conditions with the guarded hot plate apparatus.

Measurements on VIP

Preparation of samples:

The following procedure was applied to bring a defined quantity of moisture into the VIP:

First, the core material (fumed silica pressed to a panel) was dried for 3 h at 150°C, weighed, wrapped into the laminate-envelope and evacuated and then the thermal conductivity of the dry panel was measured.

After that, the VIP was opened, the core was sprayed with a roughly defined amount of water, frozen, evacuated and the thermal conductivity was measured on the VIP with moisturized core.

To evaluate and to check more precisely the amount of water in the core, after the thermal conductivity measurement the VIP was opened again, the moist core was weighed, once more dried (3 h at 150°C) and weighed in the dry state. The water content X_w in the VIP was calculated from the dry mass m_{dry} and the mass of the moist core m_{moist} : ($X_w = (m_{moist}-m_{dry})/m_{dry}$)).

In the following the moisture in the VIP is always indicated as water content X_w (in mass percent with respect to the dry mass).

Results:

The thermal conductivity was measured at mean temperature of 10°C, with 20°C on the hot plate and 0°C on the cold plate. The panel size was 30 cm x 30 cm x 2 cm. The results are shown in Figure 16.

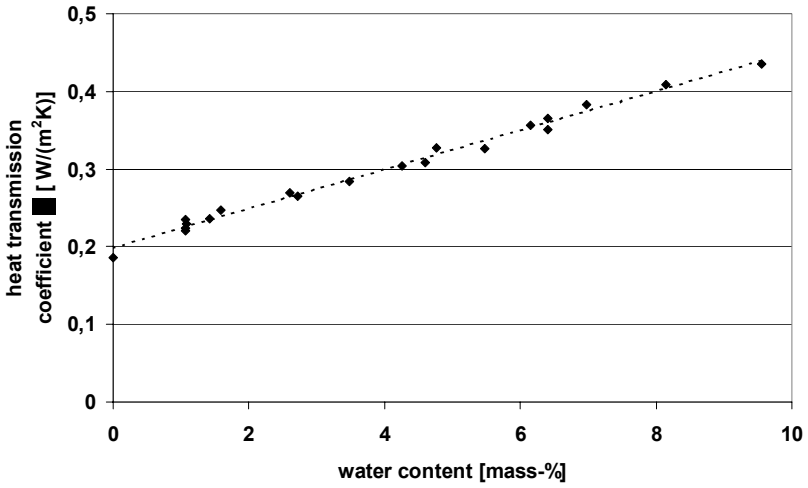

Figure 16: Measured heat transfer coefficient versus the water content for a 20 mm thick VIP. Mean temperature was 10°C.

A significant increase of the heat transfer with increasing water content is observed. These measurements only apply for the specified measurement conditions and panel size. Fitting a straight line through the data in Figure 16 and converting the heat transmission coefficient into a thermal conductivity, one gets an average increase in thermal conductivity of $0{,}5 \cdot 10^{-3}$ W/(m·K) per mass percent of water content. The total thermal conductivity of the moist board can be considered as a function of the water content Xw.

$$\lambda(X_w) \approx \lambda_{VIP,dry} + 0.5 \cdot 10^{-3} \frac{W}{m \cdot K} \cdot X_w / m-\% \qquad (10)$$

Although equation (10) only applies for the mentioned conditions it allows to estimate the influence of moisture on the thermal conductivity.

The above results give the thermal transmission coefficient under terms of stationary condition. Another interesting aspect is the development of the measurements with time. At the beginning of the measurements high heat flows arise. This increased heat flows are caused by the vaporization with transport of the phase change enthalpy. The transient behaviour when the temperature gradient is reversed by turning around the panel, is illustrated in Figure 17, which depicts an “apparent thermal conductivity“ calculated with the actual power feed into the panel.

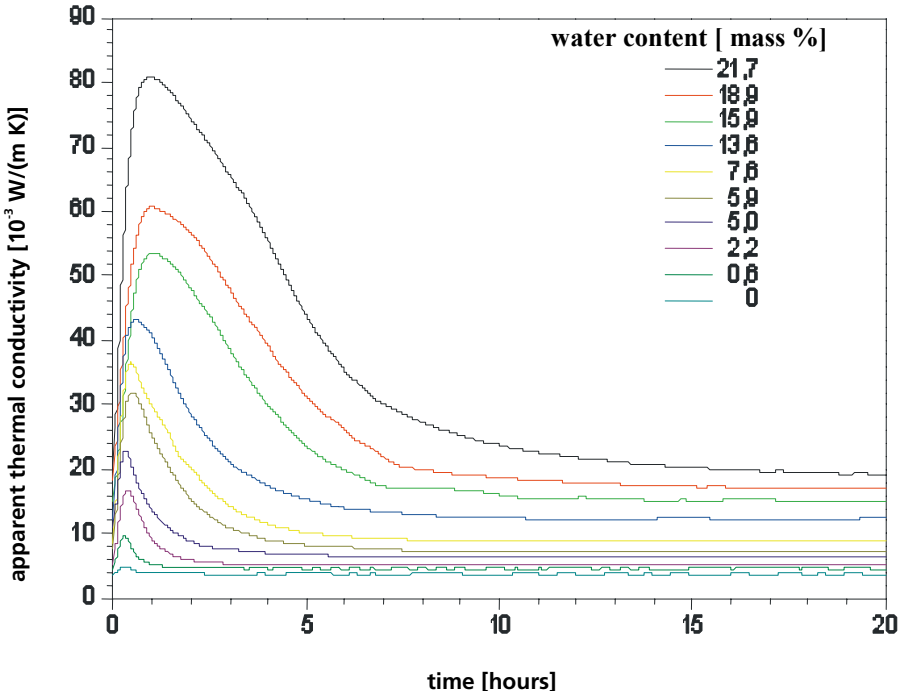

Figure 17: „Apparent thermal conductivity" developing by the time for a VIP (30 x 30 x 2 cm³) with different water contents. Mean temperature was 10°C.

Measurements on the core material

A second set of measurements not on specially prepared VIP but on the core material were performed with a guarded hot plate apparatus that can be evacuated. Water vapour in different portions was let into this device. The water content is given by the partial pressure of the water vapour (see Figure 13) and in these tests this partial pressure is the same as the total gas pressure. Thermal conductivity was measured as a function of the relative humidity for different temperatures. The relative humidity is given by the ratio of the measured gas pressure and the calculated saturation water vapour pressure.

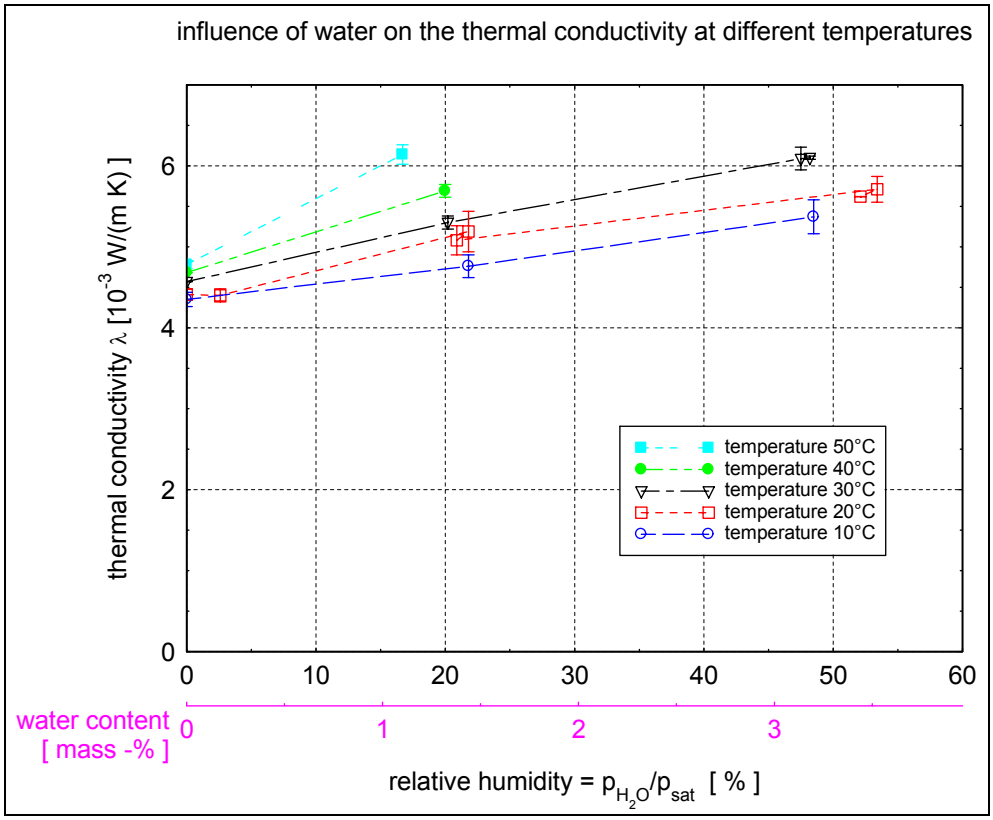

Figure 18: Measured thermal conductivity versus different water vapour pressures, depicted as relative humidity. Additional parameter is the mean temperature. Typical temperature gradient was 20 K on the samples with a thickness of about 18.5 mm.

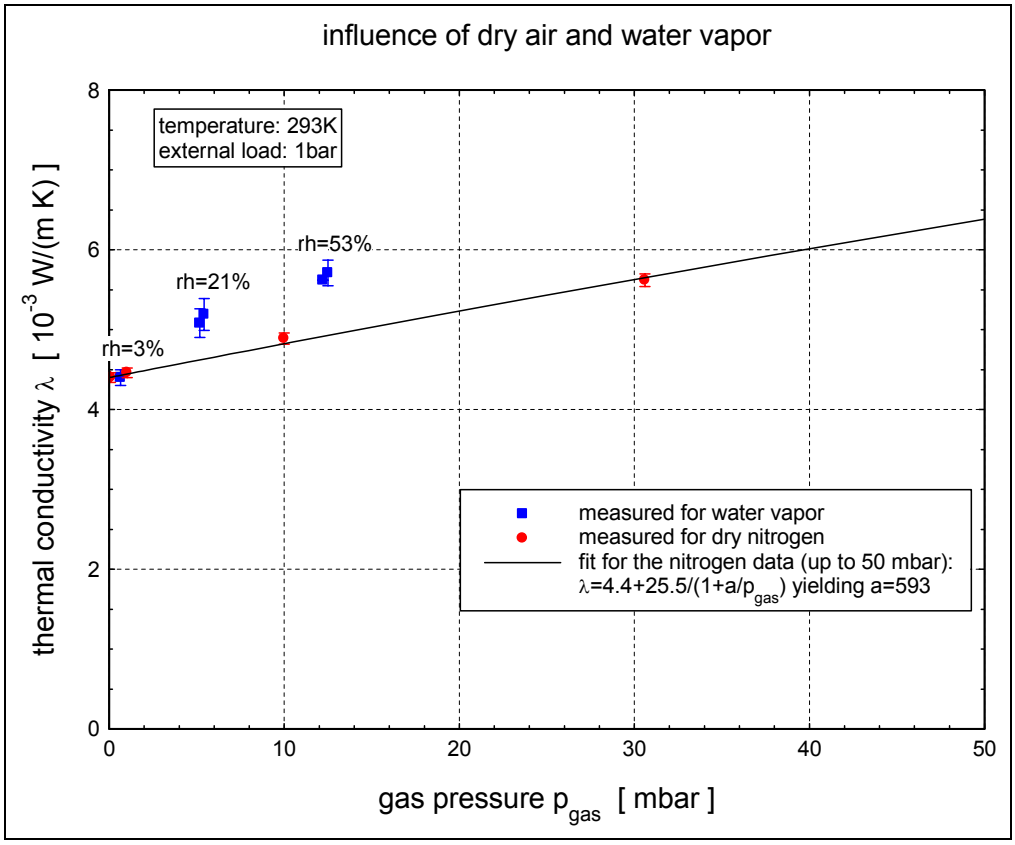

Figure 19: Thermal conductivity measured for different gas pressures of dry nitrogen and of water vapour at a mean temperature of 20°C. Additionally the corresponding relative humidity is depicted at the values given for the atmosphere of water vapour.

2.3.3 Specific Heat

The dependence of specific heat on temperature was measured using a differential scanning calorimeter SETARAM DSC 92.

The experimental parameters are the following:

- Initial Temperature: 30°C
- Final Temperature: 200°C
- Temperature step: 5°C
- Step duration: 480 s
- Heating rate: 2°C/min
- Number of cycles: 34

The results are listed in Table 19 and presented in Figure 20. The mean value is about 850 *J/kg K* for each material.

Table 19: Specific Heat.

Temperature	**Specific Heat**	
°C	*J/kg.K*	
	SIL 1	**SIL 2**
43	726	648
53	895	922
58	935	908
73	811	938
83	890	902
103	786	802
123	822	852
143	761	849
153	788	794
168	996	877
178	915	921

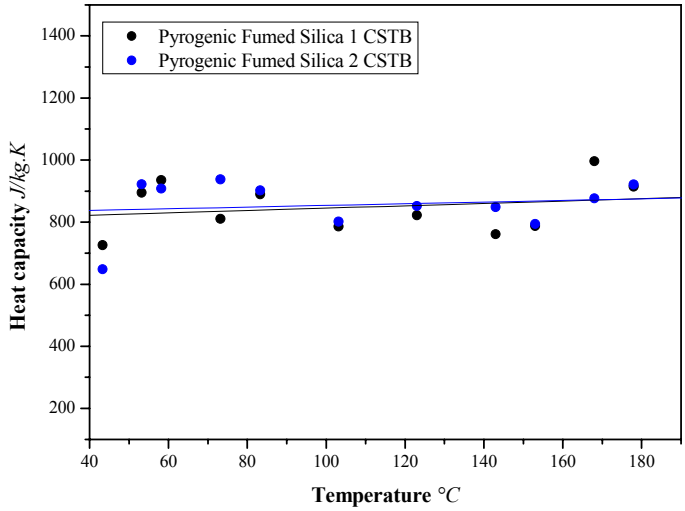

Figure 20: Specific heat versus temperature.

The specific heat of dry materials does not vary significantly versus temperature in the range 40-180°C.

2.4 Gas Permeability

The intrinsic gas permeability *k* (*m²*) of a porous material is defined by the Darcy's law [15] and [16]:

$$V = -\frac{k}{\eta}\frac{\Delta P}{L} \tag{11}$$

v: fluid velocity m/s

η: dynamic viscosity Pa.s

L: thickness m

P: pressure Pa

The fluid flow Q = v A through a media of thickness L and section area A is written:

$$Q = -\frac{k}{\eta}\frac{A.\Delta P}{L} \tag{12}$$

Then, the intrinsic permeability k is as follows:

$$k = -\frac{Q}{A}\frac{\eta.L}{\Delta P} \tag{13}$$

and the gas permeability K_g (s^{-1}):

$$K_g = k\frac{\rho_g}{\eta_g} \tag{14}$$

ρ_g (*kg/m³*) is the gas density and η_g (Pa s) the dynamic viscosity of the gas.

The air permeability depends on the water content through relative permeability $k_{rg}(u)$ which ranges between 0 and 1:

$$K = K_g.k_{rg}(\tau) \tag{15}$$

The tests were carried out according to the French Standard NF B 20-104: "Insulating products made with mineral fibres – Felts, mats and panels - Determination of air permeability".

The samples were cylinders of diameter, ∅ = 110 mm and variable thickness depending on the tested samples (about 20 mm). The measurements were performed only for dry materials, thus the relative permeability krg is equal to 1. The results, listed in Table 20, show that both materials have a similar and very low intrinsic permeability.

Table 20: Intrinsic Permeability

Reference	Intrinsic Permeability	ΔP
	$x10^{-15}$ m²	*bar*
SIL 1	2.6	0.98
SIL 2	3.0	1.01

2.5 Fire behaviour

The fire behaviour of both core materials is characterised by two techniques:

1: The fire reaction using the radiation test described in the French Standard NF P 92-501: Protection against Fire – Building – Fire reaction testing of materials – Radiation test for rigid materials or equivalent (glued coating materials) and soft materials with a thickness higher than 5 mm.

2: The measurement of the gross calorific value according to the French Standard NF P 92-510: Protection against Fire – Building – Fire reaction testing of materials – Determination of gross calorific value.

The sample sizes were 40 cm x 30 cm and the tests provide information about:

- the fire behaviour rating,
- the calorific value.

The results are listed in the Table 21.

Table 21: Fire reaction testing

Reference	Fire reaction rating	Calorific Value
		kJ/kg
SIL 1	non flammable	-206
SIL 2	non flammable	1204

The negative calorific value of SIL 1 results from an endothermic reaction and due to the absence of any combustible products inside.

For SIL 2 the positive calorific value ensues from some organic materials, certainly the fibres. This result confirms the SEM analysis that shows soft fibres in SIL 2.

Remarks: The mean calorific value of rock wool is lower than 1'000 kJ/kg and lower than 1500 kJ/kg for glass wool.

2.6 Thermo Gravimetric Analysis (TGA)

For this analysis, the temperature ranges from 30°C to 1000°C with a temperature step of 10°C/min. Nitrogen is used up to 700°C and oxygen from 700 to 1'000°C.

For both materials, the weight loss is lower than 2% between 30 and 100°C; it corresponds to the desorption of water. Between 100 and 1'000°C, the weight loss is only 1% for SIL 1

whereas it is more than 5% for SIL 2 between 250 and 450°C. This difference is certainly due to the nature of fibres that seems to be different from each other.

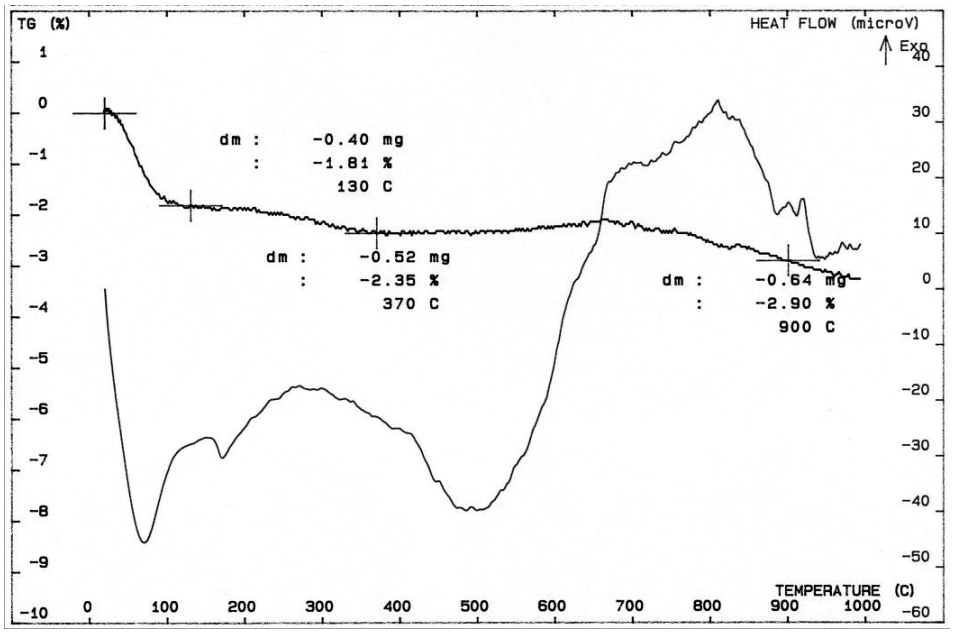

Figure 21: Thermo Gravimetric Analysis - SIL 1

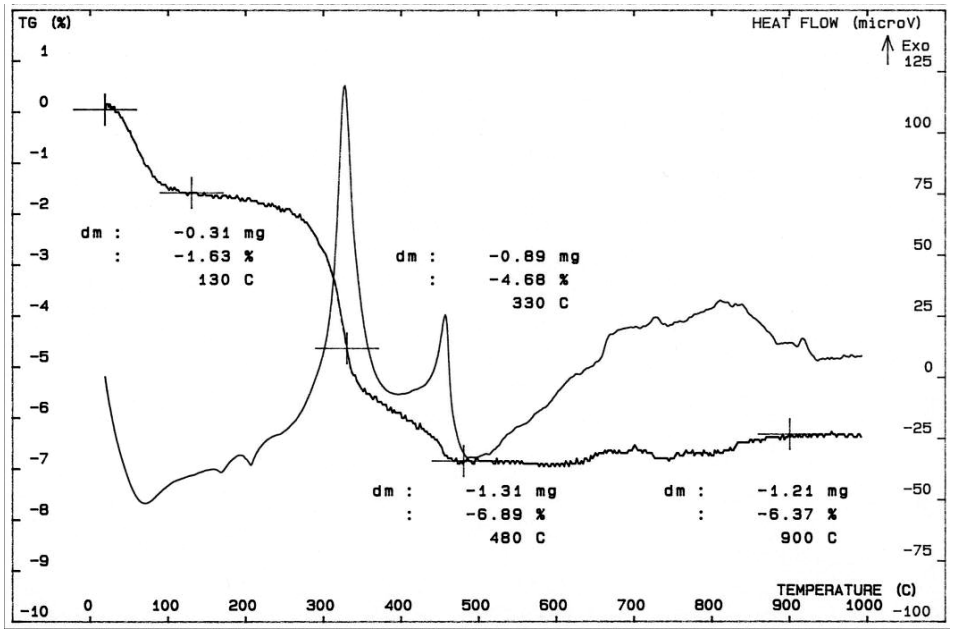

Figure 22: Thermo Gravimetric Analysis - SIL 2

2.7 Summary "Core"

Both materials SIL 1 & SIL 2 investigated in this study are comparable fumed silica with minor differences, especially the nature of fibres that are used for reinforcement.

For both materials, the porosity is higher than 90% and the specific area higher than 200 m^2 /kg. The densities are slightly different, 160 and 190 kg/m^3 respectively.

At low pressure (0.01 hPa), the effective thermal conductivity that is mostly due to the solids is close to $3 \cdot 10^{-3}$ W/(m·K) whereas this value rise up to $20 \cdot 10^{-3}$ W/(m·K) at ambient pressure in dry condition.

The compression strength of core should be high enough to allow the application of VIP for sub-floor heating applications. Nevertheless, the flexion resistance and cohesion are very weak and consequently the handling of core requires special attention.

Finally, these nano-structured materials are very sensitive to moisture. Due to the high specific area and the small size of pores, these materials are nice getters for gases, especially for water vapour. Consequently a significant influence of adsorbed water and of water vapour on the thermal conductivity was found, that causes an increase of 1 to $2 \cdot 10^{-3}$ W/(m·K) at ambient conditions.

3 Envelope

3.1 Objectives

The most critical component of a Vacuum Insulation Panel (VIP) is the outer coverage, which is responsible for the maintenance of the vacuum inside the panel. As a standard, polymer film laminates are used for this purpose. The permeability of these laminates is the determining criterion for the shelf life of the panel because the pressure in the panel may not rise above 100 mbar after 30 – 50 years.
The objective of this section of the investigation was the characterization of the currently used laminates in terms of measured transmission rates, especially for water vapour. The impact of different parameters such as temperature, moisture, ageing and production process should be examined.

In building applications a shelf life of at least 30 - 50 years is required for the panel. Derived from that and taking into account that certain core materials may act as moisture absorbers (getters) the permeability of the laminate has to be below ~10^{-2} cm³/(m² d bar) bar for the oxygen transmission rate (OTR) and ~10^{-4} g/(m² d) for the water vapour transmission rate (WVTR), which is not yet possible to achieve. State-of-the-art standard equipment has a measurement limit of about 10^{-2} g/m² d for WVTR. Therefore the task was the development of permeability measurement equipment with a sensitivity limit of at least 10^{-4} g/(m² d).

3.2 Theoretical Background

3.2.1 Introduction

Polymer films containing inorganic barrier layers have become increasingly important to the packaging industry owing to numerous advantages over other materials with respect to convenience, economy and even environmental issues. However, comprehensive knowledge of the barrier mechanisms is required to select them for the appropriate packaging use. Meanwhile, extensive studies led to a well-accepted model for the permeation of oxygen through polymer films containing an inorganic barrier layer, as Al or SiO_x. Current understanding of the permeation mechanism of water vapour is nothing better than a working hypothesis.

3.2.2 Permeation through polymer films

The permeation mechanisms of gases and water vapour through pure polymer films depends on

- how many molecules can be dissolved in the polymer, e.g. the solubility coefficient S of the permeating substance through the polymer and
- how fast the molecules can move inside the polymer, e.g. the diffusion coefficient D.

The permeability P is given by their product, P = D x S, in first approximation taken as constants, as to be seen in Figure 23.

After laminating different polymer films together, the total permeability (P_{total}) can be calculated from the individual permeabilities (P_1, P_2, ...) of the components by the simple equation, also used for conductivities in series as the electrical analog of (Kirchhoff's Law):
$P^{-1}_{total} = P^{-1}_1 + P^{-1}_2 + ...$

The driving force is the difference in gas concentration between both sides of the polymer film. Different substances can be assumed to permeate homogenously through the laminates.

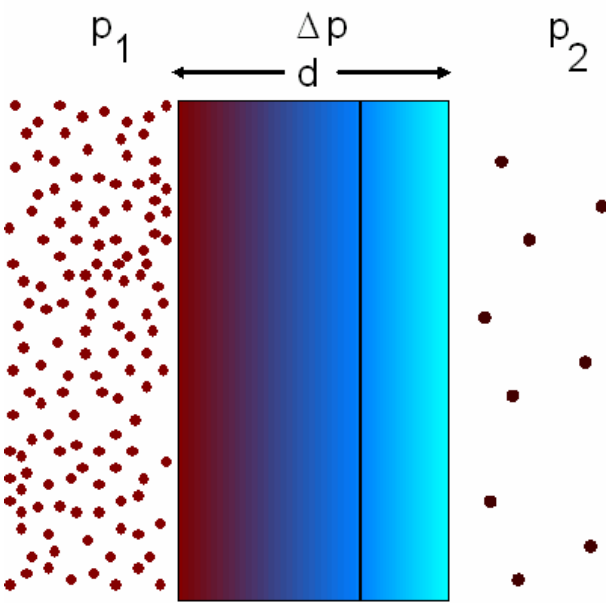

Figure 23: Permeation mechanism (schematic) through a laminate containing two homogenous polymers.

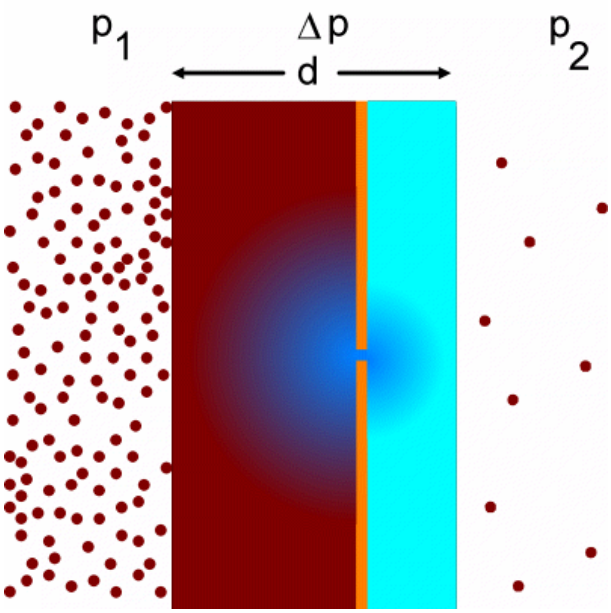

Figure 24: Permeation mechanism (schematic) through a three layer stack containing an inorganic barrier layer.

3.2.3 Permeation through vacuum web coated barrier layers

The oxygen permeation through vacuum web coated barrier layers, like Al, AlO_x, SiO_x and also Melamine, predominantly occurs at macroscopic defects in the range of 0,1 µm² to 1 µm² ([31], [32]). There is practically no permeation through the bulk material of the layers, as to be seen in Figure 24.

There is another mechanism for the permeation of water vapour through the barrier layers due to non-linear effects, mainly generated by high solubility/condensation of substances that can either be really dissolved in the polymers or condensed in capillaries (water). Capillaries can form at microscopic defects and grain boundaries. In contrast to oxygen permeation dominated by the macroscopic defects in the barrier layer, the permeation of water vapour depends also on the microstructure of the layer.

For oxygen, the macroscopic defects in the vacuum coated barrier layers are the bottlenecks for permeating molecules. Due to the sideways diffusion to and from the bottlenecks in the polymer layers (substrate film or adhesive) next to the barrier layer, the polymer close to the defects influences the total permeability much stronger than at the outsides of the laminate [32]. Hence, many small holes in a barrier layer are much more efficient in compromising the system's barrier properties than a few large holes with the same total area.

Due to capillary effects in the barrier layer, water vapour can also permeate at microscopic defects and maybe grain boundaries. A higher density of these diffusion channels reduces the impact of the sideways diffusion in the polymer layers next to the barrier layer. There is a lower synergy in permeation barrier between the barrier layer and the attached polymer for water vapour than for oxygen.

To obtain high barrier laminates by use of the synergy effect, the technical requirements are

- a low density of defects in the barrier layer and
- a polymer possessing a high barrier next to the vacuum web coated layer.

Thin high barrier polymer layers next to the barrier layer significantly improve the overall barrier properties. On the substrate side of the layer, pre-coating or co-extrusion can be used, on the other side of the layer barrier adhesives or barrier lacquers.

The barrier of the final laminate can be improved by reducing the number of defects. Successful options are thick enough coatings and coating onto smooth or plasma smoothed substrate films. Modifying the microscopic structure of the inorganic layer by plasma assisted deposition can improve, for example, the resistance of a water vapour barrier.

3.2.4 Important terms and relations for permeation measurement

The whole transport mechanism of gases, vapours and liquids through films is summarized under the term permeation. The terms used for oxygen transmission rate (ASTM D3985-81) and water vapour transmission rate (ASTM E96-80) measurements are given below.

Water vapour permeability is the time rate of water vapour transmission through unit area of flat material of unit thickness induced by unit vapour pressure difference between two specific surfaces, under specified temperature and humidity conditions.

Water vapour permeance is the time rate of water vapour transmission through unit area of flat material or construction induced by unit vapour pressure difference between two specific surfaces, under specified temperature and humidity conditions.

Water vapour transmission rate is the steady water vapour flow in unit time through unit area of a body, normal to parallel surfaces, under specific conditions of temperature and humidity at each surface. The unit is given as g / (m^2 h) in metric units.

Oxygen transmission rate is the quantity of oxygen gas passing through a unit area of the parallel surfaces of a plastic film per unit time under the conditions of test. A commonly used unit of OTR is the cm^3 (STP)/(m^2 d) at one atmosphere pressure difference

Oxygen permeance is the ratio of the oxygen transmission rate to the difference between the partial pressure of oxygen on the two sides of the film. The SI unit of permeance is the mol / (m^2 s Pa)

Oxygen permeability coefficient is the product of the permeance and the thickness of a film. The permeability is meaningful only for homogeneous materials, in which case it is a property characteristic of the bulk material. This quantity should not be used, unless the relationship between thickness and permeance has been verified on tests using several different thicknesses of the material. The SI unit of oxygen permeability is the mol /(m s Pa).

for mono film permeability: P = Q * d

P: permeability coefficient
Q: transmission rate
d: thickness

diffusion coefficient *D* [cm^2 / s], describes for the mobility of the gas molecules.

solubility coefficient *S* [cm^3 (STP) / (cm^3 Pa)], describes the amount of permeating molecules dissolved in the polymer.

Typical solubility constants of PET film are:
[cm^3 / STP cm^3 / Pa) ($*10^7$)
- Nitrogen 4.3
- Oxygen 7.5
- Methane 19.7
- Argon 0.8
- CO_2 130.0

Table 22: Relative values of permeability parameters; Nitrogen is defined as the normalized standard, because of the lowest permeability [33].

N_2 *(reference)*	1.0
O_2	3.8
CO_2	16.0
He	15.0
H_2	22.5

3.2.5 Basic measurement principles for gases

3.2.5.1 Manometric Method (DIN 53380, T 2, draft)

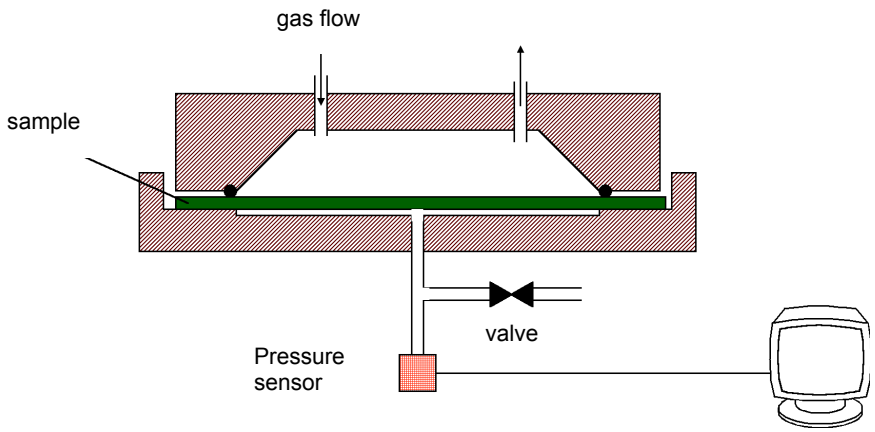

Figure 25: Principle of the set up of the manometric measurement principles for gases.

The manometric method is used to determine the amount of gas that permeates through a packaging material under defined conditions by measurement of the pressure variation in the

permeation cell. Inert gas permeabilities can be measured by this method. The lower measurement limit is 1 cm³ / (m² d bar).

3.2.5.2 Electrochemical Method for Oxygen (DIN 53380-3)

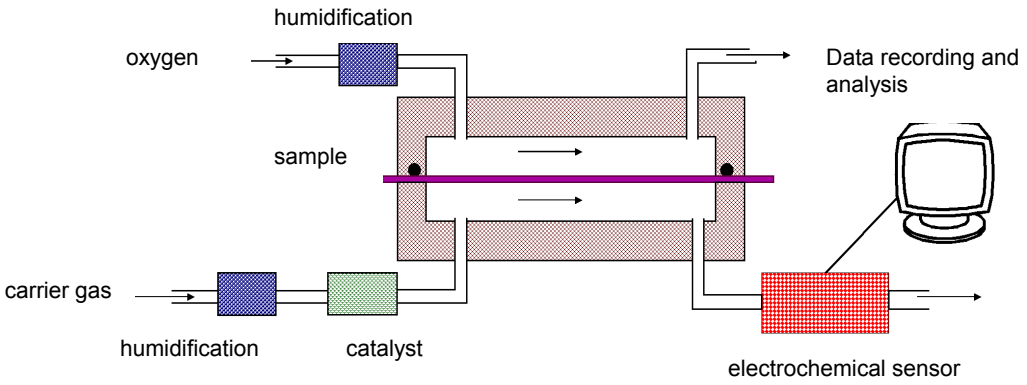

Figure 26: Principle of the set up of the electrochemical measurement principles for oxygen.

Carrier gas method to measure the amount of oxygen, which permeates through a packaging material using an electrochemical sensor. The lower measurement limit is 0.05 [cm³ / m² d bar].

3.2.6 Basic measurement principles for WVTR

3.2.6.1 Gravimetric Process (ISO 15106-3)

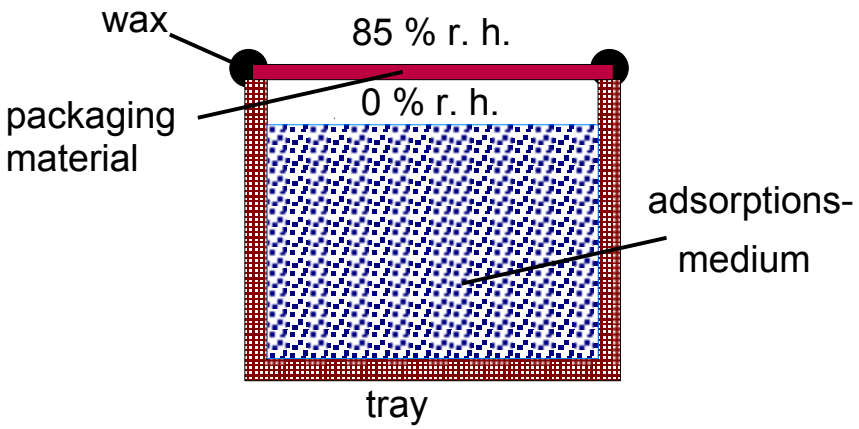

Figure 27: Principle of the set up of the gravimetric measurement for WVTR.

The gravimetric method can be used to measure materials with WVTR in the range of 1 to 1'000 g/(m^{2}d). Foils are bonded on a glass bowl filled with silica gel with a special wax, as shown in Figure 27. The samples are exposed to a constant temperature / constant relative humidity chamber and weighed in regular intervals. By plotting weight change against exposure time, the WVTR can be calculated.

3.2.6.2 Electrolytic Process (DIN 53 122-2)

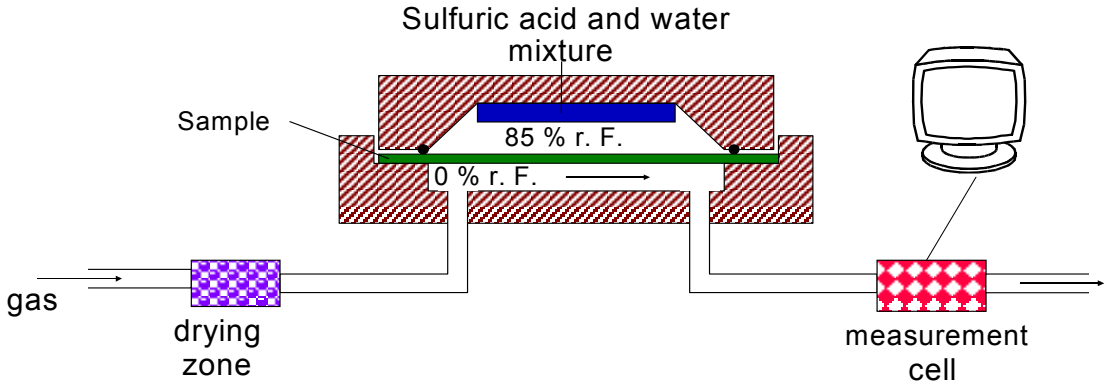

Figure 28: Principle of the set up of the electrolytic measurement method for WVTR.

A schematic description of the functional principle of the electrolytic process is given in Figure 28. The sample to be tested is mounted in a two-compartment permeation cell. A constant water vapour pressure is maintained on the upper side of the sample. On the other side, the water vapour permeated through the sample is carried by the extremely dry carrier gas into the electrolytic cell. Two spiral wire electrodes covered by a thin coating of phosphorus pentoxide are provided in the latter on the inside wall of a thin glass capillary. These electrodes are subject to a DC voltage of approx. 70 V. The water vapour present in the carrier gas flowing through the capillary is quantitatively absorbed by the P_2O_5 and electrolytically decomposed into hydrogen and oxygen. From the electrolyte current the amount of water vapour, which is decomposed, and therefore permeated through the sample can be established per unit time. In the dry section of the permeation cell a very low water vapour pressure exists.

3.2.6.3 Calcium Test

A new measurement method for WVTR is based on the corrosion of thin calcium films [34]. These films, deposited on the substrate of choice are encapsulated with a transparent adhesive/sealant and a glass lid. The calcium layer is initially a highly reflecting metallic mirror. As water and oxygen penetrate the test cell, metallic calcium reacts with oxygen and water, resulting in an increasingly transparent layer of calcium salt. Transmission rates in the range of 10^{-1} to 10^{-5} g H_2O m^{-2} day^{-1} have been determined using this method. The samples have to be prepared under oxygen and water free conditions. Therefore, the method requires tight glues for measurement of high performance barriers. The calibration is very sophisticated, because the calcium oxidation can be caused by oxygen or water. As a consequence, the quantification of the degree of oxidation of the calcium layer is crucial and also the contrast between the calcium and underlying metal is critical. Finally it is a very sensitive measurement method to be carried out under absolute water and oxygen free conditions and for standard measurements this method is too difficult.

3.3 List of companies offering WVTR measurements

Table 23: List of companies for water vapour measurements.

Company	Measurement principle	Measurement limit *[g/m²d (38 C; 90→ 0 RH)]*	Remark
Brugger	electrolytic measurement principles	0.01	equipment supplier
Desert Cryogenics, Tuscon	two vacuum chamber separated by sample and gas analysis by mass spectrometry	<<0.005	first results obtained, data still confidential
Mocon, Minneapolis	electrolytic measurement principles	0.005	equipment supplier
Pauly/Becker Fachlabor f. Permeationsprüfung; Wiesbaden	no information given by the lab	0.005	
InfraServ GmbH; Wiesbaden	MOCON equipment	0.005	
Innoform GmbH, Oldenburg	Brugger equipment	0.01	
ISEGA Forschungs- und Untersuchungs GmbH	Brugger equipment	0.01	
Labor für Kunststoffprüfung	gravimetric	1.0	
Mecadi GmbH Homburg	gravimetric plus Karl-Fischer analysis	0.00001	no prototype available
Lyssy AG, Zollikon	Capacitive moisture sensor	0.03	
Batelle Advanced Materials Application, Ohio	no information given by the lab		
Pesce Labs, Pennsylvania	no information given by the lab		
Perma Tech, Minnesota	MOCON equipment	0.01	
VTI Cooperation; Florida	Chilled mirror	0.04	

3.4 Barrier Measurements

3.4.1 WVTR and ORT measurements (IVV)

Several water vapour permeation measurements on different samples were carried out according to the electrolytic process (DIN 53 122-2). In the Figure 29 to Figure 31 a summary of the results is given. Each figure shows usually two measurements of up to six production batches of each product (one to three metallized layers).

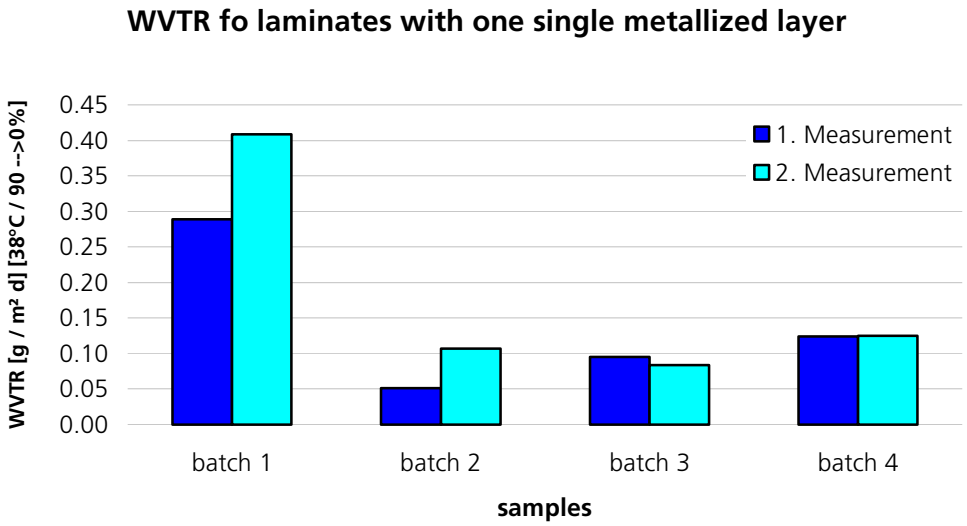

Figure 29: WVTR of four production batches of a product with one single metallized layer.

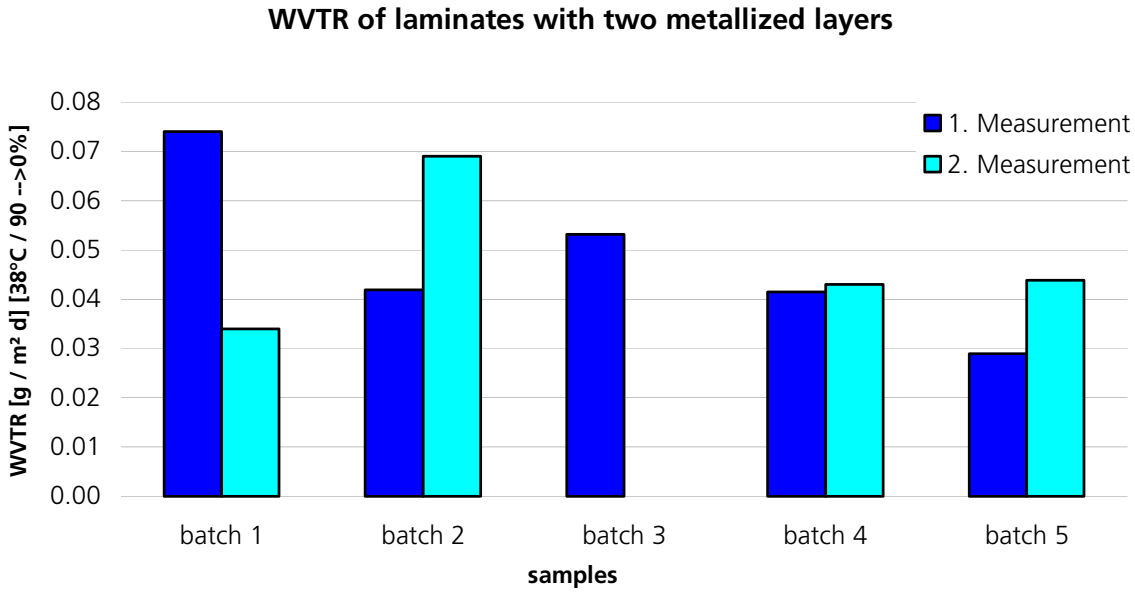

Figure 30: WVTR of five production batches of a product with two single metallized layers.

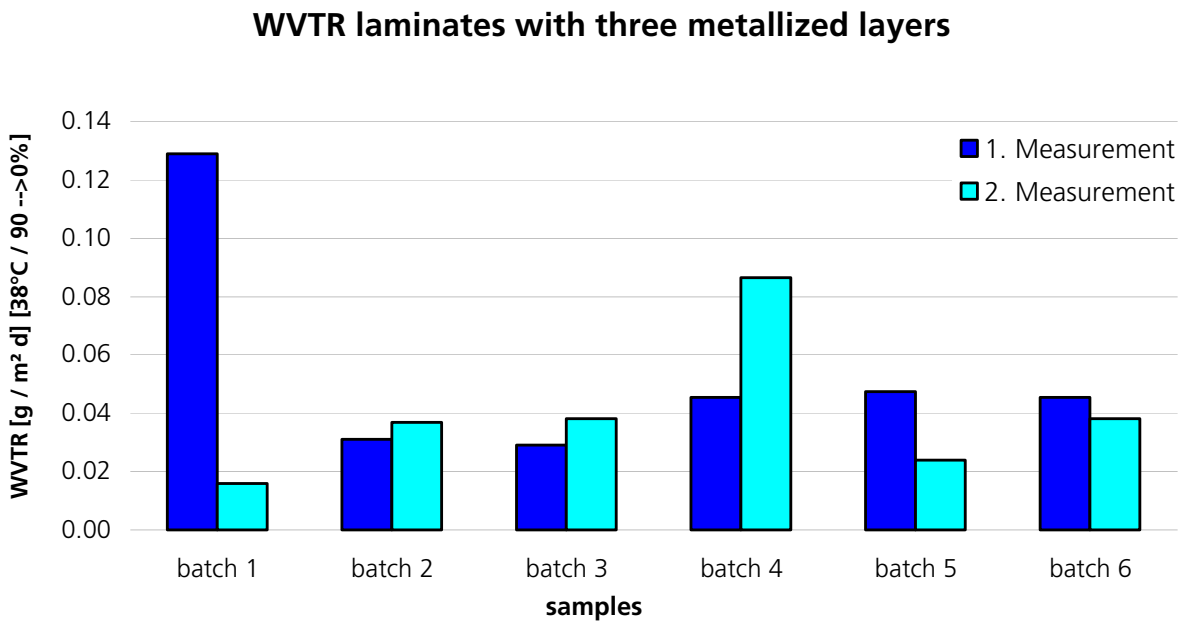

Figure 31: WVTR of six production batches of a product with one three metallized layers.

The measurements needed a long time to reach equilibrium. Figure 32 shows an exemplary measurement of this time behaviour.

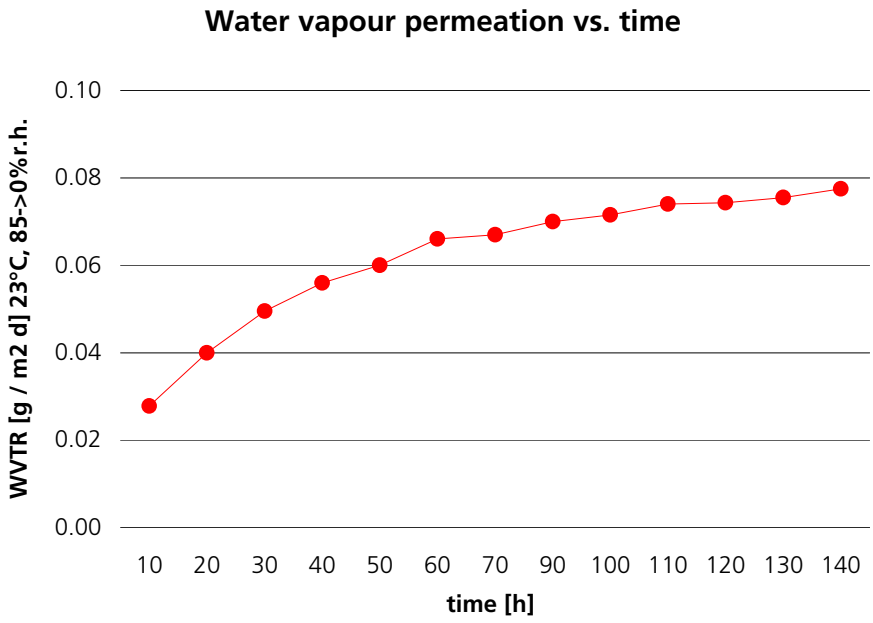

Figure 32: The time behaviour of a water vapour permeation measurement.

Parallel to the water vapour permeability, measurements of helium permeability according to the manometric method (DIN 53380, T 2) were also performed on the same samples. The measurement of the helium permeability represents a method, which can be carried out very

fast and reliably, due to the high diffusion coefficient of helium and the high permeability, the steady state for permeation is reached rather quickly. The measurement needs only some hours in many cases because the smaller helium molecules are able to permeate much faster through the polymer film laminate than water molecules. The time for measurement depends on the lag time, which is the time required for the permeation to reach equilibrium, i.e. the dissolution of the gas in the polymer reached saturation. The lag time can be determined experimentally according to the following diagram:

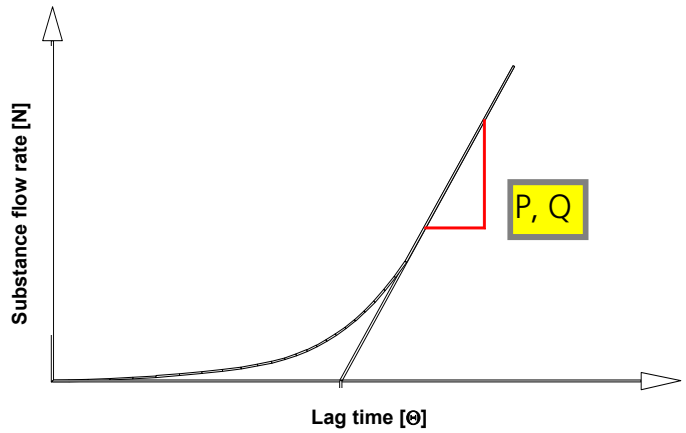

Figure 33: Determination of the lag time by measuring the substance flow rate.

The slope of this curve represents the permeation rate of the permeating substance. Approximately the lag time is calculated by the formula:

$$\Theta = d^2 / (6*D) \qquad (16)$$

d: thickness of the substrate
D: diffusion coefficient

For some metallized films, a correlation between the water vapour and helium permeability was found. However, since the permeation mechanism could differ from sample to sample and with respect to laminates, using the same correlation value for all the metallized films and laminates, would lead to errors. For these reasons the helium and water vapour permeability values of all the received films shall be measured in addition, to see whether a correlation is feasible. In Figure 34, the measurements of the helium permeability are correlated to the values of the water vapour permeability.

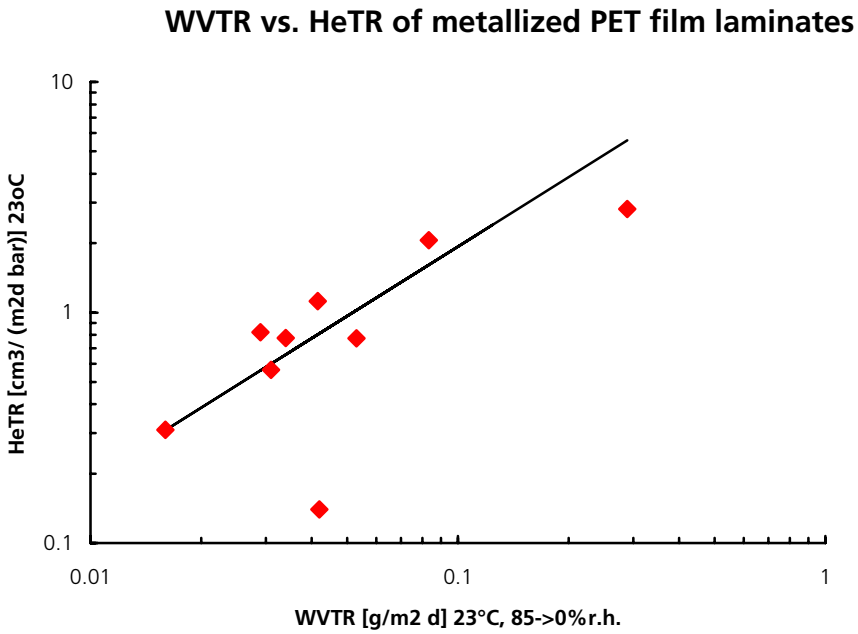

Figure 34: He values against WVTR values of metallized PET film laminates.

Moreover the time necessary to reach a steady state during water vapour permeation measurements is extremely long (see Figure 33, lag time). A period as long as 3 weeks is needed to complete such a measurement. Therefore, for a quick assessment, a fast method like Helium permeability gives great advantage for quality control in industry.

The diagram in Figure 35 and Figure 36 show the time regimes for water vapour and Helium permeation measurements.

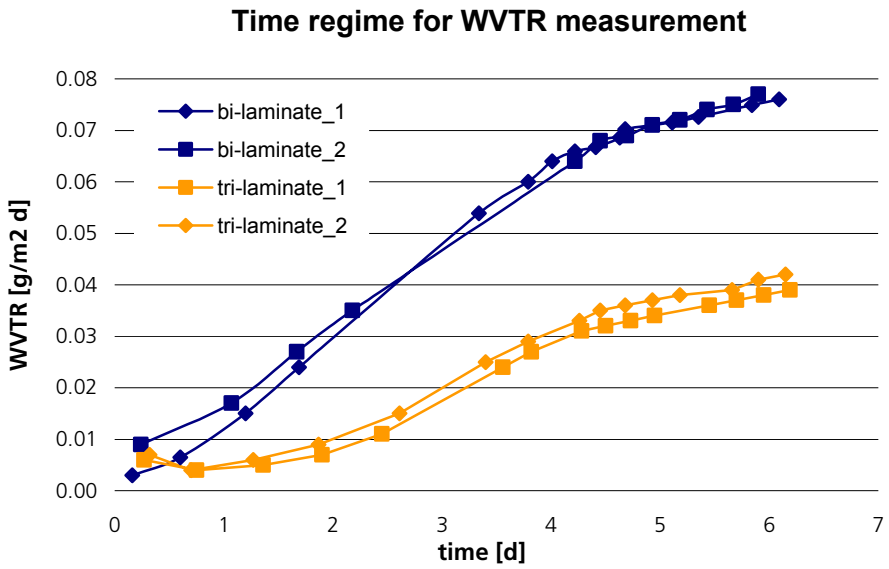

Figure 35: The time regime for WVTR measurements of a bi- (two metallized layers) and a tri-laminate product (three metallized layers). It takes more than five days for the permeation rate to reach equilibrium, i.e. the dissolution of the water in the polymer reaches saturation.

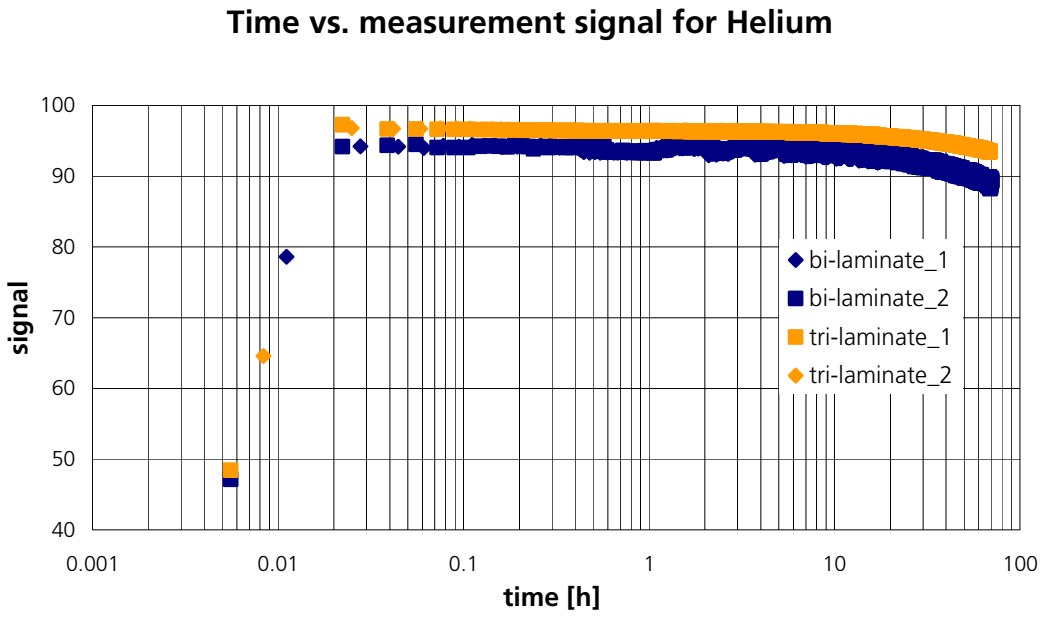

Figure 36: The measurement signal vs. time regime for Helium.

One of the problems of the helium permeability measurements is the minimum measurement limit. To overcome this problem, the measurements were carried out at higher temperatures. To verify this approach, measurements were carried out at different temperatures with the same sample and the temperature behaviour was observed. The graphs with the ln of the transmission values for He and the inverse temperature (1/T, with T in Kelvin) shown below

are drawn according to the usual Arrhenius representation. The graphs for the two samples are shown in Figure 37 and Figure 38. The diagrams show a linear behaviour of the measurements at different temperatures.

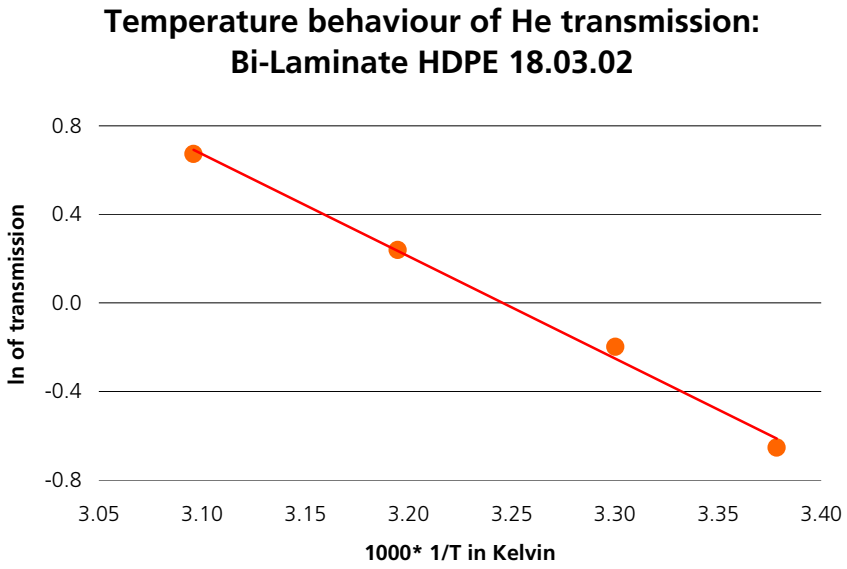

Figure 37: He transmission at different temperatures.

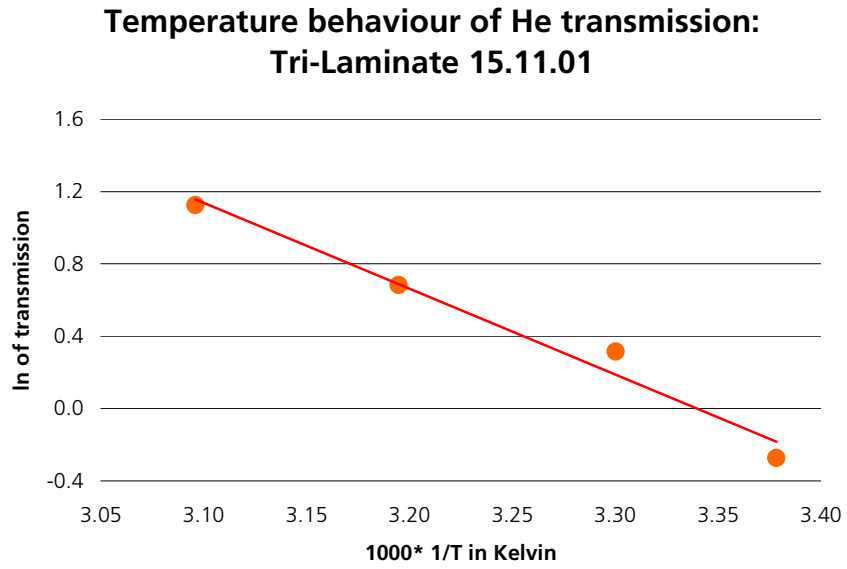

Figure 38: He transmission at different temperatures.

To establish the relationship between water vapour transmission rates and He transmission rates, measurements were carried out with identical sample pieces (sample size 10 cm x 10 cm). First the water vapour measurements were carried out at 38°C and 90% RH and then the He transmission values were measured at 23°C. In Figure 39 the relationship is

shown for the different laminate types. In each case two samples were examined. No significant experimental differences were seen for samples of the same laminate type.

The good correlation of Figure 40 shows that for well-defined samples, the Helium permeability measurements can be a good and fast method to predict the water vapour transmission.

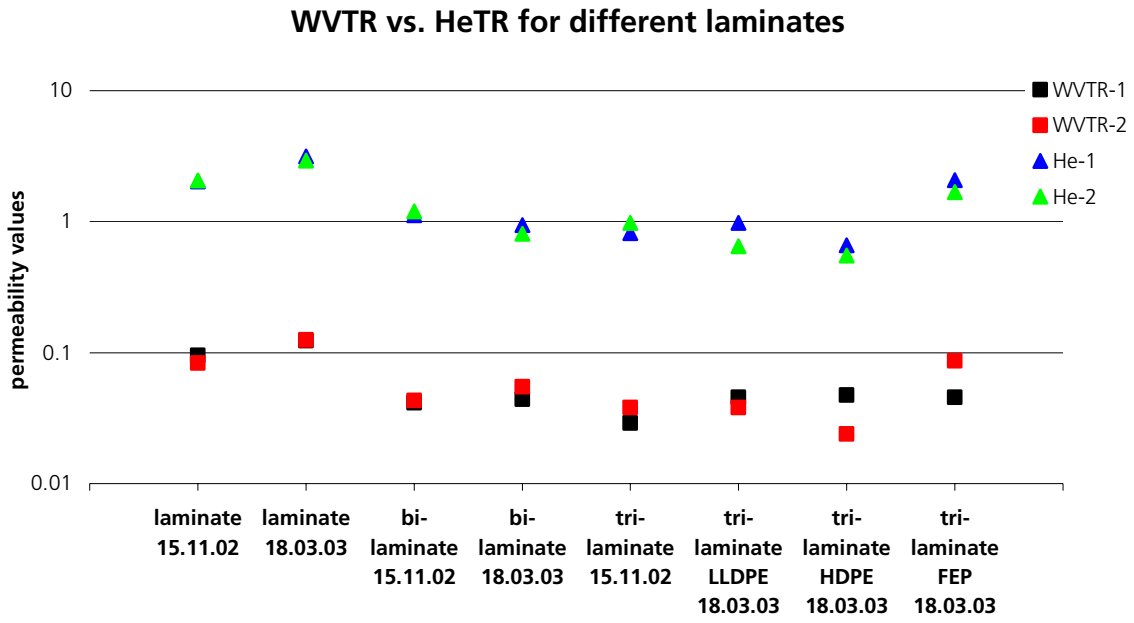

Figure 39: WVTR vs. He transmission rates for different samples.

In the following figure the correlations between Helium and water vapour transmission rates for a laminate, a bi-laminate and a tri-laminate are shown. The x-axis shows the values for the water vapour permeation and the y-axis shows the values for the Helium permeation. A logarithmic plotting is used.

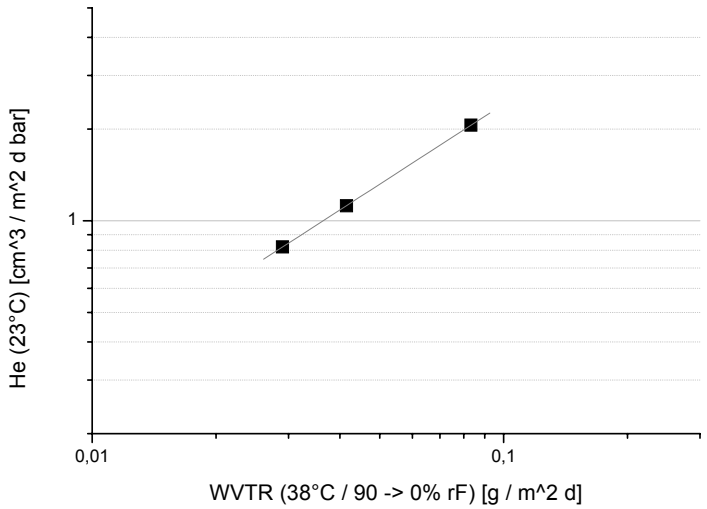

Figure 40: He values against WVTR values.

In order to understand the effect of aging on the permeability of the films, 6 batches of bi-laminates were kept for 4 weeks at 65°C and 75% RH. These conditions are also used in chapter 4 (aging of whole panels). The water vapor transmission rate values of the samples were measured before and after aging. Measurements at different conditions were carried out; at 23°C and 85% RH. and also at 38°C and 90% RH. As expected, higher values were observed for the measurements at higher temperature.

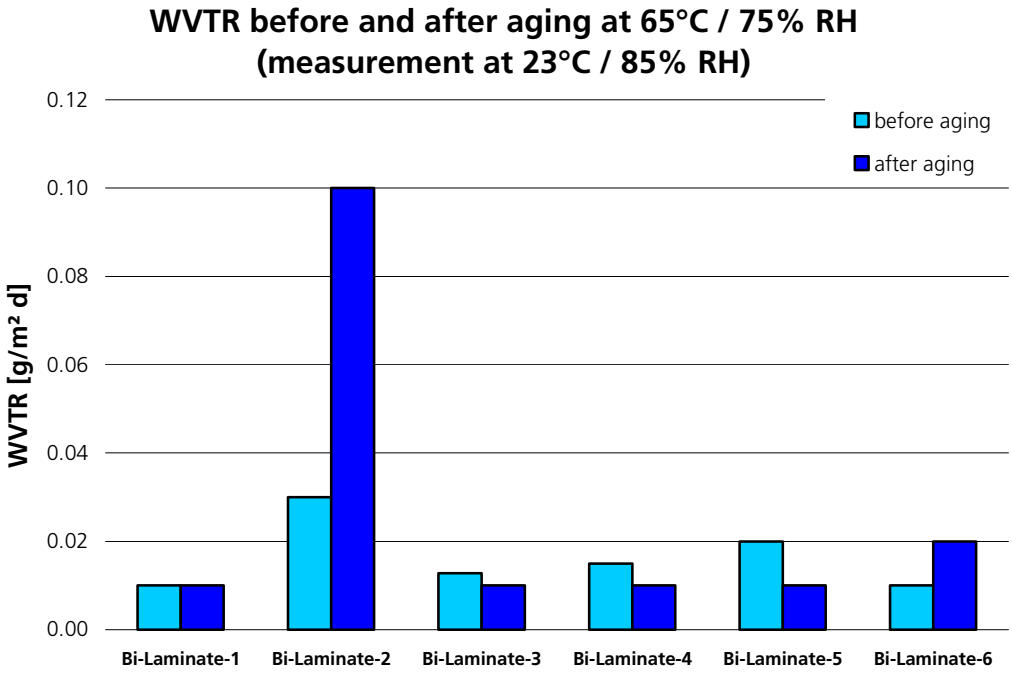

Figure 41: WVTR values measured before and after aging at 23°C and 85% RH.

After the aging process the water transmission rates were measured again at 23°C and 85% RH and also at 38°C and 90% RH. Through the aging process there was not a big effect recognizable on the permeation behaviour of the film samples (the difference in most cases was less than a factor of 2).

Interpreting these results it has to be considered that for the measurements before and after aging different samples were used and so it is possible that in some cases there was a pore or an other defect in the used sample part. The measurement limit is at 0.01 g / (m² d), when results are next to the measurement limit it is possible to observe bigger fluctuation.

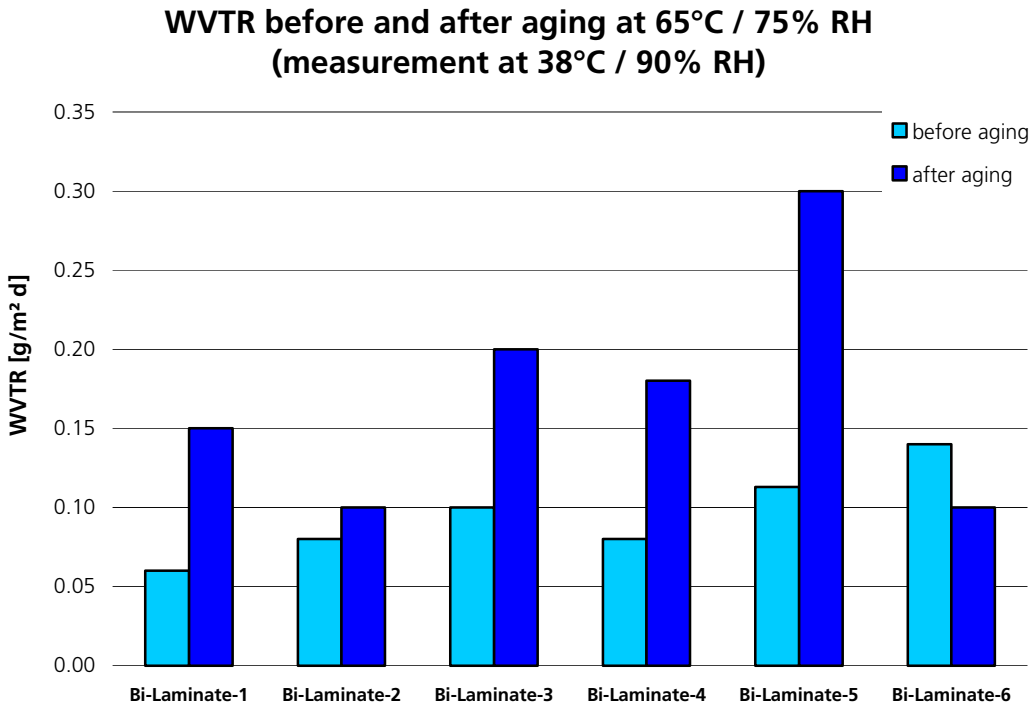

Figure 42: WVTR values measured before and after aging at 38°C and 90% RH.

Another topic was the barrier measurements of film samples taken from produced VIP.

The schematic view of the VIP envelope is given in Figure 43 with the real dimensions. The square in the middle with the lines represents the inner filler material. The slightly bigger square is part of the bag, which covers the thickness of the inner filler material. The external black ring is the sealing. The circle is an example of a sample cut for permeability measurements (sample size 10 cm diameter).

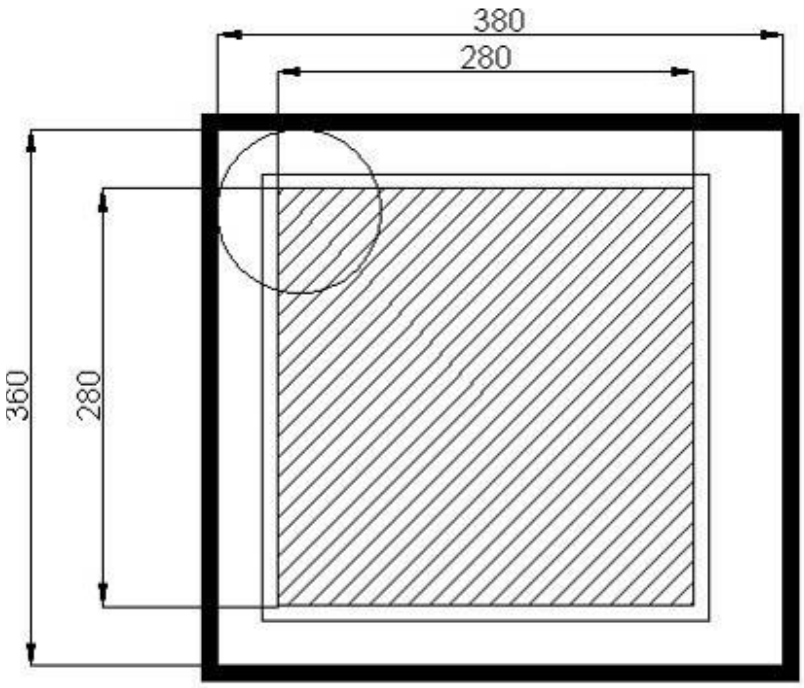

Figure 43: Schematic view of the VIP envelope (no core material inside).

For the permeability measurements, the envelope of each VIP was divided into three sections on each side; 1) corner, 2) flat surface, 3) edge. The samples do not include any seam. One side of the envelope was used for O_2 permeability (at 23°C and 50% RH) and the other side for WVTR (at 23°C and 85% RH) measurements. The regions where the samples were taken from each VIP for the permeability measurements can be seen in Figure 44.

O_2 permeability measurements **WVTR measurements**

Barrier material: Bi-Laminate 3

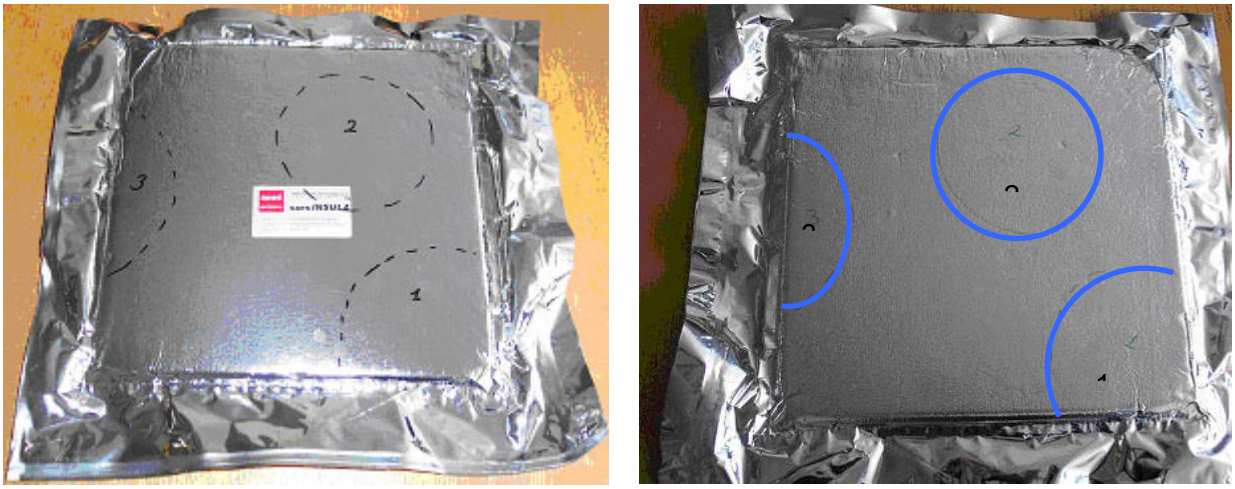

Barrier material: Bi-Laminate-6

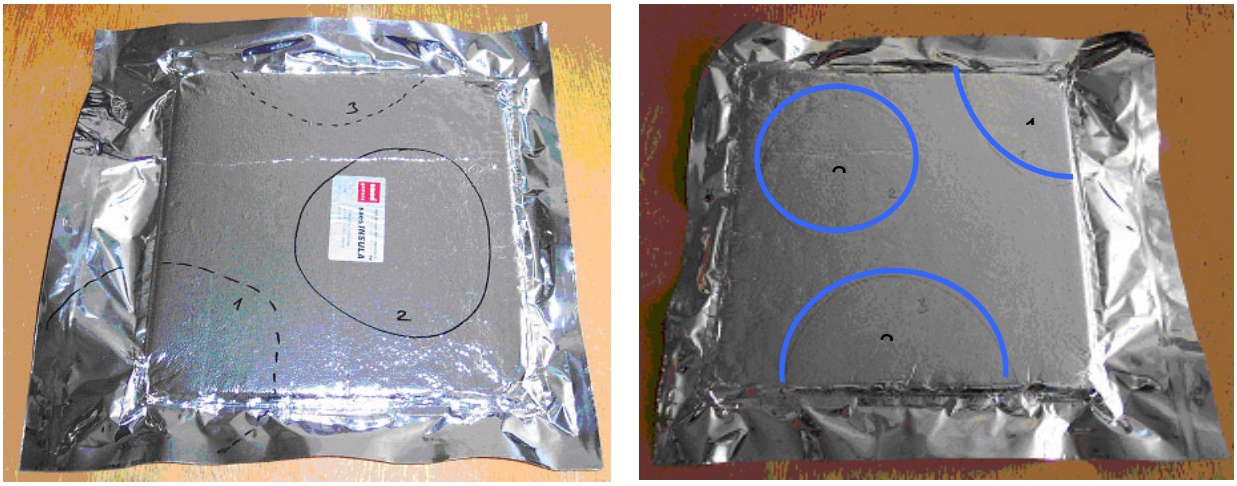

Figure 44: Sample preparation for the permeability measurements.

The O_2 permeability and WVTR values measured for the samples taken from the VIP are given in Table 24. The samples were taken from the centre of the panels, edges and corners. The size of the samples were for OTR 50 cm^2 and for WVTR 80,6 cm^2. The WVTR values are measured by the standard measurement unit (electrolytic process, see section 3.2.6.2).

Table 24: OTR and the WVTR values of the samples taken from the two VIP.

OTR [cm³/(m² d)]			
	1) Corner	***2) Surface***	***3) Edge***
VIP with Envelope 3	0.07	0.01	0.01
VIP with Envelope 6	0.07	0.02	0.04

WVTR [g/(m² d)]			
	1) Corner	***2) Surface***	***3) Edge***
VIP with Envelope 3	0.10	0.09	0.08
VIP with Envelope 6	0.10	0.09	0.07

The mean barrier properties of the samples of used films were not much affected by the VIP production process, except OTR of samples containing corners.

3.4.2 WVTR measurements (NRC)

NRC tested single and triple layer metallized laminate bags for the VIP production. The bags already had seams on three edges. From each type, six circular test specimens (15 cm in diameter) were used for vapor permeance tests according to ASTM Standard E 96. The results can be found in the Appendix. To enhance the limit of the mentioned method, dry cup measurements were done at 90% RH in the chamber. Even though the precision obtained is excellent, the results are too high compared with the results obtained by the electrolytic process (see above) or by weighing aged panels (4.4.3.2). It has to be concluded that the dry cup method can not be used for determining the WVTR of VIP envelope laminates.

3.5 Development of a new barrier measurement unit

For the objective of building an ultra-permeation measurement unit (UPA), a modification of a gas chromatograph is used. The outline of such a measurement system has been developed in the course of the project. The schematic diagram of the instrument is shown in Figure 45 and a picture of the system is given in Figure 46.

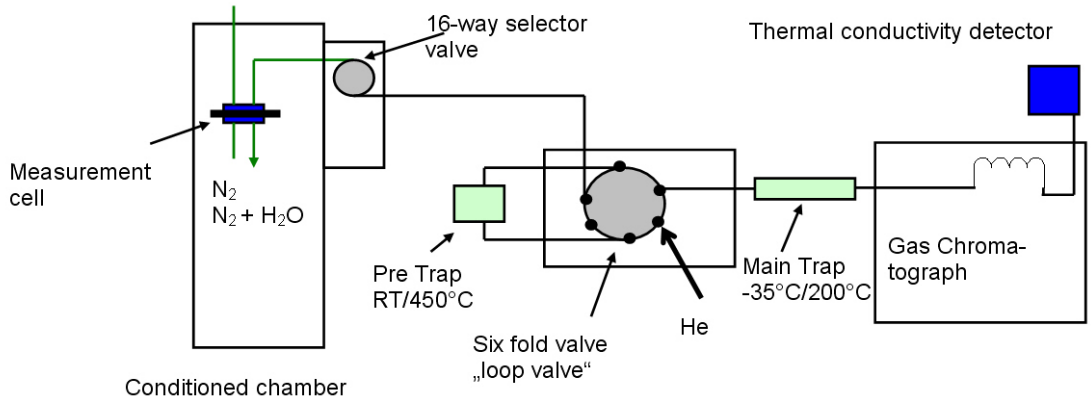

Figure 45: Schematic diagram of the ultra permeation measurement unit.

Figure 46: Ultra permeation measurement unit.

The main features of the ultra-permeation measurement unit are the following:

- The test sample is in a defined measurement cell (area 191 cm^2) placed in a conditioned chamber. One side of the film is flushed with a gas flow of defined humidity grade. The backside is faced to a dry nitrogen flow.
- During the measurements, the water vapour permeating through the film is taken up by the nitrogen gas and accumulated in a pre-trap for about 20 minutes. The pre-trap is filled with hygroscopic material and works at room temperature. In a next step the adsorbed water is transferred into an analytical trap with He gas by thermal desorption at 450°C. The trap is also filled with the adsorption material and the water is frozen to solid state at -35°C. By thermal desorption at 200°C the adsorbed water is transferred to a chromatographic column and quantified by a thermal conductivity detector. By a thermal conductivity detector it is possible to detect 10^{-9} grams of water. By adjusting the accumulation time in the pre-trap, the detection limit can be adapted. Via extrapolation to one day and

to the dimensions of the measurement cell, theoretically a transmission rate of 3.8 x 10^{-6} g / m^2 d should be attainable. However, at these very low water vapour concentrations the peak shown in the chromatograph usually does not have a regular shape (tailing is observed). The lowest transmission rate value that is measured so far by the unit is in the order of 10^{-4} g / m^2 d.

- The measurement period is defined by the amount of the permeated water and the time to reach the steady state. Due to the lower amount of permeating water, longer measurement times are to be expected.
- In order to calibrate the measurement unit, a known amount of water is injected into the system and the injected water follows exactly the same route that the permeating water vapour follows during a real permeability measurement (Figure 47). The number of counts measured by the gas chromatograph is then related to the amount of water that is injected to the system. Figure 48 shows a typical calibration chart. The y-axis represents the number of counts measured by the gas chromatograph and the x-axis represents the amount of injected water into the system. As it is seen in the graph, the number of counts increases linearly as the amount of injected water increases.

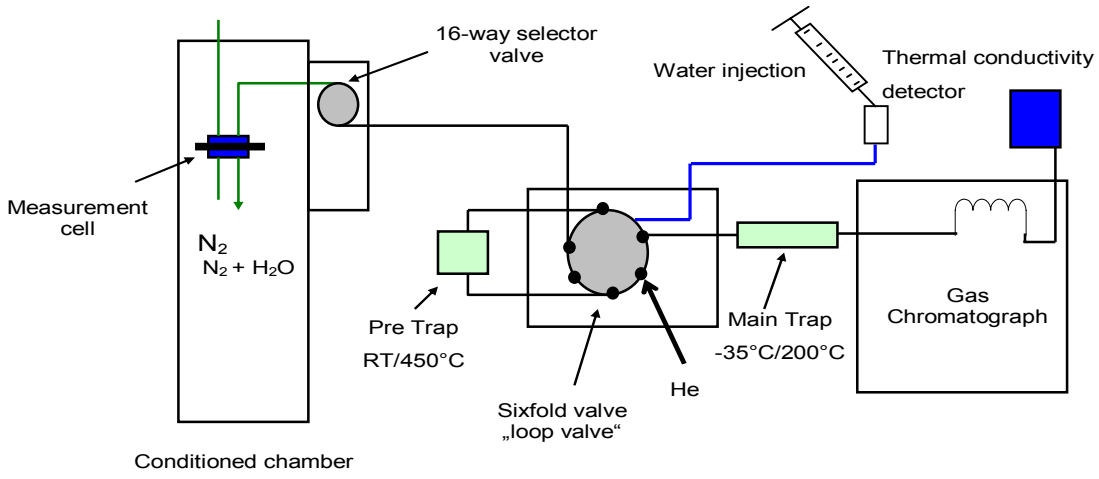

Figure 47: Injection of water to the system for calibration.

- During the water vapour permeability measurements, the number of counts is read from the gas chromatograph and Figure 48 is used in order to convert the number of counts to the total amount of water in grams. The water vapour transmission rate is then determined by extrapolating the accumulation time to one day and also by taking into consideration the area of the measurement cell.

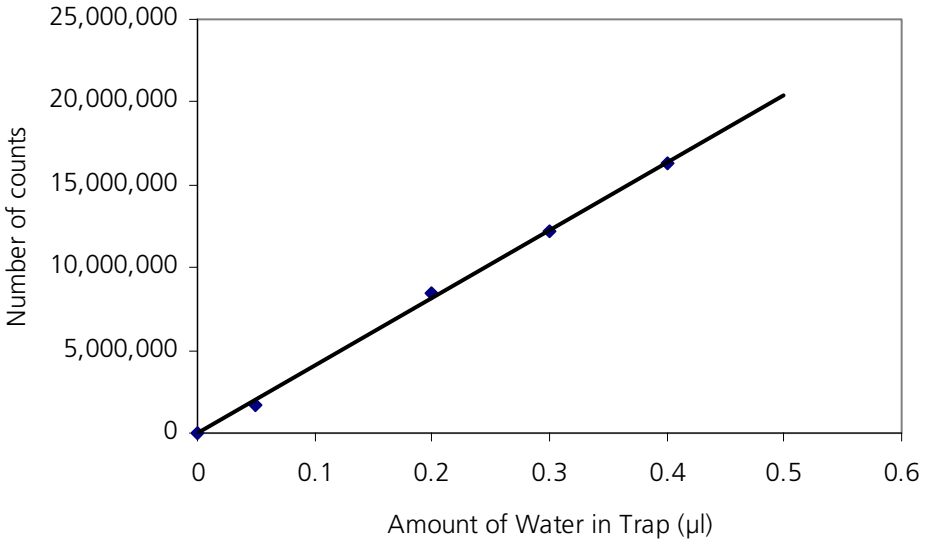

Figure 48: Calibration chart (Number of counts vs. Amount of trapped water).

To be able to evaluate the new measurement concept, industrially manufactured standard polymers were also examined. The experimental results obtained by the new unit were compared with those measured by the standard electrolysis measurement system. The measurements with the electrolysis system were carried out at 23°C and 85% RH and the measurements with the new system at 23°C and 100% RH. The good correlation between the values show that the results from the new system are reliable.

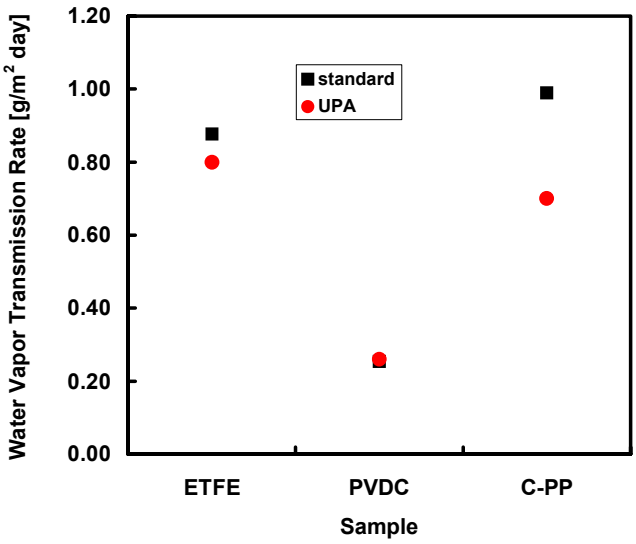

Figure 49: Comparison of the water vapour transmission rate measurement results obtained by the two systems: Standard measurement system and the new ultra permeability measurement unit (UPA).

A measurement of a film sample from a Japanese producer; TOYO, was also carried out. The structure of this sample is PA (15µm) / metallized PET (12 µm) / Al (6 µm) / PE (50 µm). TOYO reports a value much lower than 0.5 g/m².d for the water vapour transmission rate of this sample. As it is seen in Figure 50, very low values can be measured with the new ultra-permeation unit.

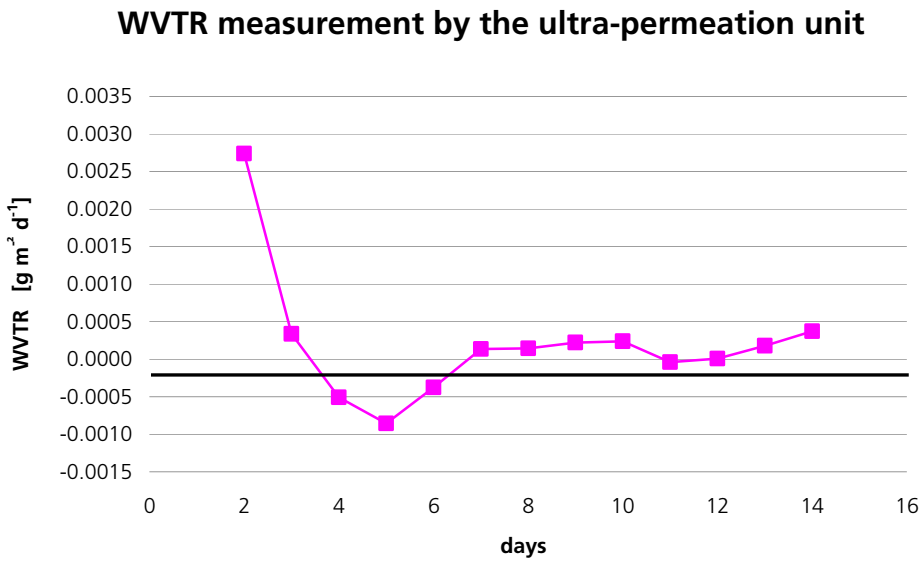

Figure 50: WVTR measurements of the TOYO film with the ultra-permeation unit [23°C / 100% RH].

Even though the existing prototype is good enough to measure the targeted water vapour transmission rate values, it is believed that the upgraded version of the existing prototype will be quite expensive for the industry. Moreover, when the barrier materials have very low water vapour transmission rates, the experimental time necessary to reach a steady state is extremely long. Most of the times, a time as long as 3 weeks is needed to complete such a measurement. Due to these reasons, investigations on the He permeability of the film materials were performed and for some of the metallized films, a correlation was found between the water vapour and helium permeability (Figure 39 and Figure 40). Therefore from the industrial point of view, a fast method like He permeability can be a more desired tool as an alternative for a quicker assessment and also quality control.

3.6 Summary "Envelope"

A measurement tool for water vapour transmission rates with a measurement limit of 10^{-5} g/m² d^{-1} has been developed. It has been shown that due to physical reasons, barrier films with a very low permeability require a measurement time of several weeks until they reach the lag time of the water vapour transmission. Therefore a correlation between WVTR and HeTR has been established, because He due to its smaller molecular size has a higher diffusion coefficient and therefore the measurement time is much shorter. However, each laminate or stack of layer has its own characteristic correlation. In industrial production the correlation has to be determined for each kind of laminate or layer stack once and then the same correlation can be used for the whole product line.

Edges and corner effects on the WVTR and the OTR in VIP have been determined and they have been found to be much lower than expected.

4 Panels

4.1 Introduction

4.1.1 Panel production technology

The panel production process is basically a standard evacuation and sealing process applied to the barrier bag containing a pressed and dried fumed silica board that is often enclosed in a permeable fleece envelope. The bag is formed either by four seams around the perimeter or by preparing a tube with one seam and two seams at the two remaining open sides (Figure 51).

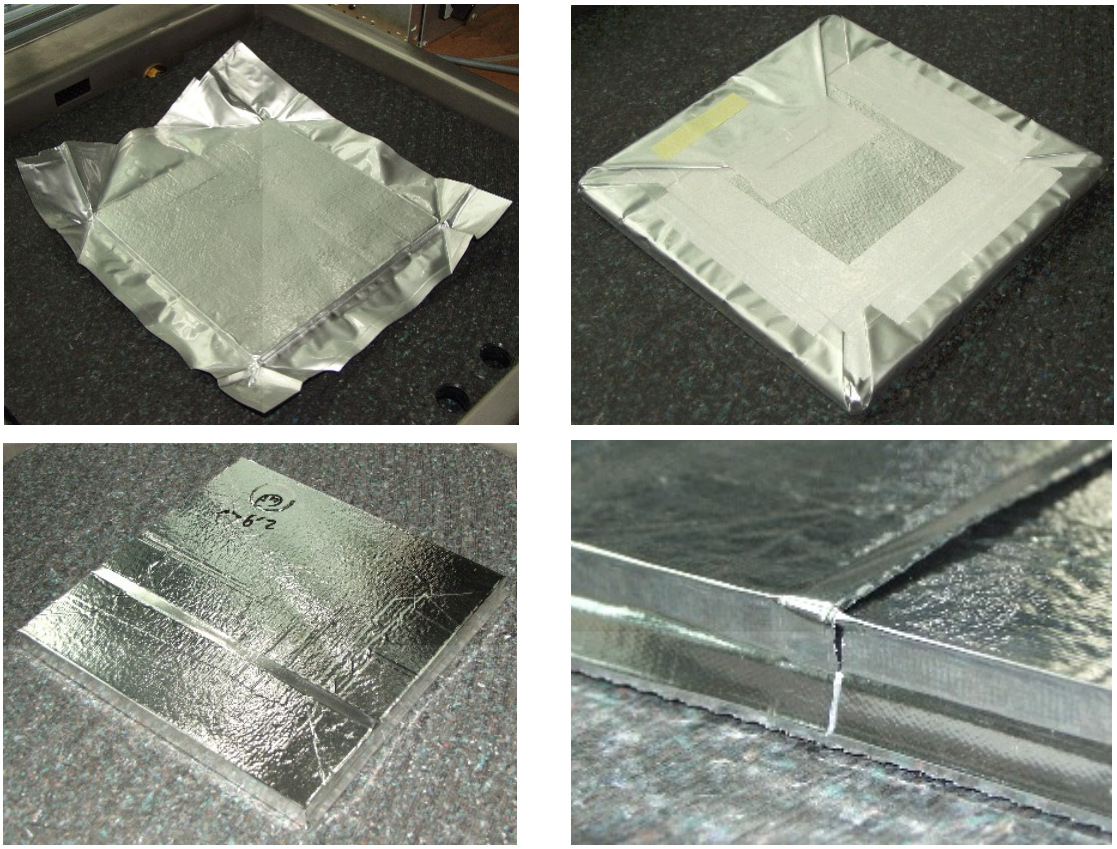

Figure 51: Two types of VIP packaging technologies.

Sealing is performed by heat-welding the PE layers at the open side(s) of the bag while the pressure in the depressurization chamber is maintained at a few tenths of a millibar. In order to end up with a rectangular board the parts that stick out of the envelope have to be wrapped and fixed on one face of the panel. Whereas pre-welding, filling, evacuation and sealing

sealing of the bag is processed semi-automatically, wrapping or other finishing steps are presently done manually.

4.1.2 Aging and service life

In the present context "aging" is understood as an irreversible change of one (or more) properties leading to a degradation of relevant performance characteristics. Service life is the time between production and failure, which is related to approaching a certain end-of-life criterion of a defined performance indicator. Clearly the service life of an individual specimen is a random value. The service life of a population of individuals is often described by using a graphical representation called the bathtub curve (Figure 52). It consists of three periods: an infant mortality period with a decreasing failure rate followed by a normal life period (also known as "useful life") with a low, relatively constant failure rate and concluding with a wear-out period that exhibits an increasing failure rate.

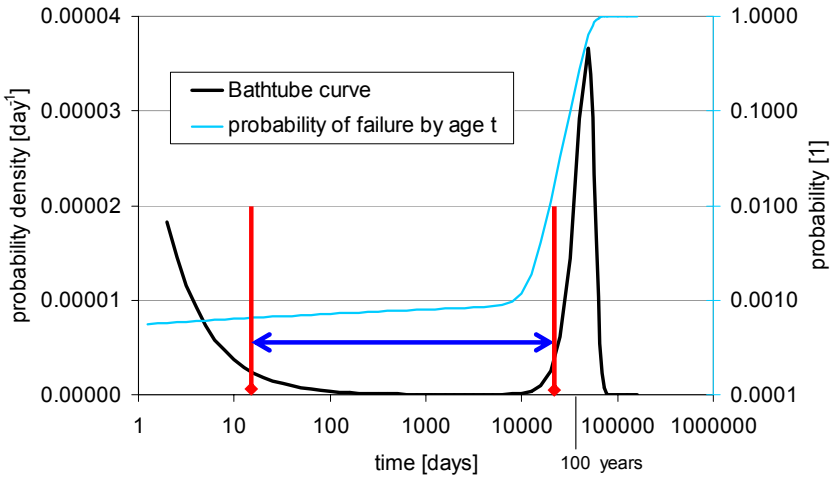

Figure 52: The Bathtub Curve describing the service life of a population population: Time vs. failure rate.

Failures during infant mortality are highly undesirable and are always caused by defects and blunders: material defects, design blunders, errors in assembly, etc. Normal life failures are considered to be random cases of "stress exceeding strength." Wear-out is a fact of life due to fatigue or depletion of materials or – in the VIP context – inevitable permeability of the envelope barrier.

Regarding infant mortality the best approach is generally to identify defects caused by manufacturing or material variations that can lead to failure and to take action to remove the root causes of these defects. While with conventional thermal insulation products early failure almost does not exist, process or material "errors" are often critical with VIP. Early failure caused by imperfect production frequently appeared in the first stage of VIP manufacture. Since then the early failure rate was strongly reduced due to improved process and quality control. Today the production failure rate for high quality products is presumably well below one percent. An effective measure is for instance the storage of freshly produced panels over a period of some 10 days before final control and shipping.

Another cause of early failure is mechanical damage of the delicate envelope during transport or installation, observed at several construction sites that were visited during IEA Annex 39. Therefore on-site installation of unprotected VIP is a really challenging task requiring specialists. To avoid this problem pre-fabrication of assemblies with built-in VIP is favourable.

Since the thermal resistance of the core under environmental pressure and moisture conditions is reduced by about a factor 5 the conservation of the initial low pressure and dry state inside of a VIP is the main concern when thinking of a long-term application in building. In the "normal life" period, pressure increase as well as moisture accumulation will take place due to slow permeation of atmospheric molecules through the barrier surface. The permeation rates will depend on the environmental temperature and humidity conditions as well as on the barrier properties. It is well known that sustainable high barriers can be achieved with massive metal layers having a thickness ~ 10 μm. In fact, VIP were made with PE laminated aluminium foils in this thickness range in the first stage of VIP production. However, thermal conductance measurements and numerical calculations [30] show that the heat flow through the edge of a metal foil envelope can be much larger than the heat flow through the entire VIP core volume. In order to reduce the thermal bridge problem, metallized polymer films are now widely used. To reduce the gas permeation problem specially developed laminated high barrier polymer based envelopes include up to three metallic layers with a thickness in the range of 30 - 100 nm each.

There is no standardised end-of-life criterion for this continuous aging process yet. If for instance the criterion is 100 mbar for the internal pressure of the dry core, then a dry gas pressure increase rate of 2 mbar per year would give a total service life of 50 years. Disregarding humidification of the core the thermal conductivity would change from initially about $4 \cdot 10^{-3}$ W/(m·K) to $6 \cdot 10^{-3}$ W/(m·K) after 25 years and ending with about $8 \cdot 10^{-3}$ W/(m·K) after 50 years. Another more application related criterion could be the centre-of-panel thermal resistance or thermal conductivity that could be in the range of 0.007 to 0.010 W/(m·K), depending on the demands given by the building design.

4.2 Properties and aging mechanisms

4.2.1 Envelope

In addition to chapter 3, general information about VIP barriers and aging mechanisms are briefly summarized here. As an example of an actual polymer based high barrier material for VIP the layer sequence of a laminate with three metallized layers is indicated in Figure 53. The envelope consists of three aluminized PET or PP films which are PU laminated. An additional PE layer towards the VIP inside is used to thermally weld two adjacent barrier sheets. Other laminates of metallized polymer films for VIP are produced, normally with 2 to 3 metallization layers.

For those types of multiple metallized polymer laminates, oxygen transmission rates (OTR) as low as 0.0005 $cm^3(STP)m^{-2}d^{-1}bar^{-1}$ at 23°C, 50% RH are found in manufacturer's declarations. An often used estimate for the nitrogen transmission rate is NTR ≈ OTR / 4. If this is valid the permeation behaviour with respect to air, weighted by the partial pressures of N2 and O_2, is well described by just the OTR times 0.4. Permeation of moisture is normally much faster compared to other atmospheric gases: a water vapour transmission rate (WVTR) for a high barrier of 0.005 $g/(m^2d)$ corresponds to a permeability of about 6 $cm^3(STP)m^{-2}d^{-1}bar^{-1}$, which is roughly 104 times the OTR in similar units. At present there is no final explanation for this large gap.

As indicated before the permeability values are not constant but increasing with temperature and/or humidity. This point will be addressed in more detail in the following subsections.

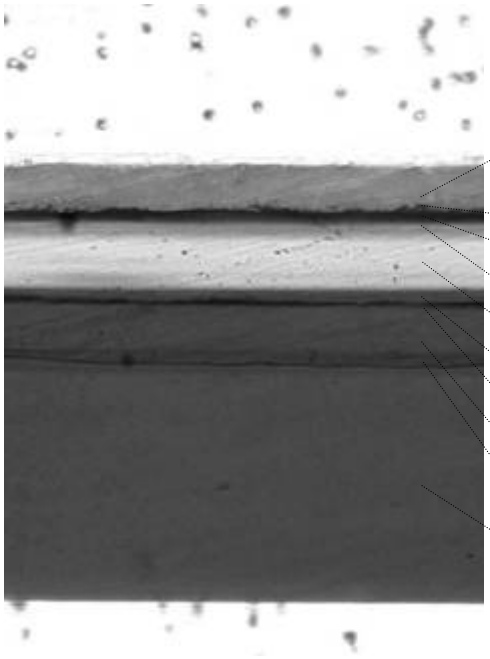

Layer #	Material	Function	Thickness
1	PET	Protecting layer (substrate for 2)	12 μm
2	ALU	Barrier layer	30 nm
3	PUR	Glue	2 μm
4	ALU	Barrier layer	30 nm
5	PP	Substrate for 4	18 μm
6	PUR	Glue	2 μm
7	ALU	Barrier layer	30 nm
8	PET	Substrate for 7	12 μm
9	PUR	Glue	2 μm
10	PE-LD	Sealing layer	60 μm

Figure 53: Visualization of a laminated polymer based high barrier envelope containing three aluminium barrier layers with an optical microscope (top and bottom areas are embedding material).

On a long-term scale, aging of all envelope components has to be taken into account. Because the metal layer is extremely thin (typically between 30 nm and 100 nm), a short survey check for the 50 years life is done here about the oxidation speed of aluminium. A fresh aluminium surface has a 1 nm oxide layer. This layer acts as an oxidation barrier and slows down further aluminium oxidation asymptotically up to a thickness of few tens of nm in contact with air.

Also a fully oxidized first layer can act as a barrier, as Al_2O_3 is also used as a barrier material [18] so that the second and third metallic layers have much lower oxygen exposure. Moreover, accelerated aluminium surface oxidation is primarily observed at high air humidity above 60 - 80% RH [19] and temperatures in a range of 80°C or above. Within these limitations, oxidation should not be critical in most building applications, as far as high humidity is not correlated with high temperature. Also the base level of moisture or water in the environment must be limited to pH-values less than 8.5 ([20],[21]), which should be considered particularly if concrete or other alkaline substances are present in the immediate vicinity.

PU layers may be subject to degradation by hydrolysis in contact with hot water [22]. Subsequent delamination of the barrier would clearly cause premature failure of a VIP. Delamination could be accelerated by interfacial H_2O condensation as well as shear stress from different hygro-thermal expansion properties of metallic and polymeric layers.

Concerning the polyethylene layer used for sealing the envelope, maximum service temperatures of PE-LD are given as 80°C for short-term and 60°C for long-term application when stabilized by phenolic antioxidants. For PET 130°C is permissible under long-term exposure [23]. Various stabilizers to prevent UV as well as thermal aging are available for each type of polymer [24]. PET is listed as quite UV resistant. If regular exposure to solar radiation in the application is foreseen, specially stabilized types are required. It should be noticed that short

high-intensity UV irradiation does occur during the plasma-treatment before metallization [25]. For this reason O_2 or Ar plasma is favourable [26]. Also PE as the most sensitive polymeric material in the VIP envelope was proven to be stable in a long-term building application by means of appropriate stabilization [27].

Addressing potential fracture of the barrier at low temperature, aluminium normally becomes more ductile with decreasing temperature. Polymers under normal circumstances, however, become brittle below the glass-rubber transition temperature. The combined effect in a laminated aluminium-polymer or a laminated metallized polymer film at the lowest temperatures occurring in the built environment (-20°C) results in fracture behaviour of the high barrier films that can be characterised as relatively ductile. This means that the lower limit of the service temperature is outside the range of application in buildings. Besides, the water vapour and gas permeation rate through the high barrier envelope decreases exponentially with decreasing temperature. So, in the lower temperature region, i.e. in cold climates, problems due to shortened service life are not likely to occur.

For all those reasons barrier materials should be carefully protected against moisture or even water from the environment, as well as against temperatures above an approved maximum service temperature. Occasional condensation can be accepted if drying is ensured. If these restrictions are taken into account the service life of a panel should not be limited by envelope materials degradation. However, it should be noted that there is no real life polymer aging data covering a life span of 30 or even 50 years. That is, some uncertainty remains concerning the integrity of envelope materials over time periods of this length.

4.2.2 Core

Within IEA Annex 39 all investigated VIP consisted of a fumed silica core. Detailed information on its properties are found in chapter 2. Below are some approximate relations for the core properties that can be useful to estimate panel characteristics. An approximate linear relation for the hygroscopic isotherm behaviour is:

$$s = \frac{dX_w}{d\varphi} \approx 0.08\%\text{-mass per \% RH} \qquad (17)$$

s: *slope of the sorption isotherm*
X_w: *moisture content, %-mass*
φ: *relative humidity,%*

The linear approximation is valid in the range up to about 80% RH For example, the moisture content at 50% RH is X_w ~ 4%-mass.

The influence of gas pressure and moisture content on the heat transfer in the silica core was discussed in detail in section 2.3. The following approximate linear relations describing the impact on the thermal conductivity may be used for practical estimates:

$$\frac{\partial \lambda}{\partial X_w} \approx 0.5 \frac{mW}{mK\ \%-mass} \tag{18}$$

$$\frac{\partial \lambda}{\partial p} \approx 0.035 \frac{mW}{mK\,mbar} \text{ in the range up to 100 mbar} \tag{19}$$

λ: thermal conductivity, W/(m·K)

p: "dry gas" pressure in the pores, mbar

Starting with an approximate initial thermal conductivity of about $4 \cdot 10^{-3}$ W/(m·K) for the dry core, the combination of (17) and (18) gives a value of about $6 \cdot 10^{-3}$ W/(m·K) for moisture equilibrium at 50% RH. And, according to (19), a pressure increase of 30 mbar results in a thermal conductivity increase of about $1 \cdot 10^{-3}$ W/(m·K).

Aging in terms of degradation of the fumed silica core at its own was not considered further as it is seen to be very stable in the temperature range occurring in building applications.

4.2.3 Panel

Since the thermal conductivity of the SiO_2 core is increased by about a factor 5 between low pressure (1 mbar) and standard atmospheric pressure (chapter 2), gas permeation through the envelope is clearly the most important aging mechanism of a VIP.

The penetration of atmospheric gases will give rise to a continuous pressure increase as well as accumulation of moisture in the hygroscopic core according to the sorption isotherm. Referring to the OTR of recent multi-layer metallized polymer barrier films a yearly pressure increase in the order of 0.01 to 0.1 mbar could be expected in a 1 x 1 x 0.02 m^3 panel. However, this is too simple for several reasons:

i) A typically non-linear increase of the permeation rates at higher temperature and/or humidity will accelerate the pressure increase. The temperature dependence of a permeation rate P for polymeric materials is often described in form of an Arrhenius acceleration factor:

$$P(T)/P(T_{ref}) = exp\left(-\frac{E_a}{R(T-T_{ref})}\right) \tag{20}$$

T: temperature, K

T_{ref}: reference temperature, K

E_a: activation energy, J/mol

R: gas constant, 8.31 J/(mol K)

High water vapour pressure surrounding a VIP is equivalent to a high pressure difference over the high barrier envelope, resulting in a high water vapour permeation rate through the foil. High humidity also influences the permeability properties of the barrier film with respect to water vapour permeation, which, however, is a very complex interaction and not yet completely understood. In a realistic model, the effects of temperature and humidity have to be combined e.g. by a parameterized Arrhenius function or in form of an Eyring model ([28]).

Therefore temperature and humidity conditions, under which a vacuum insulation panel has to operate, have a large influence on its service life.

ii) Increased permeance of the edge area - mainly because of a higher defect density at wrinkles, edges, corners and the seal - will result in higher panel permeance values than calculated just for the unstressed planar barrier area. This applies to both the main atmospheric gas components as well as water vapour. There is no evident analytic model to quantify the additional edge contribution to the total permeance. Therefore realistic service life estimates for VIP can hardly be derived from permeation properties of the envelope film, but must be investigated experimentally with assembled panels. As a consequence of different contributions from surface and perimeter size effects have to be taken into account.

iii) As indicated earlier, due to the relatively high moisture permeation through polymeric barriers the internal water vapour pressure will possibly approach equilibrium with the environment, which is typically in a range of 10 - 20 mbar. This pressure increase is in principle acceptable, but the corresponding average moisture content of the hygroscopic core in the range of 3 to 6%-mass will raise the thermal conductivity as described by Equation (18).

With the assumption that the effects of pressure increase and moisture accumulation can be superimposed independently, the change rate of the thermal conductivity of the core may be expressed as:

$$\dot{\lambda} = \frac{\partial \lambda}{\partial p}\dot{p}(T,\varphi) + \frac{\partial \lambda}{\partial X_w}\dot{X}_w(T,\varphi) \qquad (21)$$

$\dot{\lambda}$: *change rate of the thermal conductivity,* $\cdot 10^{-3}$ *W/(m·K·yr)*

$\dot{p}$: *pressure increase rate, mbar/yr*

$\dot{X}_w$: *moisture accumulation rate, %-mass/yr*

T : *Temperature,°C*

This is the basic relation that will be used in the subsequent section on service life prediction. For example, for constant $\dot{p}$ = 2.0 mbar/yr and $\dot{X}_w$ = 0.15%-mass/yr (neglecting saturation effects), the thermal conductivity after 10 years is approximately:

$$\lambda \approx (4.0 + 0.035 \cdot 2.0 \cdot 10 + 0.50 \cdot 0.15 \cdot 10)10^{-3}\, W/(m\,K) \qquad (22)$$
$$= 5.5 \cdot 10^{-3}\, W/(m\,K)$$

The impact of pressure increase and moisture accumulation on the service life of VIP will be discussed in section 4.5. There is a number of other properties that may be relevant in applications or during installation as well:

- Requirements on dimensional stability apply for most applications.
- Compression and compressive creep behaviour should be considered in load-bearing constructions.
- Flexural properties may be important for applications in sandwich panels or façade elements (c.f. Appendix).
- Minimum resistance to point load is required for handling and durability reasons.
- Resistance to chemicals is essential e.g. in contact with concrete or water solved chemicals. A more detailed discussion of requirements on testing and declaration of properties is found in section 5.

It is in general not possible to quantify the impact of an arbitrary combination of stresses and the service life of a VIP. On the other hand it is often possible to minimize additional mechanical and/or chemical stress factors to a large extent by appropriate construction design.

4.3 Experimental methods

4.3.1 General and specific test methods

In the field of conventional thermal insulation products, a large number of test methods is available (e.g. [29]). It is obvious to apply those methods where applicable, in order to get comparable performance properties as far as possible. Most of the test methods for dimensional and mechanical properties can be adapted without substantial changes. Also the thermal conductivity or thermal resistivity measurement methods are applicable as far as the conducting barrier envelope does not disturb the measured heat flow unintentionally. A non-standardized method is the determination of the pressure inside of a VIP. Those methods widely applied within this project are shortly described in the following paragraphs.

4.3.2 Thermal conductivity

The most important property is of course the thermal resistance or “thermal conductivity”, to be determined e.g. with a guarded hot plate (ISO 8302). However, since the sensitivity of the thermal conductivity to slight pressure changes is weak, this method is rather inappropriate to quantify gas permeation effects on an undamaged VIP. It should also be taken into account that the thermal resistance is influenced both by pressure increase and moisture accumulation in the silica core.

As an example, Figure 54 shows a sketch of the guarded-hot-plate apparatus LOLA V (ZAE-Bayern) for the determination of the thermal conductivity at the centre of the VIP.

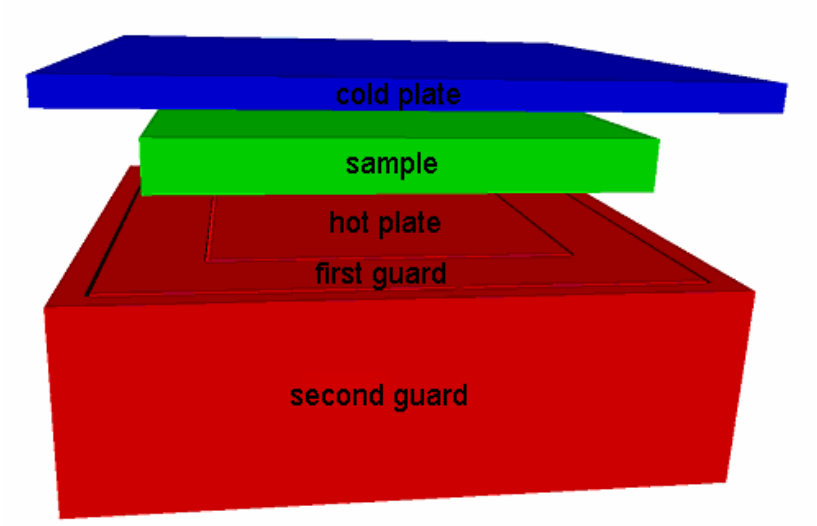

Figure 54: Device LOLA V (low lambda) for measuring the thermal conductivity; the guard system secures a one-dimensional heat flow through the sample. The sample is somewhat larger than the guarded area and provides, due to its extremely low thermal conductivity, the best possible lateral thermal insulation.

The thermal conductivity measurements are performed under stationary conditions. The quadratic heating area A is heated electrically with a constant heating power Q and is kept at the temperature T_h on the warm surface. The temperature for the interior and exterior guard are controlled in order to prevent a lateral or downward heat flow. The temperature of the cold plate is kept at the temperature T_c. Thus, the thermal conductivity λ of a sample of the thickness d can be calculated, according to the Fourier law:

$$\lambda = \frac{Q \cdot d}{A \cdot (T_h - T_c)} = \Lambda \cdot d \qquad (23)$$

Λ: *heat transmission coefficient of a sample with thickness d in the region of the central hot plate.*

With this guarded hot plate system the thermal conductivity at the centre of the VIP (effects of the edges are prevented by the two guards) can be derived with an uncertainty of about 5%.

4.3.3 Internal pressure

Rise of the internal pressure and accumulation of moisture in the core material are the two primary aging effects influencing the long-term heat resistance and hence the service life of VIP. Whereas moisture permeation can easily be measured just by weighing, a common method for the measurement of the internal pressure does not exist. A depressurization based method has been successfully applied by ZAE-Bayern, EMPA and NRC: the pressure around a VIP specimen is continuously reduced in a vacuum chamber. In Figure 55 the

envelope laminate lift-off procedure is depicted. If the pressure in the chamber diminishes to below the VIP pressure, the VIP envelope lifts off the core surface. This can be recorded visually or by using photo electric sensors. At EMPA the distance of the envelope surface is continuously measured with one or more laser distance meters at fixed locations on the VIP surface as a function of the chamber pressure. The "equilibrium pressure" is subsequently determined by analysis of the distance curve with an accuracy of about 0.3 mbar plus 5% (Figure 56), taking into account that the detachment behaviour may be influenced by local effects to some extent.

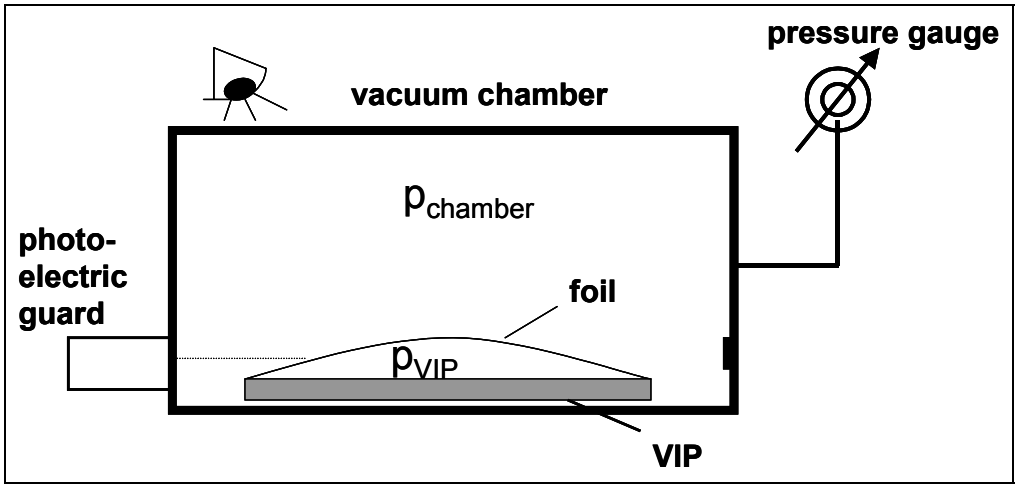

Figure 55: Sketch for the envelope lift-off procedure [35].

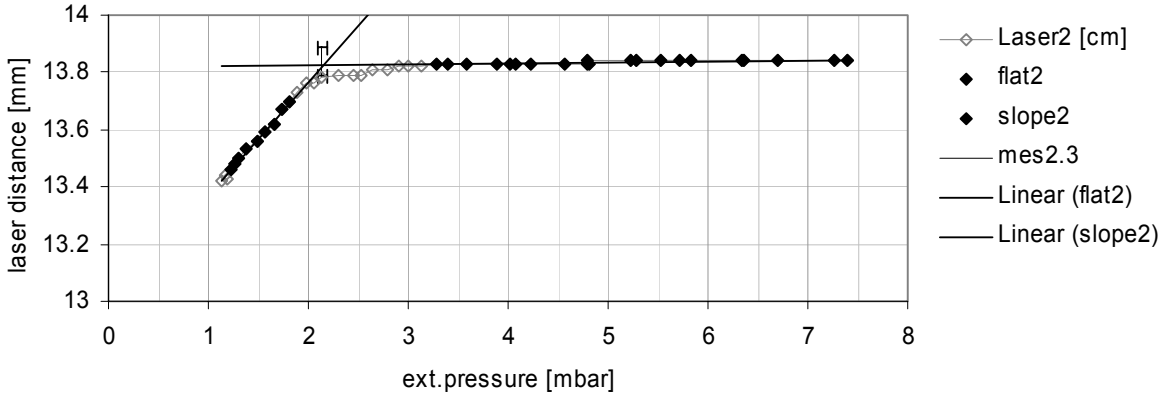

Figure 56: Determination of the internal pressure at EMPA. The pressure of detachment is identified in the distance-pressure diagram (b) as the intersection of the two linear portions of the distance function. Below the intersection the VIP is expanding.

4.3.4 Accelerated aging

In the framework of this project „accelerated aging" was performed in the sense of speeding up gas penetration through a VIP envelope by exposure of panels to higher temperature and/or humidity loads compared to typical ambient conditions in an application. That is,

acceleration was restricted to system degradation in terms of pressure increase and moisture accumulation. Referring to 4.2 actual chemical or hygro-thermal degradation of barrier materials was not investigated and is therefore not included in the lifetime projections that are based on temperature – humidity driven aging experiments on the time scale of a few weeks to months.

Also potential effects of combined hygro-thermal-mechanical stress was not investigated within this project, since mechanical stress besides the static atmospheric gas pressure is thought to be largely avoidable in VIP applications. A reasonable static mechanical load perpendicular to the main faces e.g. in floor applications is not expected not affect the service life significantly.

However, cyclic or dynamic hygro-thermal stress variation normally occurs in building applications, which is not really accounted for in static climate chamber exposure. Although some few experiments were done with cyclic conditions, collection of real life aging data from different applications are very important for the correlation with and validation of laboratory based aging and service life prediction calculations.

4.4 Experimental results

4.4.1 EMPA

As heat and moisture loads are always present in buildings, aging experiments at EMPA were focused on elevated temperature and humidity. The specimens, typically with a size of 250 x 250 mm^2 (“small”) and 500 x 500 mm^2 (“large”) and a thickness of 20 mm, were recent VIP products on the European market. Properties of the two investigated polymer based barriers are listed in Table 25.

To check the impact of a wide range of conditions, a first series was performed on small VIP at the manufacturer-declared maximum service temperature of 80°C, applying a relative humidity of 80% at the same time (80°C / 80% RH). The barrier material was MF3, a three-fold metallized polymer laminate produced in 2002. For comparison, cyclic conditions and 80°C exposure at ambient vapour pressure were also investigated. Subsequent tests were performed at 30°C / 90% RH, considered to cover a reasonable range of applications.

Table 25: Polymer based laminates used in the aging tests (WVTR values converted from 38°C, 90% RH) at 23°C, 50% RH, as indicated by the manufacturers.

Label	Layer sequence	OTR $cm^3(STP)/(m^2\ d)$	WVTR $g/(m^2\ d)$
MF3	12 μm PETmet / 18 μm PPmet / 12 μm PETmet / 60 μm PE-LD	< 0.05	< 0.025
MF4	12 μm PETmet / 12 μm PETmet / 12 μm PETmet / 50 μm PE-HD	0.0005	0.0025

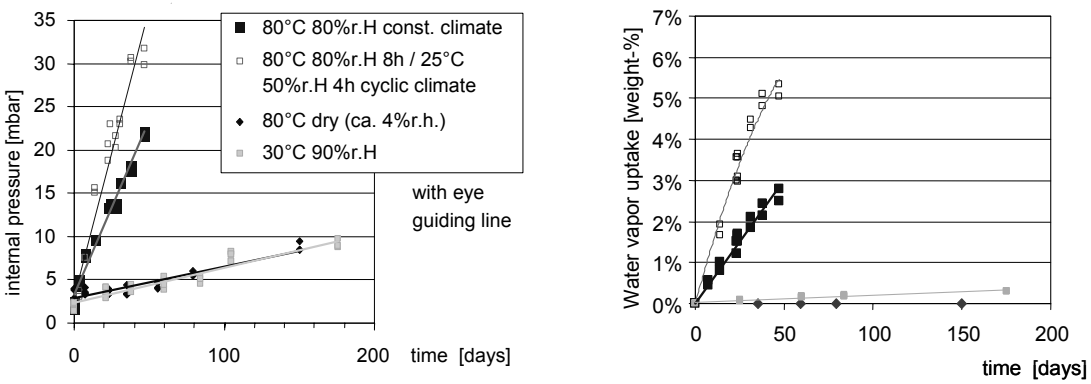

Figure 57: Increase of internal pressure (a) and moisture content (b) in "small" VIP at elevated temperature / humidity. The measurements were done at room temperature after cooling down the samples for some hours.

Results are summarized in Figure 57. At 80°C / 80% RH it is obvious that the pressure increase as well as the moisture accumulation is too fast for a long-term application. As can be seen in the figure cyclic conditions (8 hours at 80°C / 80% RH ↔ 4 hours at 25°C / 50% RH) are even harder than a constant 80°C / 80% RH exposure. Pressure and moisture content increase rates are almost doubled. Higher permeance under cyclic conditions may arise either from shear strain between polymer and metal layers due to a mismatch of thermal expansion properties, and / or by cyclic condensation of water on the “cold” VIP surfaces being delayed in temperature - humidity rise periods by the thermal inertia of the core material.

A clear correlation exists between the external vapour pressure and the extrapolated yearly increase rates of internal pressure and moisture content, indicating that the vapour pressure is a major driving force for the degradation. Another indication of the high moisture sensitivity is the behaviour at 80°C and low (ambient) vapour pressure: the pressure increase rate is much lower, but is still above 10 mbar/year (remember an acceptance range of about 2 mbar/year). The moisture content remains close to zero in this case. At 30°C / 90% RH the pressure increase rate is (by accident) quite similar.

The behaviour of 3 different products, each in two formats, was compared by continuous exposure to 65°C / 75% RH conditions (Table 26).

Table 26: Moisture content and internal pressure increase rates of VIP specimens in two sizes at accelerated conditions 65°C, 75% RH with different barrier materials.

	Size *[cm]*	**%-mass/year** extrapol. from 103 days	**mbar/year** extrapol. from 103 days
AF1	25x25x2	0.04% ± 0.01%	[3]
	50x50x2	0.02% ± 0.02%	[3]
MF3	25x25x2	7.1% ± 0.3%	63 ± 3
	50x50x2	5.5% ± 0.1%	38 ± 1
MF4	25x25x2	5.3% ± 0.5%	34 ± 5
	50x50x2	6.4% ± 0.4%[2]	19 ± [1]

[1] *4 samples of 25x25x2 cm^3, 2 samples of 50x50x2 cm^3 the only sample having stress on middle seam failed near 4% at 29 d and 73 d,*

[2] *Higher value than small size is hint to coming leakage at the middle seam, which occurred about 3 weeks after the 103d while stored at lab conditions.*

[3] *could not be detected.*

Product AF1 with a massive 6 μm aluminium barrier is very stable, regarding both the moisture content and the internal pressure. Product MF3 and product MF4 have basically a similar barrier, namely a 3-fold laminate of metallized polymer film. The metal layer thickness is about 30 nm (MF3) and 100 nm (MF4). While MF4 is more resistant to N_2 and O_2, both polymer based products are rather open to water vapour. The almost tripled aluminium thickness in MF4 does not block H_2O much better. Edge effects are also apparent from Table 26, as the rates depend on the format of the specimens.

Less severe, but non-negligible effects are detectable also for the more typical conditions 23°C, 50% RH, regarding both water uptake and pressure increase (Table 27). For those conditions the moisture accumulation rate is in the order of 0.1 mass-percent per year, and the pressure increase rate in the range of 1.5 mbar per year for the “large” format.

Table 27: Moisture content and internal pressure increase rates of VIP specimens in two sizes at standard conditions 23°C, 50% RH with different barrier materials.

	Size *[cm]*	**%-mass/year** extrapol. from 103 days	**mbar/year** extrapol. from 103 days
AF1	25x25x2	0.02% ± 0.01%	0.7 ± 0.1
	50x50x2	0.03% ± 0.01%	0.6 ± 0.2
MF3	25x25x2	0.15% ± 0.02%	3.3 ± 0.9
	50x50x2	0.10% ± 0.01%	1.8 ± 0.2
MF4	25x25x2	0.16% ± 0.01%	1.4 ± 0.6
	50x50x2	0.12% ± 0.01%	1.0 ± 0.1

From the tabulated data, size effects can be quantified by linking the permeation data for different formats. For example, perimeter and surface area related permeation rates Q_L and Q_A can be identified by means of measured data from at least two formats 1 and 2 by:

$$Q_1 = Q_L \times L_1 + Q_A \times A_1$$
$$Q_2 = Q_L \times L_2 + Q_A \times A_2 \qquad (24)$$

$Q_{1/2}$: *Measured rates for format 1/2*
$L_{1/2}$: *perimeter length, m*
$A_{1/2}$: *surface area, m^2*

In order to separate the pressure increase due to moisture accumulation, the following approximate relation may be used, providing hysteresis effects can be neglected:

$$\dot{p}_w = p_{sat}(T)\frac{d\varphi}{dX_w}\dot{X}_w = \frac{p_{sat}(T)}{s}\dot{X}_w \qquad (25)$$

p_{sat}: *saturation pressure (function of temperature T), mbar*
s: *slope of the sorption isotherm, see Equation (17)*

Based on these relations perimeter and area related permeation data for MF3 and MF4 have been determined from Table 27 for the conditions 23°C, 50% RH. (Table 28). The rates WVTR and ATR are separated transmission values for water vapour and dry air with respect to the area of the main faces. The permeation data for the typical panel format 1.0 x 0.6 x 0.02 m^3 are calculated from the perimeter and area related values.

In Table 28 it is seen that moisture permeation is quite similar with both barriers. The total yearly accumulation for the “standard panel” is about 0.1%-mass. The main part of the moisture permeation is through the main faces, but also the perimeter contributes to the overall value. Dry gas permeation gives a yearly pressure increase of about 1.0 or 0.5 mbar for MF3 or MF4 respectively. It seems that for MF3 the main part is due to the perimeter, while with MF4 the faces are more involved. However, the uncertainty is rather high as indicated in Table 27.

In general it can be concluded that the permeation values for both barrier types are in a range that is suitable for long-term application in construction assemblies.

Table 28: Perimeter (P) and area (A) related permeation data for barriers MF3 and MF4 at 23°C, 50% RH. The yearly rates for the format 1.0 x 0.6 x 0.02 m^3 are calculated values. "for 2 x A" stands for the permeation through the whole panel surface.

		MF3	MF4
WVTR (for 2 x A)	[g/(m^2 d)]	0.0075	0.0069
$WVTR_A$	[g/(m^2 d)]	0.0030	0.0048
$WVTR_L$	[g/(m d)]	0.0008	0.0006
ATR (for 2 x A)	[cm^3/(m^2 d)]	0.0660	0.0171
ATR_A	[cm^3/(m^2 d)]	0.0034	0.0087
ATR_L	[cm^3/(m d)]	0.0090	0.0018
Yearly rates (1.0 x 0.6 x 0.02 m^3)			
$X_{w,A}$	[%-mass/yr]	0.050	0.080
$X_{w,L}$	[%-mass/yr]	0.033	0.027
$X_{w,total}$	[%-mass/yr]	0.083	0.107
dp/dt_A	[mbar/yr]	0.12	0.32
dp/dt_L	[mbar/yr]	0.87	0.17
dp/dt_{total}	[mbar/yr]	1.00	0.49

4.4.2 NRC

Twelve 30 cm x 30 cm x 30 mm VIP were tested at the laboratory to determine the long-term thermal characteristics of VIP. After initial determination of thermal resistances, one specimen was found with faulty construction (specimen 1). Remaining eleven specimens were exposed to following conditions: Exposure to standard laboratory conditions (specimens 9 and 10); Exposure to laboratory temperature but high (about 90%) RH (specimens 4); Exposure to 32°C and 90% RH (specimens 6 and 12); Partially at 90% RH and then partially 32°C and 90% RH (specimens 3 and 8); 5 bar and 3 bar overpressure for 30 days (specimens 2, 5, 7 and 11). Details of the measurements can be found in the Annex.

The results obtained from the thermal measurements done on these eleven exposed specimens are shown in Figure 58. After two years these specimens were weighed and internal gas pressure of each VIP was measured. The results are shown in Figure 59.

Based on the information available from this investigations, the following observations can be made:

Environmental loads such as high relative humidity and higher than normal indoor temperatures produced only small effects on thermal resistivity of the VIP specimens.

Over-pressure may compact the VIP but did not accelerate clearly the aging by air intrusion during the exposure. Thus the laminate and seams appear to be very resistant towards the diffusion of air molecules.

The fumed silica core has large affinity towards water molecules. Therefore at the initial stages of water vapour diffusion majority of the water molecules that traverse the laminates and seams will be adsorbed by the core material and thus will delay any increase in the net pressure inside the VIP.

The technology used to make the seams prevents additional vapour diffusion paths across the seams.

In future work, it may be necessary to measure the net pressure rather than the thermal resistivity to follow the very slow ageing pattern shown by the VIP.

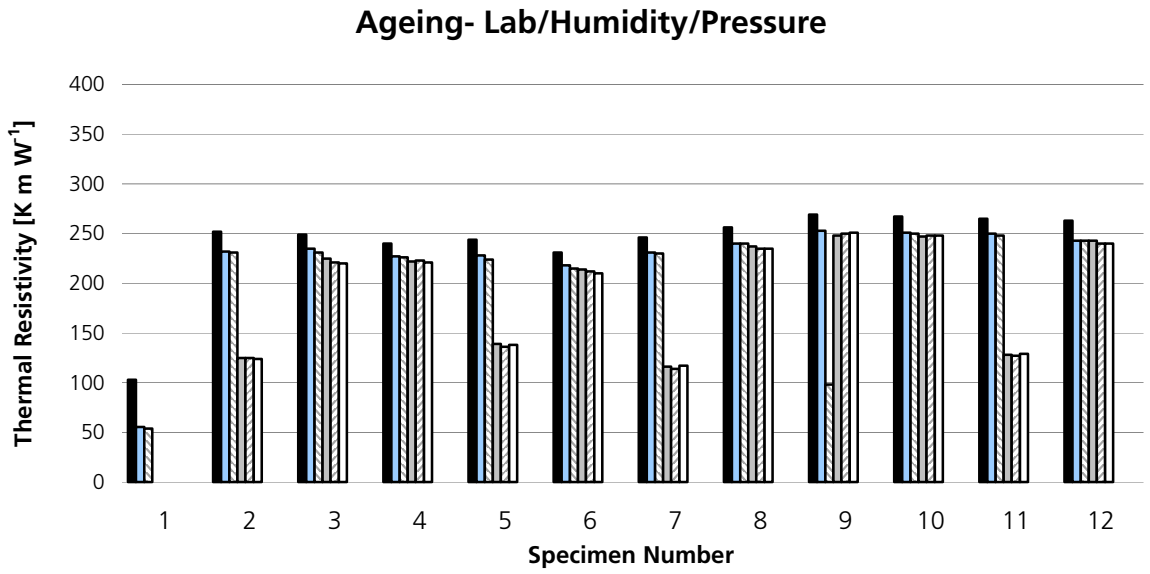

Figure 58: Initial and aged thermal characteristics of twelve VIP (see explanation in text).

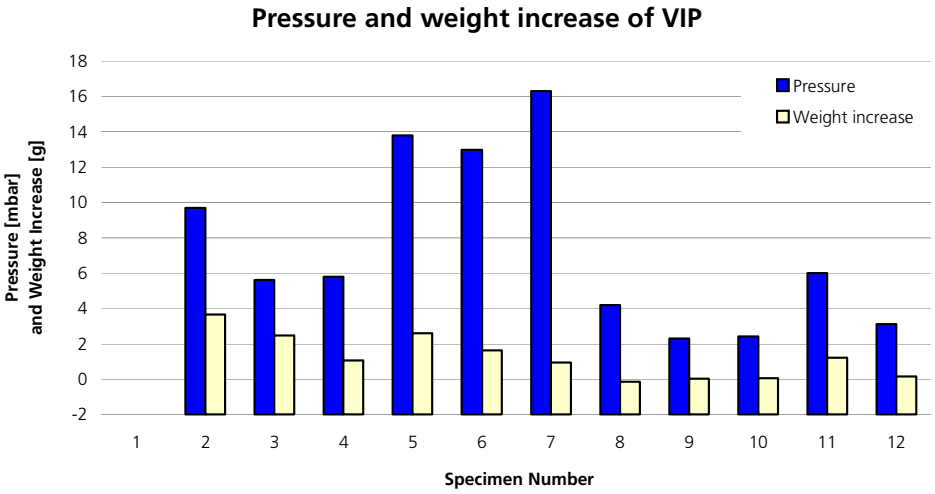

Figure 59: Internal gas pressure and weight change in VIP after two years.

4.4.3 ZAE-Bayern

4.4.3.1 Sample description and measurement program

Panels with three different laminate-envelopes were used for the tests: one laminated Al-foil (AF) and two Al-coated multi-layer films (MF1 and MF2). The measurement of the gas transmission rates were performed on VIP with fumed silica as core material. The transmission rate of air components was derived from repeated measurements of the internal panel pressure at about 20°C using the envelope lift-off procedure (see appendix). The reproducibility of the individual measurements was within ± 0.3 mbar. The water vapour transmission rate was determined from the mass increase by means of repeated weighing. The mass resolution was 0.02 g.

To determine the influence of temperature and humidity, six small boxes with temperature-controlled heating were produced. Three temperatures (25°C, 45°C and 65°C) were set. In three boxes a constant relative humidity of 75% was chosen, while the other three boxes had the same, unregulated partial water vapour pressure in accordance with the ambient air (in the laboratory room). A locally even distribution of temperature and humidity was ensured by using a fan. The panel size was (20 x 20 x 1) cm³. Into each box three VIP with foil AF, three VIP with film MF2 and one VIP with film MF1 were inserted. To be able to determine the influence of the panel size on the pressure increase, additional VIP of dimensions (10 x 10 x 1) cm³ (one VIP for each type of laminate AF, MF1 and MF2) were also used. In total, 60 panels were measured regularly throughout an overall period of approximately one year. The measurement conditions in the boxes are given in Table 29.

Table 29: Temperature and relative air humidity in the measurement boxes.

Box number	**1**	**2**	**3**	**4**	**5**	**6**
Temperature *[°C]*	25	45	65	25	45	65
Rel. humidity *[%]*	~ 45	~ 11	~ 4	75	75	75
H_2O partial pressure *[mbar]*	~ 14	~ 14	~ 14	24	73	187

In Table 30 the water vapour transmission rates (WVTR) and the oxygen transmission rates (OTR) of the laminates are given in addition to the manufacturer's details for the used material and layer thicknesses. For comparison, a laminated Al-foil (AF) was used, which, on account of the 8 µm-thick aluminium layer had the lowest transmission rates. The film MF2 had very low transmission rates, in comparison to other Al-coated films. MF1 was a low priced Al-coated film with high transmission rates.

Table 30: Laminate transmission rates according to manufacturer's specifications for the tested laminates. PET=PolyEthylenTerephtalate, PE=PolyEthylen, PP=PolyPropylen, LD=LowDensity, met=Al-layer 30 to 80 nm thick.

Name	**Laminate composition**	**OTR** *[cm³(STP)/(m²·d)]*	**WVTR** *[g/(m²·d)]*
AF[1]	12 µm PET / 8 µm Al / 100 µm PE-LD	< 0.0005 (25°C / 50% RH)	< 0.005 (20°C / 50% RH)
MF1	15 µm PPmet / 12 µm PETmet / 50 µm PE	0.07[2] (23°C / 50% RH)	0.1 (38°C / 90% RH)
MF2	20 µm PETmet / 20 µm PETmet / 25 µm PE	0.00062 (23°C / 75% RH)	0.005 (23°C / 75% RH)

4.4.3.2 Measurement results

Measurements of the pressure increase in the VIP stored within the air-conditioned boxes

Figure 60 shows the measured pressure increases for the VIP with laminates AF, MF1, MF2 and dimensions (10 x 10) cm² and (20 x 20) cm² stored in box 2 (45°C / 14 mbar). A linear pressure increase in time can be found. The pressure increases differ considerably depending on laminate type and panel size.

1 With laminated Al-foil, the transmission rates are generally lower than the threshold values of the standardized measuring methods. The values given here are threshold values of the measurement methods as defined by the American standard (ASTM F1249-30 and ASTM D3985-81 respectively).

2 According to manufacture information the low priced foil MF1 shows high variation in transmission rates. The given transmission rate represents an upper estimate. The real transmission rate may be much lower.

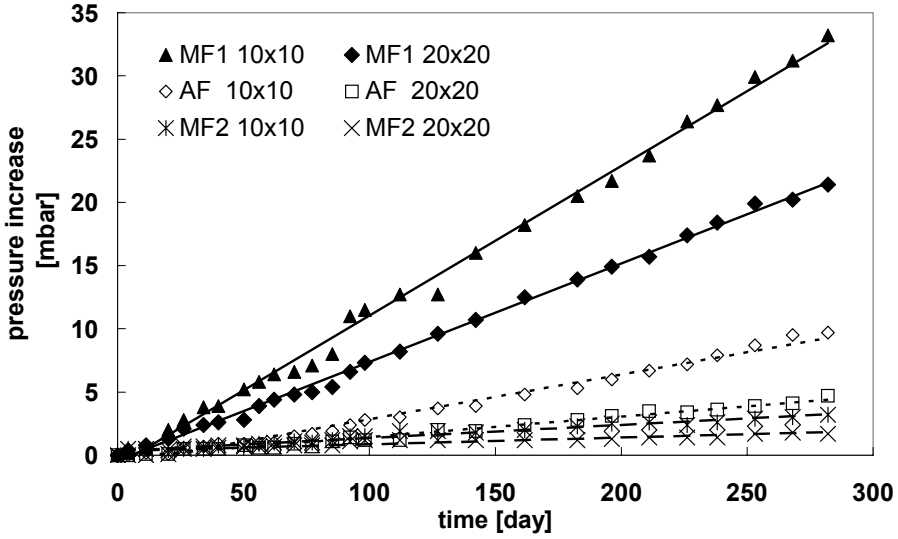

Figure 60: Measured pressure increase over time for VIP with panel sizes (10 x 10 x 1) cm³ and (20 x 20 x 1) cm³ and with laminates AF, MF1 and MF2 kept at 45°C / 14 mbar (H_2O); the measurement procedure is described in the appendix. Also shown are the corresponding straight line fits.

One can derive the mean pressure increase per year from the slope of the fit lines in Figure 60. The results for all measured VIP are summarized in the Figure 61.

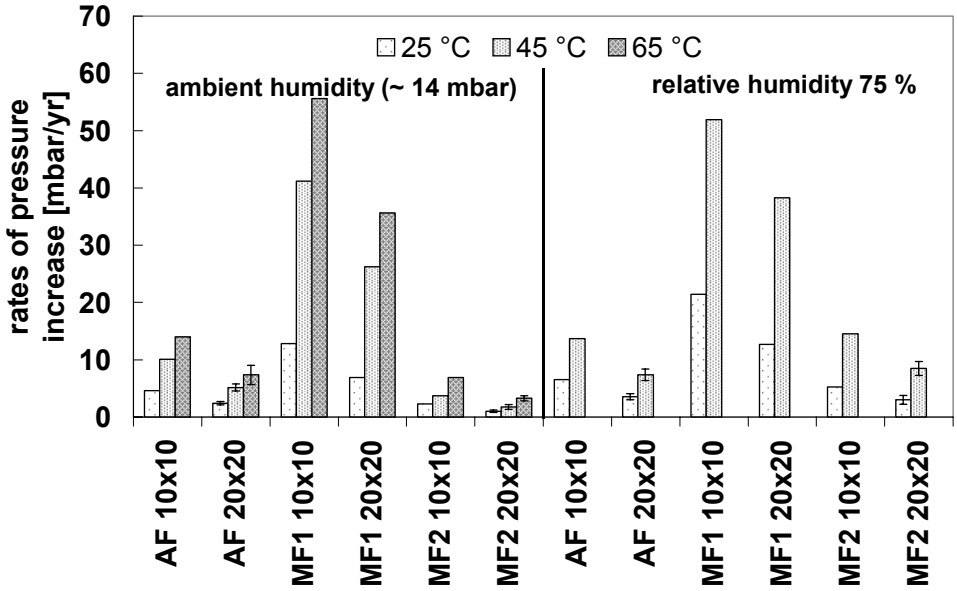

Figure 61: Determined rates of pressure increase within the VIP with the laminates AF, MF1 and MF2 stored in the air-conditioned boxes at 25°C, 45°C and 65°C (for the laminates AF and MF2 and the panel size (20 x 20) cm² the mean values and standard deviations are given). For the climate 65°C / 75% RH no values were given, as the majority of the panels with the laminates AF and MF2 failed (due to delamination) after a period of approx. a quarter of a year.

The most significant facts, that can be derived from Figure 61, are:

- VIP with different laminates show considerable differences in the rates of pressure increase. VIP with the film MF1 have the largest rates of pressure increase.
- The rates of pressure increase depend significantly on temperature.
- For VIPS stored in air with high humidity (75% RH) larger rates of pressure increase are recorded.

If the panel perimeter L is doubled, approximately one half of the rate of pressure increase occurs. This indicates, that for the laminates tested here, the pressure increase is mainly caused by the perimeter-related gas transmission rate.

Measurements of the mass increase of the VIP stored within the air-conditioned boxes

Figure 62 shows the mass increases over time for VIP with the laminates AF, MF1 and MF2 and dimensions (20 x 20 x 1) cm³ and (10 x 10 x 1) cm³ stored in the air-conditioned box 3 (25°C / 75% RH). A linear mass increase over time and a strong influence of the laminates types is observed. For VIP with the laminates MF1 and MF2 the (20 x 20) cm² panels show mass increases which are nearly three times as high as for the (10 x 10) cm² panels. For VIP with laminated Al-film, the mass increases are about one order of magnitude lower than for VIP with Al-coated films.

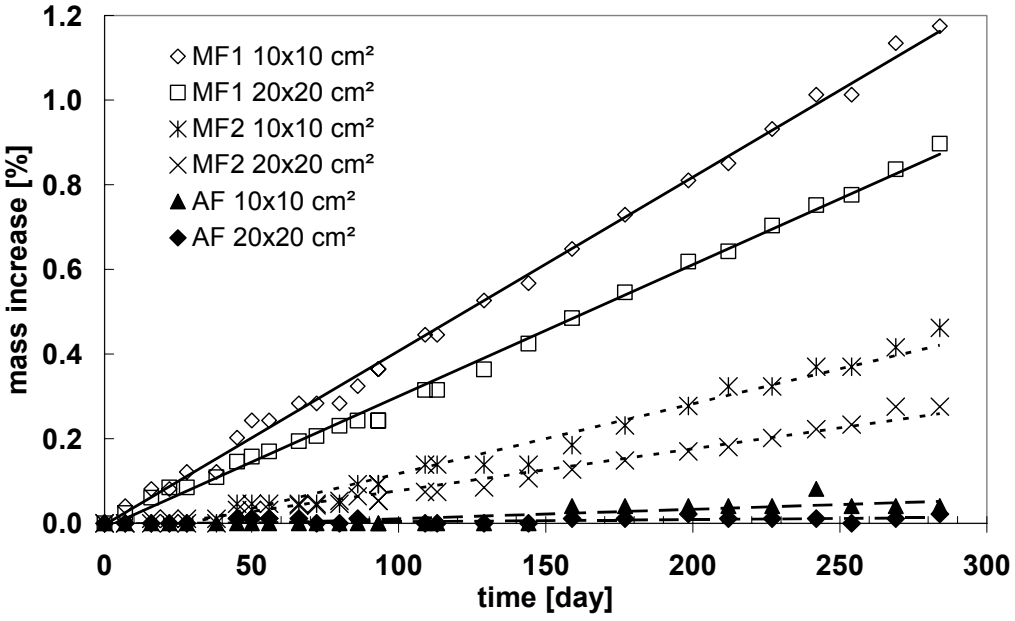

Figure 62: Measured mass increases due to water infusion over time for VIP with panel sizes (10 x 10 x 1) cm³ and (20 x 20 x 1) cm³, made with the laminates AF, MF1 and MF2 and stored in the air conditioned boxes at 25°C / 75% RH. Also shown are the corresponding straight line fits. The weight increase due to infusing amounts of N_2 and O_2 is negligible.

From the slope of the fit lines in Figure 62 the total water vapour transmission rates $WVTR_{total}$ are obtained. In Figure 63 the values of the total water vapour transmission rate divided by the panel area $WVTR_{total}/A$ are depicted.

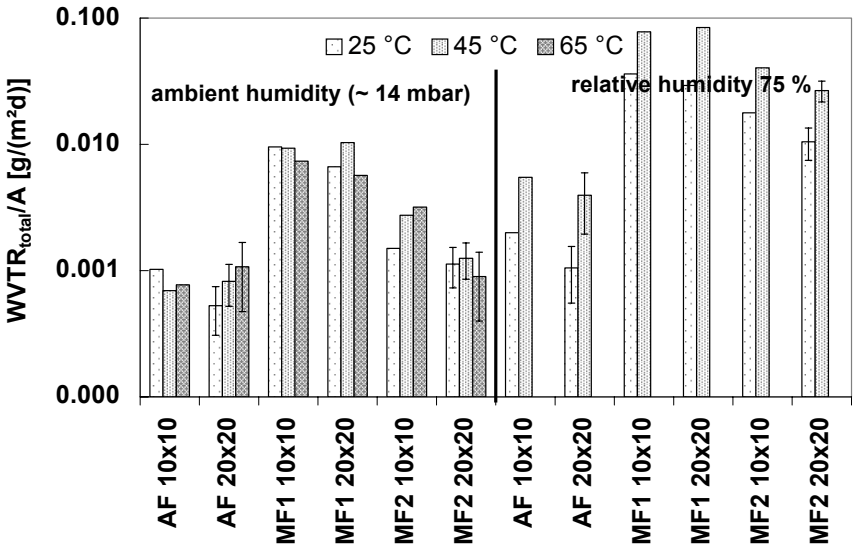

Figure 63: Total water vapour transmission rate divided by the panel area for VIP in the air-conditioned boxes; VIP with laminates AF, MF1 and MF2 and two different dimensions are investigated; mean values and standard deviations are only given for laminates AF and MF2 and dimensions (20 x 20) cm².

The large differences in water vapour transmission observed for ambient humidity and for high humidity (75% RH) may be due to the fact that at increased humidity, particularly at increased temperatures, a larger water vapour pressure is exerted onto the VIP (see Table 29). A water vapour transmission rate of 0.001 g/(m^{2}d) determined for laminates AF and MF2 at ambient humidity corresponds to mass increases of about 0.03 g after one year for the panel size (20 x 20) cm². As the resolution of the scale is 0.02 g, accurate data are difficult to obtain in this case.

An important question is, which amount of water within the VIP (rate of mass increase up to around 0.1 g/(m²·d)) is adsorbed by the hygroscopic fumed silica and which amount is in the vapour phase and influences the pressure and thus the thermal conductivity. This influence can be answered if the sorption isotherm of the core material is known.

For the fumed silica boards used within these panels for low humidities (< 50% RH) the sorption isotherm can be approximated by a linear relationship [48]. The slope amounts to approx. 0.08%-mass per percent of relative humidity. The linear approximation is used further on. With this linear approximation and knowing the increase in water content dXw/dt from our measurements, we can deduce the increase of water vapour pressure with time. To determine the partial pressure pair of the dry air components (N_2, O_2,…) in the VIP, we have to subtract the water vapour pressure from the measured total pressure ptotal.

$$p_{air} = p_{total} - p_{wv} = p_{total} - \varphi(X_W) \cdot p_{wv,satured}(T) \qquad (26)$$

$\varphi(X_W)$: *inverse function of the sorption isotherm* $X_W(\varphi)$.

4.4.3.3 Discussion

The measurements have shown large spreads in the pressure and mass increases. For the three different laminate envelopes we now discuss how the parameters panel size, temperature and relative humidity influence the pressure and the mass increases.

Influence of humidity on the pressure increase

The partial water vapour pressure in the VIP can be calculated if water content and the sorption isotherm are known. The following example shows the increase in partial pressure from infusing water vapour if a fumed silica core with a bulk density of 170 kg/m³ is used for a 1 cm thick VIP. A water vapour transmission rates of 0.1 g/(m²d), typical for film MF1 at 45°C/ 75% RH, leads to a rate of mass increase of about 4%-mass/yr. This results, at a temperature of 20°C, in a rate of increase in water vapour pressure of approx. 12 mbar/yr. With a vapour transmission rate of 0.001 g/(m²d), typical for foil AF at 25°C and ambient humidity, the humidity-related rate of pressure increase amounts to only about 0.1 mbar/yr. From these estimates it becomes obvious that particularly at high humidity the measured pressure consists of both, the partial pressure of the dry air components and the partial pressure of the water vapour.

Figure 64 shows the rates of pressure increase measured for VIP of size (20 x 20 x 1) cm³ and with laminates AF, MF1 and MF2 at ambient humidity (water vapour pressure ~ 14 mbar) and at 75% RH for temperatures of 25°C and 45°C. It also shows the rates of water vapour pressure increase, which can be calculated from the inverted sorption isotherm using as data the difference of the measured mass increase at ambient humidity and at 75% RH.

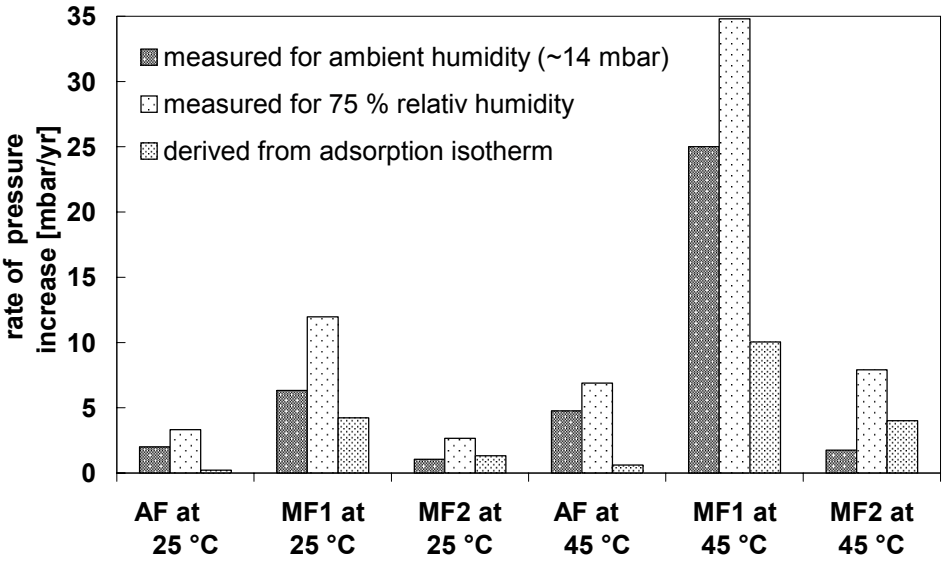

Figure 64: Comparison of the rates of pressure increases at ambient humidity and at 75% RH with the rates of vapour pressure increase estimated from the increase in water content for the VIP with the laminates AF, MF1 and MF2.

VIP with film MF1 suffer the largest rates of pressure increase. VIP with laminate MF2 and AF are roughly comparable in their overall barrier quality. For AF-enclosed cores, the pressure increase is dominated by air components, the contribution from water vapour to the

increase in pressure is small. For MF1 and MF2 covered VIP a relatively large fraction of pressure increase is caused by water vapour.

Influence of temperature on the permeation of air

The permeance of a laminate as a function of temperature is governed by the Arrhenius law. In Figure 61 the influence of the temperature on the pressure increase has been shown. For the considerations in this report we neglect the fact that the gas infusion, especially for high humidity (75% RH) and high temperatures, is also influenced by the presence of water vapour (see Figure 64). For low humidities this influence is less pronounced. In this case the measured temperature dependence of the diffusion process should correspond approximately to the temperature dependence of the dry air case. To obtain the temperature dependence of the permeation of air components as precisely as possible, the contribution of the penetrating water vapour to the pressure increase is corrected using equation (26). The transmission rates of air are calculated from the corrected pressure increases. Figure 65 shows the logarithm for the obtained air transmission rates at 25°C, 45°C and 65°C at low humidity plotted over {-1/(RT)}. Only the pressure increases of panels with dimensions (20 x 20 x 1) cm³ are assessed. The activation energies Ea, listed in Table 31, are derived from the slope of the fit lines. They are in the range expected for polymers (20 to 45 kJ/mol [45]).

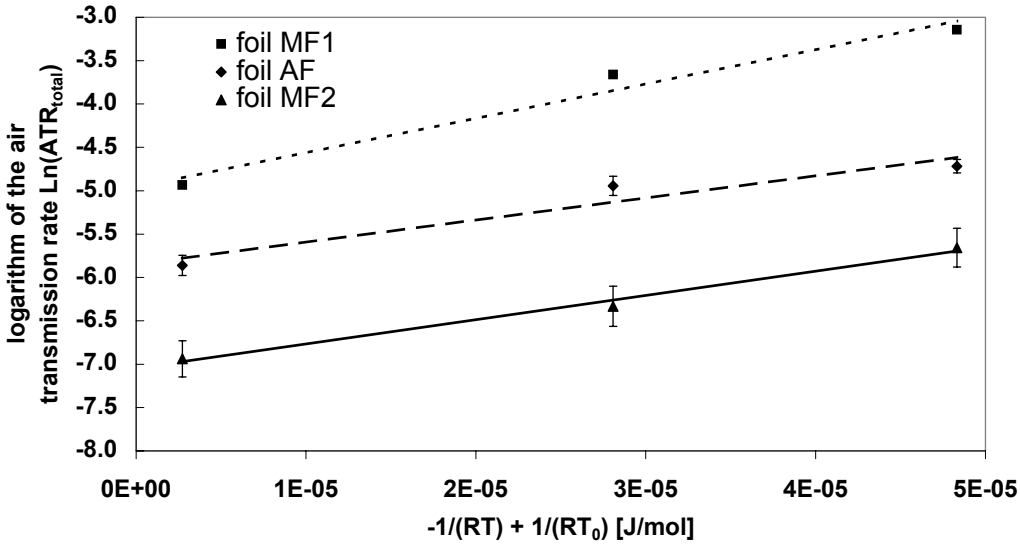

Figure 65: Logarithm of the air transmission rate ATR_{total} over $1/(R \cdot T)$ for the laminates AF, MF1 and MF2.

Table 31: Activation energies E_a for the laminates AF, MF1 and MF2.

	AF	MF1	MF2
E_a [kJ/mol]	26 ± 2	40 ± 7	28 ± 3

To illustrate how strongly the temperature affects the air permeation, Table 32 shows the factor by which the air transmission rate changes in comparison to the one given at 25°C.

Table 32: Factor exp(-E_a/(RT)+E_a/(RT_0) for the laminates AF, MF1 and MF2 with T_0=25°C.

Temperature	Foil AF	Film MF1	Film MF2
0°C	0.39	0.23	0.35
10°C	0.58	0.43	0.47
45°C	1.9	2.7	2.0
65°C	3.4	6.7	3.8
80°C	4.9	12.2	5.8

Depending on the type of laminate, the air permeation and its temperature dependence varies and should be recorded for each laminate.

Influence of the panel size on pressure increase and on the permeation of air

As the measurement results presented in Figure 61 show, the rates of pressure increase depend significantly on the panel sizes. If at 25°C the panel perimeter doubles, the rate of pressure increase is roughly reduced to one half. The rates of pressure increase for the panel sizes tested here was essentially determined by the perimeter-related air transmission rate ATR_L. Figure 66 shows the total air transmission rates derived for all panels in the air-conditioned boxes divided by panel perimeter L. As the total pressure increase (air pressure and water vapour) was taken as the basis of the calculation for permeation, the transmission rates here represent an upper estimate for the air transmission rates.

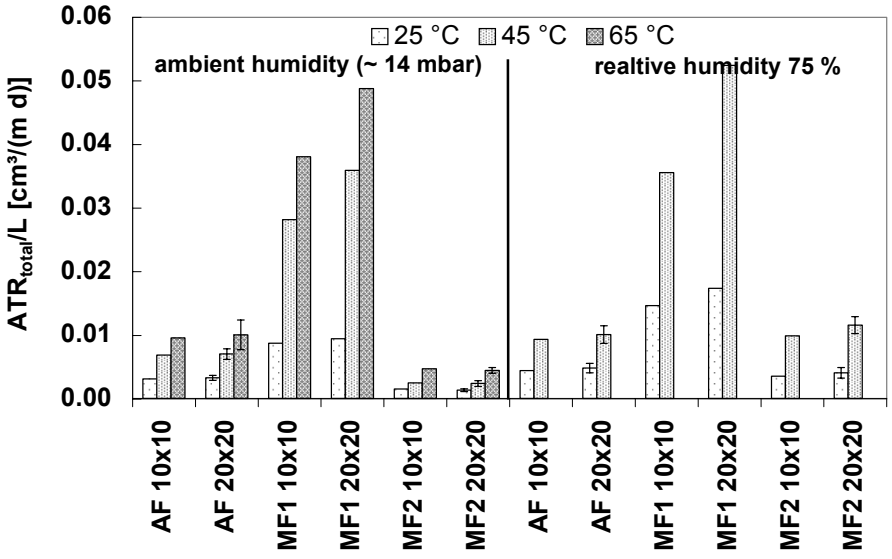

Figure 66: Total air transmission rates divided by the perimeter L recorded from the measured pressure increases for the VIP in the air-conditioned boxes with the laminates AF, MF1 and MF2; mean values and standard deviations are given for the laminates AF and MF2 and the dimensions (20 x 20) cm².

For the interpretation of Figure 66 we have to consider that $ATR_{total} = ATR_A \cdot A + ATR_L \cdot L = ATR_A \cdot 2 \cdot K^2 + ATR_L \cdot 4 \cdot K$ for squared VIP with side length K. Thus $ATR_{total}/L = ATR_A \cdot K/2 + ATR_L$

follows. For the laminates AF and MF2 almost no dependence of the perimeter-related total air transmission rate on panel size can be found. We conclude that infusion occurs predominantly through the perimeter of the VIP. For the film MF1, the quantity AT/L increases as the panel size does. Thus it is evident that surface permeation contributes to the infusion process. In principle ATR_A can be calculated from the change of ATR_{total}/L as a function of L. As is evident in Figure 66, the variation of ATR_{total}/L for the two tested panel sizes with the laminates AF and MF2 is in the same order of magnitude as the standard deviation of ATR_{total}/L. Thus it doesn't make sense to determine the surface air transmission rate[3]. A further detail that impedes the separation of ATR_L and ATR_A is the restriction to small panel formats, which resulted from the small size of the air-conditioned boxes. An analysis of the influence of panel sizes and proposals for improvement to determine the length and surface air transmission rates are given in section 4.4.4.1.

Influence of the panel size on the mass increase

As the measurements show, there is both, a mass increase across the surface as well as across the sealed seam. With the database at hand, it is not possible to separate the water vapour permeation across the surface and the edge. As the panels tested here were relatively small and the contribution of the surface permeation on the total permeation becomes larger with increasing panel size, the relative contribution of perimeter-related permeation should be negligibly small if large VIP are chosen. If we neglect the perimeter permeation and calculate the area-related water vapour transmission rate ($WVTR_A \approx WVTR_{total}/A$) from the mass increases measured for the small panel sizes (e.g. see Figure 63), then we get an upper estimate for the $WVTR_A$ and for the mass increase. If we assume only a surface permeation for water vapour, then the relative mass increase (in %-mass with respect to the dry mass of the VIP) is independent of the panel size and only indirectly proportional to the panel thickness. Table 33 shows the rates of mass increase calculated for a VIP thickness of 1 cm with an assumed bulk density of 160 kg/m³ for the core. For the calculation the values $WVTR_{total}/A$ as derived for the panel sizes 20 x 20 cm² were taken.

[3] If one performs a regression analysis to determine ATR_L and ATR_A, then the standard deviations of ATR_A are greater than ATR_L and are in the same magnitude as the theoretical surface air transmission rates that would result if the gases were to penetrate solely through the surface into the VIP (ATR_L=0).

Table 33: Rates of mass increase for 1 cm thick VIP with laminates AF, MF1 and MF2 derived from the $WVTR_A$.

	Rates of mass increase [%-mass/yr]		
Climatic conditions	**Foil AF**	**Film MF1**	**Film MF2**
25°C / ~45% RH	0.02 ± 0.01	0.3	0.05 ± 0.02
45°C / ~11% RH	0.04 ± 0.02	0.4	0.06 ± 0.02
25°C / 75% RH	0.05 ± 0.02	1.3	0.49 ± 0.14
45°C / 75% RH	0.18 ± 0.09	3.8	1.22 ± 0.23

The VIP with the laminated Al-foil AF take up clearly less mass than those with the Al-coated films MF1 and MF2. The VIP with film MF1 shows particularly high rates of mass increase. VIP with fumed silica generally have no desiccant added[4]. Thus according to adsorption isotherm, an increase in the water content also leads to an increase in the relative humidity in the VIP, even in the course of just a few years. As the water vapour pressure increases within the VIP over time, the pressure difference between the inside and outside decreases. Thus also the water vapour intake decreases over time. If one assumes standard average relative humidities of 60% RH to 80% RH, then a maximal water content of 4%-mass to 8%-mass can be expected.

A relative humidity of 80% RH at 20°C corresponds to a vapour pressure in the VIP of 18 mbar. This pressure can be expected to influence the thermal conductivity of the VIP. To estimate a humidity-related increase in the thermal conductivity, an accurate determination of the mass increase, which is strongly influenced by the climatic conditions, is important.

Influence of temperature and relative humidity on the water vapour permeance

An essential factor influencing the mass increase is the partial water vapour pressure around the VIP. The vapour pressure $p_{wv} = \varphi \cdot p_{wv,saturated}$ (T) shows an approximately exponential dependence on temperature at constant relative humidity. The varying water vapour pressure for the climatic conditions in our test is shown in Figure 67. In addition to the depend-

[4] In comparison to fumed silica, core materials like PU, XPS or fibre glass adsorb almost no water and, at the same time, increase their thermal conductivity in the pressure range of 1 mbar. That's why sufficient desiccant must be added here in order to adsorb the water vapour throughout the entire application period. Penetrating water vapour would otherwise very quickly lead to an increase in the thermal conductivity.

ence on the prevalent vapour pressure, water vapour permeation can explicitly depend on the temperature and relative humidity. To illustrate these dependencies, the water vapour permeance, which gives the water vapour transmission rate related to the vapour pressure, is also shown in Figure 67.

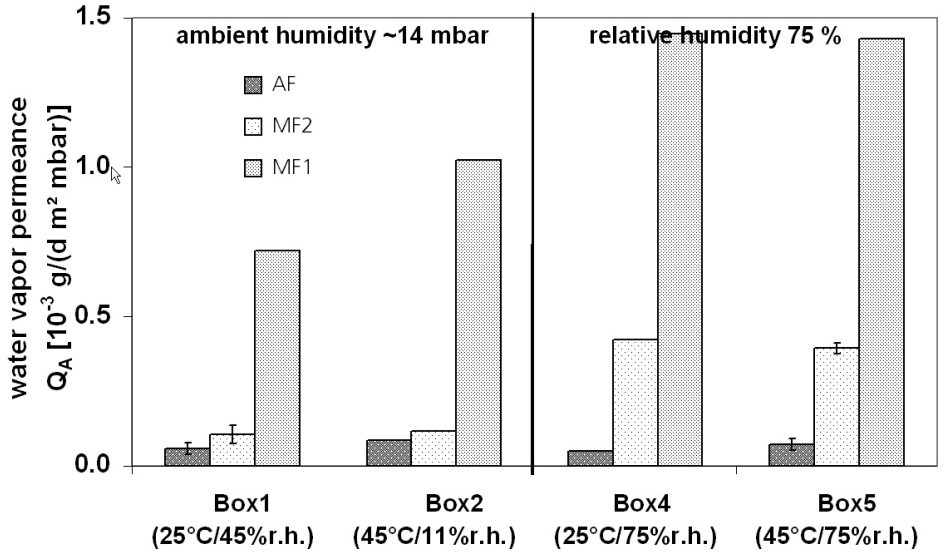

Figure 67: Water vapour permeance for the laminates AF, MF1 and MF2 at temperatures 25°C and 45°C and at ambient humidity (~14 mbar) and at rel. humidity of 75% RH (21 mbar at 25°C and 73 mbar at 45°C).

Especially for the Al-coated films the permeances at higher humidity (75% RH) are increased, while the temperature dependence is rather weak. At first glance this is surprising, as also for water vapour diffusion an Arrhenius dependence can be assumed. A possible explanation is the low activation energy of PET for water vapour of about 3 kJ/mol [45]. At such a low activation energy the temperature influence is practically negligible. As for the Al-coated films the aluminium layer is vacuum coated onto PET, the temperature dependence of PET should determine the temperature dependence of the permeation. With other polymers, a significantly stronger temperature dependence can occur. The water vapour permeance depends clearly on the relative humidity. However a precise estimate of the mass increase is not possible, as the functional dependence between permeance and relative humidity is not known.

4.4.3.4 Pressure increase rates of VIP in construction applications

For applications in the construction sector, rates of pressure increase below 2 mbar/yr are required. The above measurements often show significantly larger rates of pressure increase depending on temperature, humidity and panel size. The pressure increases in our experiments were determined at relatively high temperatures (45°C and 65°C), which would rarely occur in construction applications (insulation of walls, floors, ceilings) and only for short periods of time. The annual mean temperatures on VIP throughout the year are usually below 25°C for typical construction applications. Thus the determined pressure increases at 25°C represent an upper estimate. For this reason, let us consider the pressure increase at 25°C and ambient humidity. Table 34 illustrates the rates of pressure increase for the laminates AF, MF1 and MF2 at 25°C / ~ 45% RH for the panel format (20 x 20 x 1) cm³. As, in the construction sector, larger panel formats are generally used, the given rates of pressure increase represent an upper estimate for typical-construction panel sizes. In addition, Table 34 shows the air transmission rate per unit area that results from the pressure increase,

assuming that the gases can only penetrate through the surface into the VIP and that there is no perimeter permeation.

Table 34: Rate of pressure increase at 25°C / 14 mbar for VIP with laminates AF, MF1 and MF2 and size 20 x 2 0 x 1 cm³, as well as air transmission rate per unit area (assumption ATR_L=0).

	Foil AF	**Film MF1**	**Film MF2**
Rate of pressure increase *[mbar/yr]*	2.4 ± 0.2	6.9	1.1 ± 0.2
ATR_A *[cm³/(m²·d)]*	0.030 ± 0.002	0.087	0.014 ± 0.002

Film MF1 shows a rate of pressure increase that is too high, making it impractical for the construction sector. For VIP with film MF2 the requirements for building applications on the pressure increase are fulfilled. For thicker panels as may be common in building application the pressure increase is smaller than measured on the small and thin test panels, thus also film AF may be used.

In Table 34 rates of total pressure increase, i.e. effects of the air components and water vapour are given. Pressure increases, that are only caused by air, are obtained by subtracting the pressure increase calculated from the mass increases from the total pressure increase (see equation (26)). If we also assume, that the air components only penetrate the sealed seam of the VIP, then we can estimate the perimeter-related transmission rate for air components $ATR_{air,L}$ from the corrected pressure increase. Table 35 includes the perimeter-related air transmission rate that have been determined this way. All former air transmission rates and pressure increases are valid for the measurement conditions of 20°C and 1 bar. For comparison, Table 35 also shows the transmission rates of air components at standard conditions (0°C / 1.013 bar). Also given are the rates of pressure increase to be expected at these air transmission rates for the panel sizes (20 x 20 x 1) cm³ and (100 x 100 x 2) cm³.

Table 35: Perimeter-related air transmission rates for measurement and standard conditions, determined from the pressure increases at 25°C / 14 mbar and panel sizes (20 x 20 x 1) cm³ as well as rates of pressure increase for (20 x 20 x 1) cm³ and (100 x 100 x 2) cm³ panels.

	Foil AF	**Film MF1**	**Film MF2**
$ATR_{air,L}$ *[cm³/(m·d)]*	0.0032 ± 0.0002	0.0081	0.0012 ± 0.0003
$ATR_{air,L}$ *[cm³(STP)/(m·d)]*	0.0029 ± 0.0002	0.0075	0.0011 ± 0.0003
Rate of pressure increase *[mbar/yr]* at (20 x 20 x 1) cm³	2.3 ± 0.2	5.9	0.9 ± 0.3
Rate of pressure increase *[mbar/yr]* at (100 x 100 x 2) cm³	0.23	0.59	0.09

When compared with the rates of pressure increase from Table 34, the rates of pressure increase for (20 x 20 x 1) cm³ sized panels show the influence of the humidity. The rates of pressure increase on (100 x 100 x 2) cm³ size panels are, determined by the greater panel format, by a factor of 10 lower than those for (20 x 20 x 1) cm³ size panels. The values in Table 35 give the approximate rates of pressure increase range for the laminates AF, MF1 and MF2, which is to be expected in construction applications for typical panel sizes by the intrusion of dry air components.

4.4.4 Comparison of experimental results, general findings

4.4.4.1 Comparison of panel results and film permeability data

If the perimeter related permeation is assumed to be only caused by the penetration of air component through the sealed seam, a theoretical seam transmission rate of air components can be calculated from the permeability of the seal material and from the thickness and width of the seam. The seal material used on the laminates was LD-PE. With an air permeance of the LD-PE of 800 cm³(STP)/(m²·d·bar) for a 100 µm thick PE film [47], for a sealed seam of 100 µm thickness and 8 mm width a theoretical perimeter-related transmission rate of air of 0.0010 cm³(STP)/(m·d) results. From the measurements at ZAE-Bayern (Table 35) a somewhat greater perimeter air transmission rate for the foil AF (seam thickness 2·100 µm) is derived, while the one for film MF2 is almost twice as high and the one for film MF1 is nearly seven times as high. Similar results are derived from the measurements at EMPA (Table 28): the factor between the experimental result and the theoretical value is about 2 for MF4, and nearly 10 for MF3.

One can speculate whether the PE seal material has additives mixed into it to possibly improve the melting behaviour for sealing. The air transmission rate of modified PE can be considerably larger than the one for pure PE. Whether the high perimeter-related air transmission rate really is caused by an increased seam permeance, or whether there are other causes for this, has not yet been examined. Another reason for the increased air permeation could also be a damaged aluminium barrier layer along the VIP perimeter, which is subjected to bending and crumbling. Point damages and weakness of the barrier layer were observed visually using light-microscopy.

The increased perimeter-related air transmission rates show that the theoretical estimates merely give a lower threshold. The actual perimeter air transmission rates can only be determined by measurements. On the other hand, the observed differences in the perimeter permeation indicate that there is still room for optimization. By using seal materials with smaller air permeability, like HD-PE or PET, the perimeter permeation can be further reduced. Such improvements are already pursued by manufacturers.

Regarding water vapour transmission a corresponding statement can be made: The surface-related WVTR values extracted from mass increase measurements on VIP are typically higher than the values expected for the unstressed laminates (factors roughly between 1 and 2). This can be seen e.g. by comparison of Table 30 and Table 37.

4.4.4.2 Discussion of the results from panel measurements

The following example illustrates the influence of the panel size on the pressure increase. Figure 68 shows the perimeter and surface-related rates of pressure increase for 1 cm thick VIP with high air transmission rates for surface and perimeter (ATR_{L1} = 0.01 cm³/(m·d) and ATR_{A1} = 0.02 cm³/(m²·d)) and with low transmission values (ATR_{L2} = 0.001 cm³/(m·d) and ATR_{A2} = 0.0006 cm³/(m²·d)). ATR_{L1} and ATR_{L2} correspond roughly to measured perimeter transmission rates of the films MF1 and MF2 at 25°C and ambient humidity. ATR_{A1} and ATR_{A2} correspond approximately to the surface transmission rates according to manufacturer's information. The chosen panel formats are (10 x 10) cm², (20 x 20) cm ², (50 x 50) cm²

and (100 x 100) cm². The overall rates of pressure increase are marked with 15% error bars. This error corresponds roughly to the variation observed in the measurements.

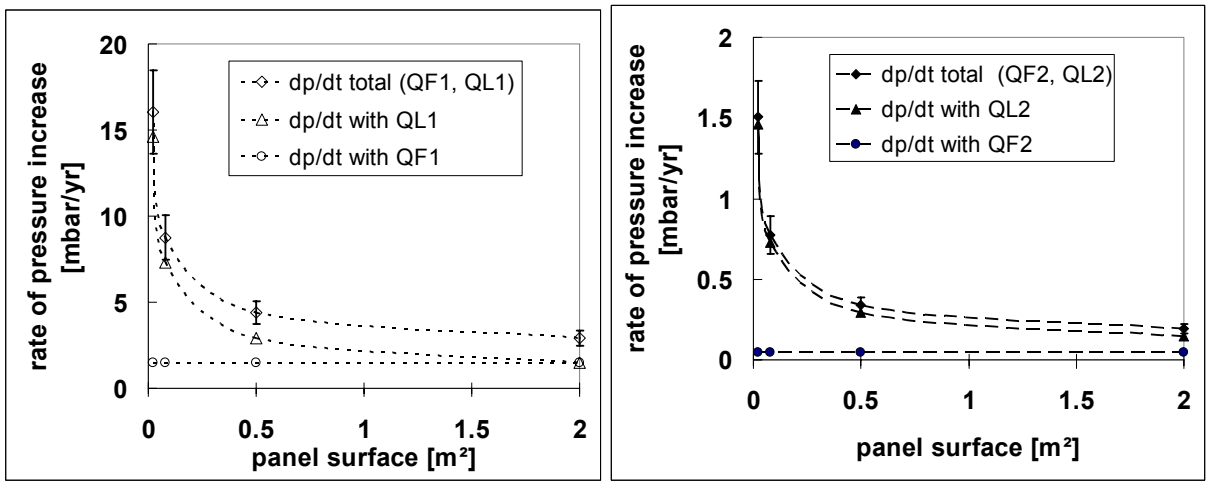

Figure 68: Pressure increases per year as a function on panel size. Two laminates with different air transmission rates for perimeter and surface related leakage are considered (values are given in the text).

In Figure 68 the perimeter-related rate of pressure increase rises with decreasing panel size. Below a specific panel size, which depends on the ratio of surface to perimeter transmission, the pressure increase is almost completely determined by the perimeter transmission. With increasing panel size the pressure increases becomes smaller, thus (depending on pressure increase and resolution of the pressure measuring procedure) often long periods of time are required to determine this quantity. In addition, pressures within large panels are difficult to measure with the envelope lift-off procedure and upon repeated measurements larger panel often buckle.

Measurements on only small panel formats yields too large pressure increases. Pressure increases measurements on larger, more construction-typical panel formats provide a good estimate for the conventionally used panel format. However, with special formats (small fitted pieces, or thin VIP strips as used to insulate window frames) a clearly greater pressure increase could occur. This is why the surface and perimeter transmission rates should be determined for each laminate barrier by measurements on various differing panel sizes.

4.4.4.3 Summary of panel aging data

Based on the data from the panel aging experiments, perimeter and surface area related permeation characteristics for all investigated barriers types with multiple metallized polymer laminates are shown in Table 36. The values are normalized for the conditions 23°C, 50% RH and atmospheric pressure 1 bar.

Table 36: Area (subscript A) and perimeter (subscript L) related transmission characteristics of VIP with metallized polymer laminates for 23°C, 50% RH and 1 bar.

Barrier type	$WVTR_A$, g/(m^2 d)	$WVTR_L$, g/(m d)	ATR_A, cm^3/(m^2 d)	ATR_L, cm^3/(m d)
MF1	0.0233	-	0.0160	0.0080
MF2	0.0057	-	-	0.0039
MF3	0.0030	0.0008	0.0034	0.0091
MF4	0.0048	0.0006	0.0088	0.0018

It is seen that except for MF1 the permeation values are in comparable ranges. MF1 clearly shows higher area related water vapour and dry gas transmission rates. The values in Table 36 have been used to calculate the yearly moisture and pressure increase at standard conditions for 2 cm thick VIP with the formats 0.25 x 0.25 m^2, 0.25 x 0.50 m^2, 0.5 x 0.5 m^2, 0.5 x 1.0 m^2, and 1.0 x 1.0 m^2. The respective areas are 0.0625 m^2, 0.125 m^2, 0.25 m^2, 0.50 m^2, and 1.00 m^2. As indicated in Figure 69 there is a clear trend toward higher pressure increase rates for smaller formats due to the perimeter contribution. The format dependence is less significant regarding moisture accumulation, since the surface contribution is more dominant. It can be stated that except for MF1 the moisture accumulation rate is below 0.2 %-mass/yr for all formats. Omitting again MF1 the pressure increase rates are close to or below 2 mbar/yr except for the smallest format, and below 1 mbar/yr for formats above 0.5 x 1.0 m^2.

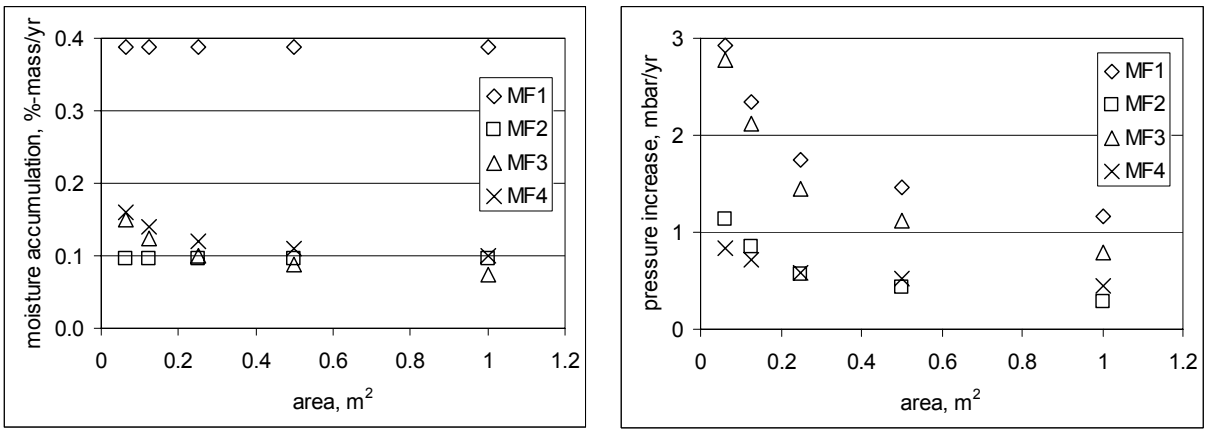

Figure 69: Moisture accumulation and pressure increase rates at 23°C, 50% RH (1 bar) for various VIP formats, calculated with the values from Table 36. The uncertainty may be in the order of 10 to 15%.

4.4.4.4 General findings

The measurements of the pressure increase have shown a complex influence of temperature, relative humidity and panel size on the pressure increase. The temperature influence can be accounted using the Arrhenius law. The penetrating water vapour will be partially adsorbed by the fumed silica. The non-negligible influence of the water vapour on the pressure increase was determined by the sorption isotherm. The panel size also influences the pressure increase. Estimates of the pressure increase for applications in the construction sector were made. It was found that VIP with laminated Al-foils and high-quality Al-coated multi-layer laminates show dry air pressure increase rates below 1 mbar/yr for formats above

0.5 x 1.0 m^2 and environmental conditions. The values may become higher for smaller formats. For a more precise estimate, the perimeter- and surface-related transmission rates of air in dependence on temperature and relative humidity and the respective climatic conditions must be known.

The measurements at ZAE-Bayern have shown that for panel sizes typical for construction application the mass increase essentially takes place across the laminate surface. The same holds for the high-quality barrier measured at EMPA. For a detailed product characterization, again perimeter and surface related water vapour transmission properties must be determined. For Al-coated films, in comparison with laminated Al-foils, larger rates of mass increase have been detected. For high humidity and high temperature mass increase rates up to 1%-mass/yr have been determined. Over the years thus a significant increase of humidity and water vapour pressure in the VIP is established. For typical environmental conditions a water content from 3 to 6%-mass may be expected.

Overall, the results show that for VIP made of fumed silica and commercially available advanced metallized polymer laminate barriers, sufficiently low leakage rates can be achieved for an application in the construction industry. Improvements of barrier materials are still needed, in particular with regard to water vapour permeability.

4.5 VIP service life prediction

4.5.1 Model definition

To predict the increase in thermal conductivity over time, it has to be known how the thermal conductivity depends on gas pressure and water content.

For a simplified calculation model it is assumed that gas pressure and water content contribute independently to the thermal conductivity. Thus the two contributions can be simply added up:

$$\lambda(p_{gas}, X_w) = \lambda_{evac} + \lambda_{gas}(p_{gas}) + \lambda_w(X_w) \qquad (27)$$

λ_{evac}: thermal conductivity in the evacuated and dry state (refers to solid conduction and radiative transfer in the core material),

$\lambda_{gas}(p_{gas})$: gaseous thermal conductivity at pressure p_{gas} inside of the VIP. It is assumed that the pressure is caused by the dry air components infusing the VIP (without the partial pressure of the water vapour) and

$\lambda_w(X_w)$: thermal conductivity, caused by the water content X_w.

The gaseous thermal conductivity of different VIP core materials in dependence on gas pressure (see Figure 70) was extensively investigated [36], [38], [14] and can be described by the following relation:

$$\lambda_{gas}(p_{gas}) = \frac{\lambda_{free,gas}}{1 + \frac{p_{1/2,gas}}{p_{gas}}} \quad (28)$$

$\lambda_{free\ gas}$: thermal conductivity of the free and still gas (free = not bounded by the pores of the material, still = no convection),

$p_{1/2,gas}$: pressure, at which the contribution of the gas is on half of $\lambda_{free\ gas}$,

$\lambda_{free\ gas}$: In the evacuated state, i.e. $p_{gas} << p_{1/2,gas}$, the gaseous thermal conductivity is negligible (see Figure 70). $p_{1/2,gas}$ depends strongly on the pore width of the core material and is influenced by the gas type.

Upon increasing water content, the influence of the water on the heat transport has to be considered. With a function $\lambda_w(X_w)$ one can describe this influence. For the core material fumed silica $\lambda_w(X_w)$ is, in a good approximation, describable by a linear function [42] (measured at a mean temperature of 10°C):

$$\lambda_w(X_w) = b \cdot X_w \quad (29)$$

for X_w < 10%-mass

X_w: water content in the VIP related to the dry mass of the VIP and

b: constant, which depends on the sorption isotherm of the core material.

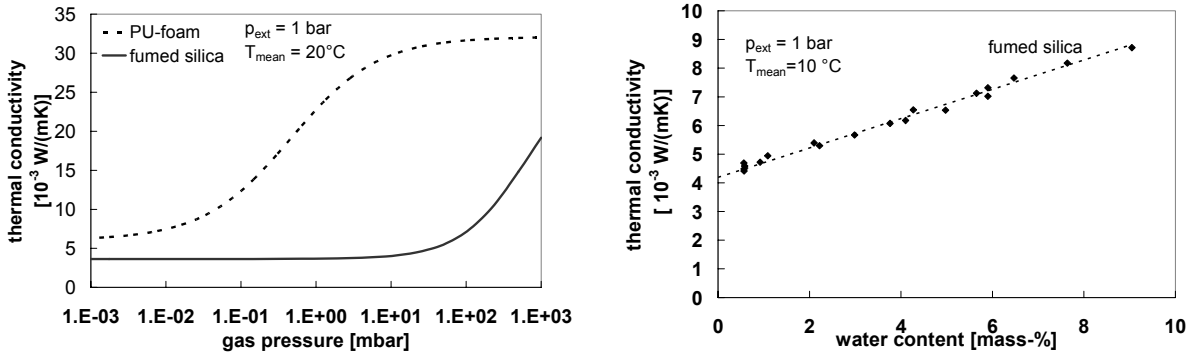

Figure 70: Thermal conductivity of fumed silica and PU-foam in dependence on nitrogen pressure at 20°C (left) [14] and of fumed silica in dependence on water content at 10°C (right) [42]. The VIP were loaded with an external pressure of 1 bar.

To predict the change in thermal conductivity, which depends on air pressure and water content according to equation (27), one has to know gas transmission rate of the envelope in order to determine the increase in pressure and water content.

Normally the gas transmission rates are defined for laminates and not for envelopes. Volumetric methods to determine the oxygen transmission rate OTR are described in the German Industry Standard DIN 53380-1 or in the American Standard Test Method ASTM D 1434. DIN 53122-1 or ASTM E 96 describe gravimetric methods for the determination of the water vapour transmission rate WVTR. According to the German Industry Standard the WVTR is

given in g/(m²d) and the OTR is given in cm³(STP)/(m²d) at standard condition (STP = standard temperature with T0 = 0°C and standard pressure p0 = 1.013 mbar).

Gases can permeate the VIP-cover through the surface, the seal seam and the edges. These gas transmission rates, which depend on temperature and humidity [46], can be added up to the total gas transmission rate GTR_{total}:

$$GTR_{total} = GTR_A(T,\varphi)\cdot A + GTR_L(T,\varphi)\cdot L \qquad (30)$$

GTR_A: surface gas transmission rate of the laminate cover per panel area A (in this report the area A is the total surface of the VIP with front and rear side, the surface-related gas transmission rate GTR_A corresponds to the gas transmission rate of the laminates) and

GTR_L: perimeter-related gas transmission rate of the laminate cover along to the perimeter[5] L of the VIP.

Instead of the gas transmission rate one often uses the permeance to characterize the permeation.

$$Q_{gas,total} \equiv \frac{GTR_{total}}{\Delta p_{gas}} \qquad (31)$$

$Q_{gas,total}$: the total gas permeance gives the amount of substance per time and per pressure difference, that permeates into the VIP.

Δp_{gas}: pressure difference across the laminate-cover.

The permeated gases cause a pressure increase. According to equation (31) and (30) and with the ideal gas equation the pressure increase with time dp_{gas}/dt becomes:

5 In our examinations we consider only VIPs with one seam layer along the VIP perimeter. For quadratic panels of edge length K thus perimeter L=4·K holds.

$$\frac{dp_{gas}}{dt} = \frac{Q_{gas,total} \cdot \Delta p_{gas}}{V_{eff}} \cdot \left(\frac{T_m \cdot p_0}{T_0} \right) = \frac{GTR_{total}}{V_{eff}} \cdot \left(\frac{T_m \cdot p_0}{T_0} \right) \quad (32)$$

$Q_{gas,total}$: the total gas permeance $Q_{gas,total}$ in cm³(STP)/(d bar) indicates, which gas volume penetrates the laminate cover at standard conditions (STP with p=1.013 bar and T= 0°C) per day and pressure difference. Here numbers mostly are given at measurement conditions (20°C, 1 bar).

GTR_{total}: total gas transmission rate.

Δp_{gas}: pressure difference across the laminate barrier. For the VIP considered here $\Delta p_{gas} \approx p_{atm}$ holds, as the gas pressure inside functional VIP is negligible compared to the external air pressure p_{atm}.

V_{eff}: effective pore volume in the VIP. V_{eff} is obtained by multiplying the volume of the core material with its porosity.

$(T_m \cdot p_0)/T_0$: conversion factor from standard (index 0) to measurement conditions (index m).

With equation (32) the pressure increase with time can be calculated from the known GTR_{total} and vice versa the GTR_{total} can be determined from the measured pressure increase. If the pressure increase is caused by a gas mixture, e.g. air gas, this total air transmission rate ATR_{total} can be determined from dp_{air}/dt.

For the mass increase with time dm_w/dt the following relation between the total water vapour permeance $Q_{total,wv}$ and the total water vapour transmission rate $WVTR_{total}$ holds:

$$\frac{dm_w}{dt} = Q_{wv,total} \cdot \Delta p_{wv} = WVTR_{total} \quad (33)$$

Δp_{wv}: difference in water vapour pressure across the laminate; with time this quantity becomes smaller as vapour pressure within the VIP increases.

The effect of water vapour inside the VIP depends on the core material. The hygroscopic fumed silica adsorbs the penetrating water vapour. The sorption behaviour of the core is determined by the sorption isotherm [48]. With the sorption isotherm, respectively its inverse function $\varphi(X_w)$, the water vapour pressure p_{wv} can be determined, if the water content Xw and the saturated water vapour pressure $p_{wv,saturated}$, which depends on temperature T, are known.

$$p_{wv} = \varphi(X_W) \cdot p_{wv,saturated}(T) \quad (34)$$

φ: in hygroscopic materials the relative humidity $\varphi = p_{wv}/p_{wv,saturated}$ depends on water content.

With equation (33) and (34), the change in water content with time $dXw/dt = (dm_w/dt)/m_{VIP,dry}$ can be derived:

$$\frac{dX_w}{dt} = \frac{Q_{wv,total}}{m_{VIP,dry}} \cdot \left(p_{wv,out} - p_{wv,in}\right) = \frac{Q_{wv,total}}{m_{VIP,dry}} \cdot p_{wv,saturated}(T) \cdot \left(\varphi_{out} - \varphi_{in}(X_W)\right) \qquad (35)$$

$p_{wv,in}$, $p_{wv,out}$: water vapour pressure, in- and outside of the VIP,
$\varphi_{wv,in}$, $\varphi_{wv,out}$: relative humidity, in- and outside of the VIP,
$m_{VIP,dry}$,: dry mass of the VIP-core.

From equation (32) a linear increase in pressure over time results, if constant climatic conditions and a constant air pressure difference Δpair ≈ p_{atm} are assumed:

$$p_{air}(t) = \frac{Q_{air,total} \cdot p_{atm}}{V_{eff}} \cdot \left(\frac{T_m \cdot p_0}{T_0}\right) \cdot t = \frac{ATR_{total}}{V_{eff}} \cdot \left(\frac{T_m \cdot p_0}{T_0}\right) \cdot t \qquad (36)$$

$p_{air}(t)$: pressure in the VIP, resulting from the different air components that permeate into the VIP.

As shown in [48], the sorption isotherm can be approximated by a linear relation $X_w = k \cdot \varphi$ for relative humidities $\varphi \leq 50\%$. Then equation (35) has an analytical solution (with initial condition $X_w(t=0)=0$):

$$X_w(t) = k \cdot \varphi_{out} \cdot \left(1 - exp\left(\frac{-Q_{wv,total} \cdot p_{wv,saturated}(T)}{m_{VIP,dry} \cdot k} \cdot t\right)\right) \qquad (37)$$

By inserting equation (36) into (28) and equation (37) into (29) and use of equation (27) the increase in the thermal conductivity of the VIP as a function of time can be derived:

$$\lambda(t) = \lambda_{evac} + \frac{\lambda_{free,air}}{1 + p_{1/2,air} \Big/ p_{air}(t)} + b \cdot X_w(t) \qquad (38)$$

The following values apply to VIP with fumed silica kernels of density ρ_{VIP} ≈ 170 kg/m³, $\lambda_{evac} = 4 \cdot 10^{-3}$ W/(m·K) [8], $p_{1/2,air} \approx p_{1/2,N_2} = 600$ mbar [8], $\lambda_{air} = 25 \cdot 10^{-3}$ W/(m·K) at 10°C [52] and $b = 0.5 \cdot 10^{-3}$ W/(m·K)/%-mass at a mean temperature of 10°C [42]. From the sorption isotherm k = 0.08%-mass per percent of relative humidity follows.

Equation (36), (37) and (38) are the model equations to calculate the increase in thermal conductivity, depending on the laminate cover and panel size.

To correlate the service life with measured data, the air and water vapour transmission rates for three different laminate covers were determined at constant climatic conditions, by meas-

uring the increase in pressure and water content for two different panel sizes (see chapter 4.4.3).

4.5.2 Constant boundary conditions

In Table 37 permeation data of the laminates AF, MF1 and MF2 found for the condition 23°C and 75% RH are compiled. This data are based on the tests on the small test panels (size 10 x 10 cm² and 20 x 20 cm²) as described above and some additional tests on larger panels, 40 x 40 cm² in size, which yield more precise results for the permeation data related to the surface [40]. However air transmissions rates through the surfaces of the laminates AF and MF2 was not significant. Thus only permeation proportional to the perimeter was taken into account.

The data in the table are used to calculate the increases in pressure, water content and thermal conductivity for two distinct panel sizes: 50 x 50 x 1 cm³ and 100 x 100 x 2 cm³. These sizes might be assumed as typical for VIP applied in buildings. In Table 38 the increase in pressure per year and the pressure after 25 years are given (calculated by linear extrapolation according to equation (36)).

Table 37: Permeation data used in the estimates of the service lives, found for the laminates AF, MF1 and MF2 at 23°C and 75% RH.

	$WVTR_A$ *[g/(m²·d)]*	**ATR_A** *[cm³/(m²·d)]*	**ATR_L** *[cm³/(m·d)]*
AF	0.0006	-	0.0018
MF1	0.035	0.016	0.0080
MF2	0.0086	-	0.0039

Table 38: Annual pressure increase and total pressure after 25 years for VIP with different laminates and panel sizes.

	Foil AF		**Film MF1**		**Film MF2**	
panel size *[cm³]*	50x50x1	100x100x2	50x50x1	100x100x2	50x50x1	100x100x2
Pressure increase per year *[mbar/yr]*	0.58	0.15	3.2	1.2	0.88	0.22
pressure after 25 years *[mbar]*	14.6	3.7	80.3	29.2	21.9	5.5

Whereas VIP with the laminates AF and MF2 are expected to have pressure increases below 1 mbar/yr, the VIP with laminate MF1 show non-acceptable pressure increases for building applications. The quality of the laminate obviously determines the pressure increase for a given VIP size. The large VIP are to be preferred, as they have four times smaller pressure increases, due to the double thickness d and perimeter L.

Figure 71 illustrates the mass increase over a period of 25 years, calculated by equation (37). Due to the large differences of the water vapour transmission rates of the laminates the water content saturates at 6%-mass after 25 years for VIP with laminate MF1, while the increase in water content for VIP with laminate AF is still linear in time, even after 25 years.

This behaviour, depending also on panel size, must be taken into account when determining the thermal conductivity.

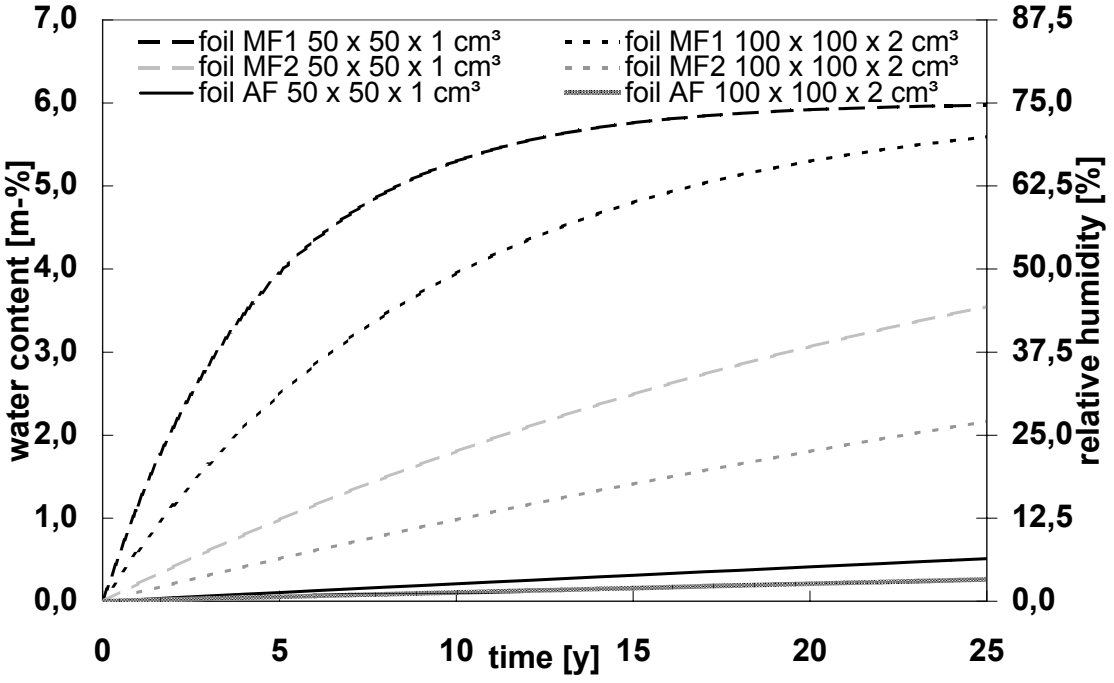

Figure 71: Calculated increase in water content of VIP with different panel sizes (50 x 50 x 1 cm³ and 100 x 100 x 2 cm³) and different laminates (AF, MF1 and MF2) calculated by equation (37) with permeability determined at 23°C / 75% RH. In addition the relative humidity is indicated ($\varphi = X_w / k$, for the calculation we assume here a linear relation from 0% RH till 75% RH).

With equation (38) the thermal conductivity can be calculated as a function of time. Figure 72 depicts the change in thermal conductivity over 25 years for VIP with the laminate AF. Starting from $4 \cdot 10^{-3}$ W/(m·K) the thermal conductivity increases slowly and even after 25 years stays below $5 \cdot 10^{-3}$ W/(m·K). Due to the small water vapour permeabilities the increase in water content is very small. Thus the behaviour at 25 years is far away from saturation.

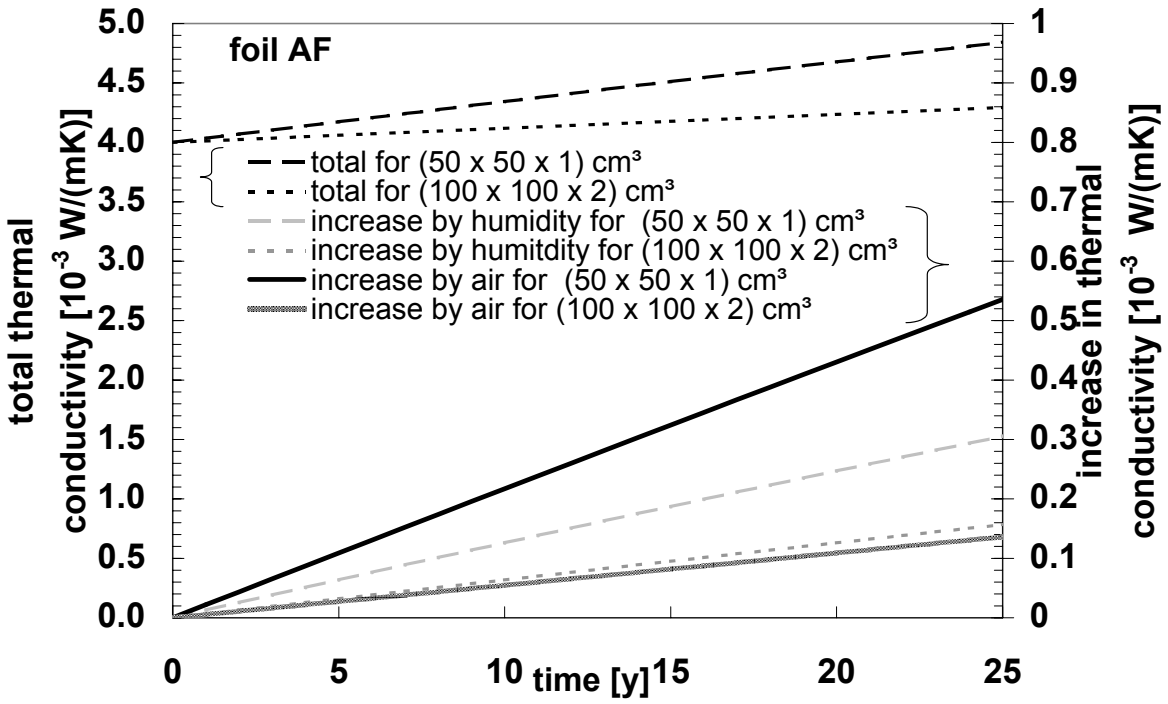

Figure 72: Total thermal conductivity as a function of time (upper part, left ordinate) and increases in air-related and humidity-related thermal conductivity (lower part, right ordinate) of VIP with laminate AF for different panel sizes.

The changes in the thermal conductivity of VIP with film MF2 (Figure 73) are larger than for VIP with the foil AF. This is due to the higher transmission rate of water vapour of Al-coated films compared to laminated Al-foils. Depending on panel size the thermal conductivity reaches values between $5.9 \cdot 10^{-3}$ W/(m·K) and $7.5 \cdot 10^{-3}$ W/(m·K) after 25 years. The influence of the humidity could be reduced by adding a drying agent to adsorb the water vapour.

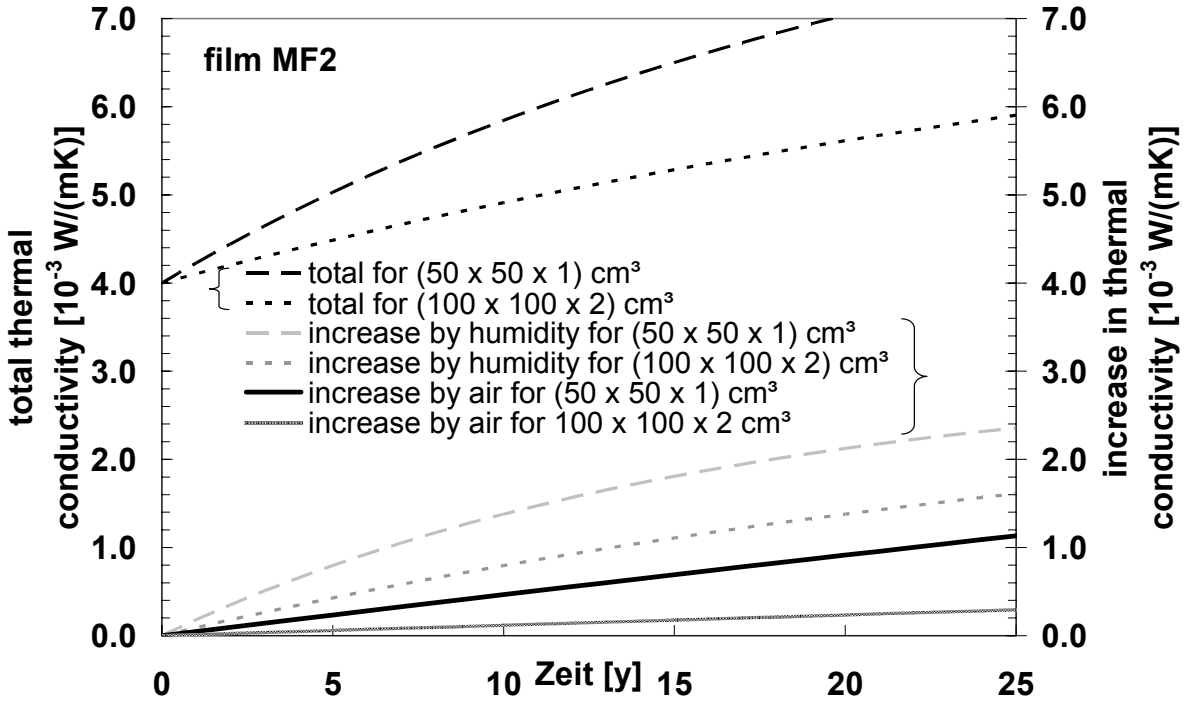

Figure 73: Total thermal conductivity as a function of time (upper part, left ordinate) and increases in air-related and humidity-related thermal conductivity (lower part, right ordinate) of VIP with film MF2 for different panel sizes.

The changes in thermal conductivity of VIP with the film MF1 are the largest (Figure 74), particularly during the first 5 years, when the thermal conductivity is mainly determined by the strong increase in water content. As the water content reaches saturation level, the humidity-related increase in thermal conductivity levels off after about 10 years. Thereafter, due to the relatively strong infusion of air, the thermal conductivity shows a further linear increase with time. After 25 years values between about $8 \cdot 10^{-3}$ W/(m·K) and $10 \cdot 10^{-3}$ W/(m·K) are to be expected.

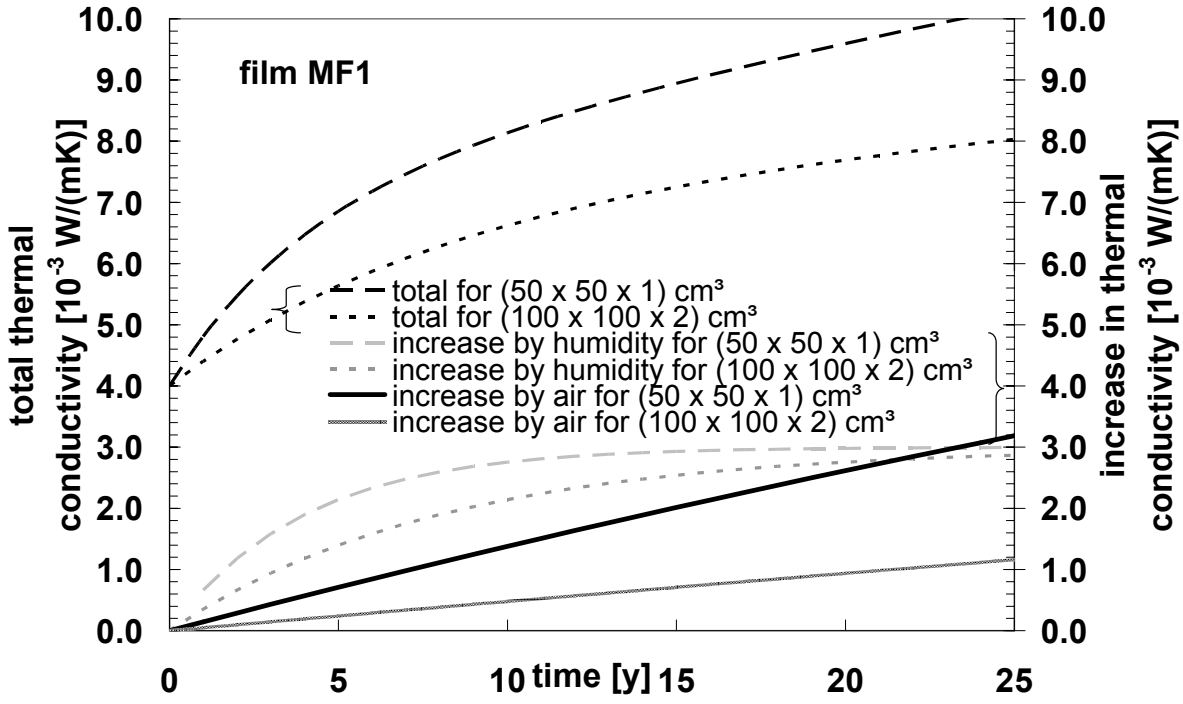

Figure 74: Total thermal conductivity as a function of time (upper part, left ordinate) and increases in air-related and humidity-related thermal conductivity (lower part, right ordinate) of VIP with film MF1 for different panel sizes.

As one now is able to predict the changes in thermal conductivity one can determine the theoretical VIP service life. This quantity is defined here as the time period, after which the maximum allowed thermal conductivity is reached. In Table 39 the service lives of VIP with the laminates AF, MF1 and MF2 are given assuming a maximum allowed thermal conductivity of λlimit = $6 \cdot 10^{-3}$ W/(m·K) (starting at $4 \cdot 10^{-3}$ W/(m·K)).

Table 39: Calculated service lives for VIP with fumed silica kernels, different panel sizes and different laminate covers calculated for a maximum allowed increase in thermal conductivity of 50%.

	Foil AF		**Film MF1**		**Film MF2**	
panel size *[cm³]*	50x50x1	100x100x2	50x50x1	100x100x2	50x50x1	100x100x2
service life *[years]*	80	245	5	10	16	38

VIP with foil AF have a long service life, which is large enough for building applications. With good Al-coated films like MF2 service lives from 16 to 38 years can be reached. This is still acceptable for building applications, especially if one considers that the service life can be prolonged by adding a drying agent. In spite of the higher increases in thermal conductivity, VIP with Al-coated films should be preferred to VIP with laminated Al-foils, because of the much higher thermal flux across the edges of the VIP with laminated Al-foils. Thermal bridges can cause a considerable reduction in the overall thermal resistance of VIP covered with laminated Al-foils [43] [30].

4.5.3 Dynamic conditions

In building applications the boundary conditions are mostly dynamic. VIP in roof or wall constructions will normally experience large daily and seasonal temperature and humidity variations, mainly on the outside. Dynamic effects by solar absorption on the building envelope may even be in the range of hours. Since detailed dynamic modelling of the gas and especially of the moisture transfer between the inside of VIP and the environment is rather complex. Rather simplified methods are discussed here to estimate the long-term changes of the VIP. The first step is always the calculation (or measurement) of the temperature and humidity conditions around the VIP, which have a strong influence on the internal pressure and the moisture content changes as seen before. This task is not easy, as coupled heat and moisture transport in the building element containing VIP is involved. The situation is often simplified by a one-dimensional (centre-of-panel) model. It may be further simplified if one of the following assumptions can be made:

- Constant relative humidity: In (almost) vapour tight cavities containing hygroscopic materials besides VIP a constant relative humidity may be assumed. The problem is then reduced to a transient temperature calculation for the main faces.
- Ambient vapour pressure: In a diffusion open environment that is in direct contact with room or outside air the vapour pressure corresponding to the air temperature and relative humidity may be used.

Once the time dependent boundaries, typically in one-hour steps, are known there are various options for the calculation of temperature - humidity related aging effects. In the following paragraphs three possible approaches are briefly described.

4.5.3.1 Time averaging

In order to calculate an approximate increment of the internal pressure and moisture content the most simple approach is the calculation of the time average values of temperature and humidity conditions around the VIP. The permeation properties for dry air and water vapour as determined by laboratory experiments for constant boundary conditions are then applied for service life estimation as described in section 4.5.2. Obviously the observed non-linearity of the transmission rates with regard to temperature and/or moisture is neglected with the time averaging.

4.5.3.2 Weighted averaging

The non-linearity of transmission rates may be taken into account by including for instance a known Arrhenius-like temperature dependence of the pressure increase rate in the averaging process. The procedure is illustrated by means of permeation data determined for VIP at various temperatures and a constant relative humidity of about 80%, which corresponds to a cavity situation as described before. The pressure increase rate p_a is indicated in Figure 52 in a log (p_a) versus *1/T* plot. The linear shape of the curve clearly indicates an Arrhenius-like behaviour of the acceleration function. Under the assumption that the yearly pressure increase can be superimposed by the time weighted increase at a given temperature/humidity, the Arrhenius fit parameters A and E_a can be used to estimate the yearly pressure increase rate with respect to dynamic boundary conditions with the following weighted average:

$$p_a = \sum_i A \exp\left(-\frac{E_a}{RT_i}\right)\Delta t_i \Big/ \sum_i \Delta t_i = A \exp\left(-\frac{E_a}{RT_{effective}}\right) \quad (39)$$

Due to the exponential temperature weighting factor the effective temperature $T_{effective}$ defined by Equation (39) is always higher than the time average temperature.

A similar approach is applicable to evaluate the yearly moisture accumulation rate X_a, which is due to the exponential temperature dependence of the external vapour pressure. In a diffusion open application, where ambient vapour pressure is always present, the time average of the environmental vapour pressure would be sufficient to select the corresponding yearly moisture accumulation rate.

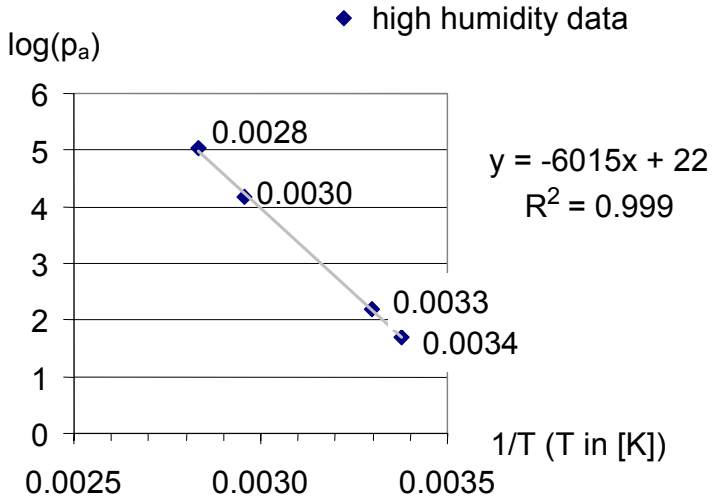

Figure 75: Arrhenius plot of the temperature dependence of the pressure increase rate in the high humidity range (80% RH).

The procedure was applied to a VIP insulated flat roof of a terrace building on a hill side, which is a typical construction in densely populated areas in Switzerland. The climate data from the Design Reference Year (DRY) for Zurich Airport (Switzerland) were chosen. Details of the construction and of the boundary conditions are described in section 4.6.2.1. Calculated results which show the influence of the different averaging methods are shown in Table 40. It can be seen that on the interior VIP surface the arithmetic and the Arrhenius weighted average are the same because of the small range of temperatures (interior air temperature fixed at 22°C). On the exterior surface with more dynamic conditions (from -18 to 44°C) the difference between the weighted and the normal average is about 4 K, giving a significant increase of the transmission rates compared to the non-weighted average. On the other hand, the average load at the interior face is obviously higher than on the exterior face, irrespective of the averaging method.

Table 40: Results of the thermal and aging calculation for the inside and outside surface of a 20 mm VIP layer (size 50 x 50 cm^2) in a terrace construction.

		VIP inside	***VIP outside***
Maximum temperature	*[°C]*	*22.5*	*44.1*
Minimum temperature	*[°C]*	*19.9*	*-18.2*
Temperature (Average)	*[°C]*	*21.5*	*11.9*
Effective temperature (Arrhenius)	*[°C]*	*21.5*	*16.0*
Pressure increase rate (Average)	*[mbar/yr]*	*2.6*	*1.3*
Pressure increase rate (Arrhenius)	*[mbar/yr]*	*2.6*	*1.8*
Moisture accumulation (Average)	*[%-mass/yr]*	*0.21*	*0.09*
Moisture accumulation (Arrhenius)	*[%-mass/yr]*	*0.21*	*0.14*

4.5.3.3 Time integration model

During the service life of a VIP in the course of a day as well as in the course of a year the climatic conditions are permanently changing. Additionally climatic conditions on one side of a VIP differ from those on the opposite side.

To include these effects in a transient model, two enhancements have been applied to the model described in chapter 4.5.2:

To account for the different conditions on both sides of a VIP, the equations in chapter 4.5.1 were modified in a way that adds up the permeation through each side considering the specific climatic condition at these sides. This holds for the permeation through the surface area. For the permeation related to the perimeter in an approximation it was assumed that at one half of the perimeter the conditions are as on the front side of the panel, at the other half as on the rear side.

To calculate the increase in internal gas pressure and in water content under varying conditions the differential versions of equation (36) and (35), describing permeation per time, have to be integrated over time. In practice this mathematical approach was approximated by an accumulation of permeated quantities over short intervals, e.g. 15 minutes, with constant conditions. For each interval different climatic conditions around the VIP as mentioned before as well as the increasing internal amount of water within the VIP was taken into account. According to the temperature gradient across the VIP the relative humidity within the panel varies locally. It was assumed that the vapour pressure does not vary within the VIP. It depends on the temperature of the cold side of the VIP and on the amount of water in the VIP. For details of this more detailed model see [41].

One has to point out that the “dynamic” models described in this report are based on the assumption that the permeation rates instantly establish as measured under stationary conditions. However in the chapter on barrier measurements it has been described that especially for water vapour permeation there is a retardation time of tens of hours or even several days one has to wait until equilibrium for the water vapour permeation rate is reached (e.g. see Figure 32). Under this aspect the models given above still are a crude estimation, especially for the water uptake.

4.6 VIP in buildings and components

4.6.1 VIP in four different wall constructions (ZAE-Bayern)

In recent years several R & D projects were carried out in which vacuum insulation panels were incorporated in buildings [55]. ZAE-Bayern promoted this technique from 1999 by installing about 30 m² of VIP in its new experimental building in Würzburg [14]. During the research project “Vakuumdämmung für Gebäude (Vacuum Insulation for Buildings)” the practical integration of VIP into buildings was further pursued [58].

4.6.1.1 Constructions and sensors used

To measure the climatic conditions, temperature and humidity sensors were mounted onto the front and rear surfaces of VIP in various building constructions. One of these constructions was designed in such a way that the VIP could be removed from it, in order to measure the pressure increase within the VIP as well as the mass increase.

Temperature and relative humidity were measured and recorded once per hour in four different constructions. The thermocouple temperature elements had a precision of ± 0.3°C. The humidity measurement with capacitive film sensors and software-controlled temperature compensation had a precision of ± 2% RH. The integrated VIP were investigated over a period of approximately one year.

The following constructions were employed in the investigations:

- A vacuum-insulated balustrade element in which a VIP was sandwiched between a glass pane and an Al-sheet. The glass pane and Al-sheet were separated by a spacer along the perimeter so that the system could be integrated in a window frame (Figure 76).
- A vacuum-insulated external thermal insulation composite system that was mounted onto a wall made of lightweight concrete (Figure 77).
- A removable wood construction that was screwed onto a wall of lightweight concrete (Figure 78).
- VIP as internal insulation, where the VIP were fastened directly onto the inner side of the wall (Figure 79).

The following figures illustrate the investigated constructions. The positions of the integrated temperature-humidity sensors that are installed on the rear and front side of the VIP (position 1 and 2) are drawn (in the balustrade element only one temperature-humidity sensor were installed at the front side of the VIP).

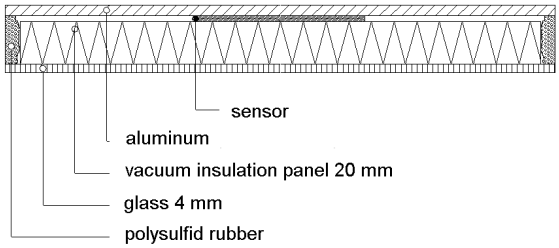

Figure 76: Vacuum-insulated balustrade element, which were integrated into a window frame.

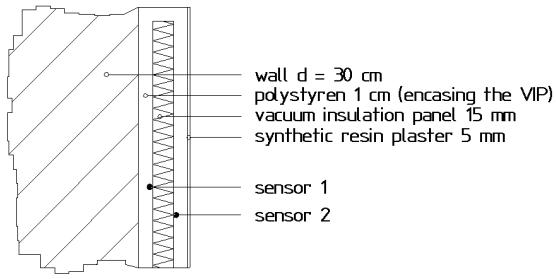

Figure 77: Thermal insulation composite system with polystyrene protected VIP.

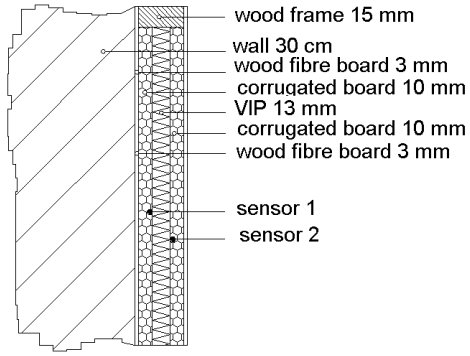

Figure 78: Wood construction on lightweight concrete wall; the VIP were removable so that their pressure and mass increase could be measured.

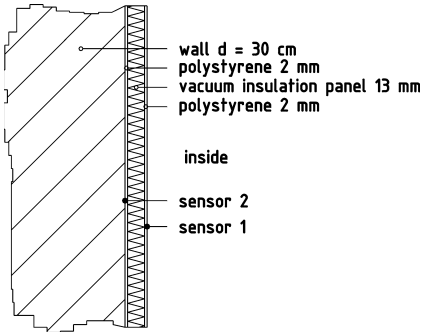

Figure 79: Inside insulation, the VIP were protected by a thin layer of polystyrene (fixed with hot-melt adhesive) and were pasted onto the wall with plaster (for measurement purposes). The sensors were pasted onto the laminate-cover of the VIP.

The thermal insulation composite system and the removable wooden construction were positioned southeastward, while the balustrade element was oriented southward. The wooden construction was opened approximately every three months; the VIP then were removed, the pressure and mass of the VIP were determined, then the VIP were re-installed.

4.6.1.2 Measured temperatures, relative humidity and water vapour pressure

The climatic conditions were measured hourly. For a better display the figures present mean values averaged over 6 hours. Figure 80 shows the temperature, relative humidity and water vapour pressure outside the VIP in the balustrade element as a function of time.

The measurements show strong fluctuations, which can primarily be attributed to the solar insolation. Temperatures of up to 65°C and water vapour pressures up to 50 mbar around the VIP occurred for short periods. The relative humidity in the balustrade element did not exceed values over 60% RH. Most of the time the temperature stayed between 5°C and 15°C and the water vapour pressure was below 10 mbar. Figure 81 gives a histogram of the measured climatic conditions.

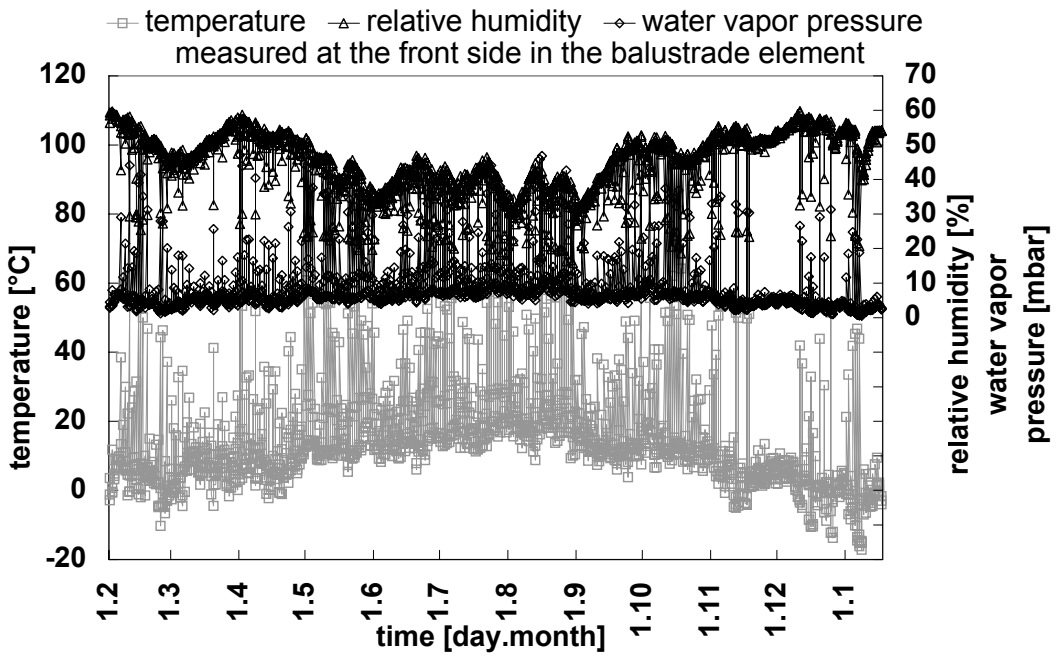

Figure 80: Temperature, relative humidity and water vapour pressure at the front side of the VIP as a function of time; the VIP were integrated into the south-oriented balustrade element (see Figure 76).

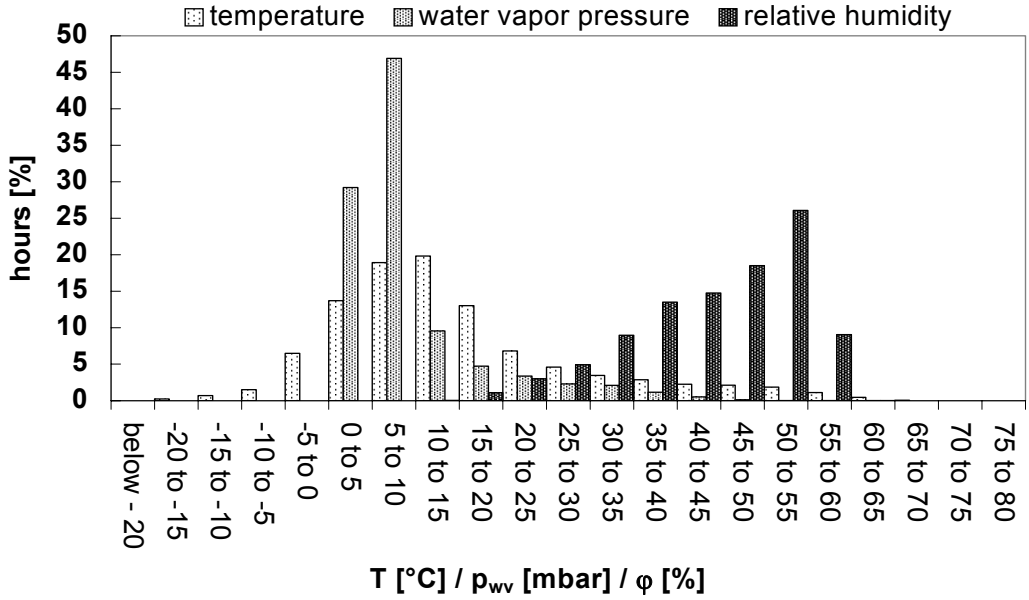

Figure 81: Histogram of the temperature T, relative humidity φ and water vapour pressure p_{wv} measured at the front side in the south-oriented balustrade element.

Figure 82 depicts the temperature, relative humidity and water vapour pressure on the outside of a VIP in the external thermal insulation composite system (see Figure 77) as a function of time.

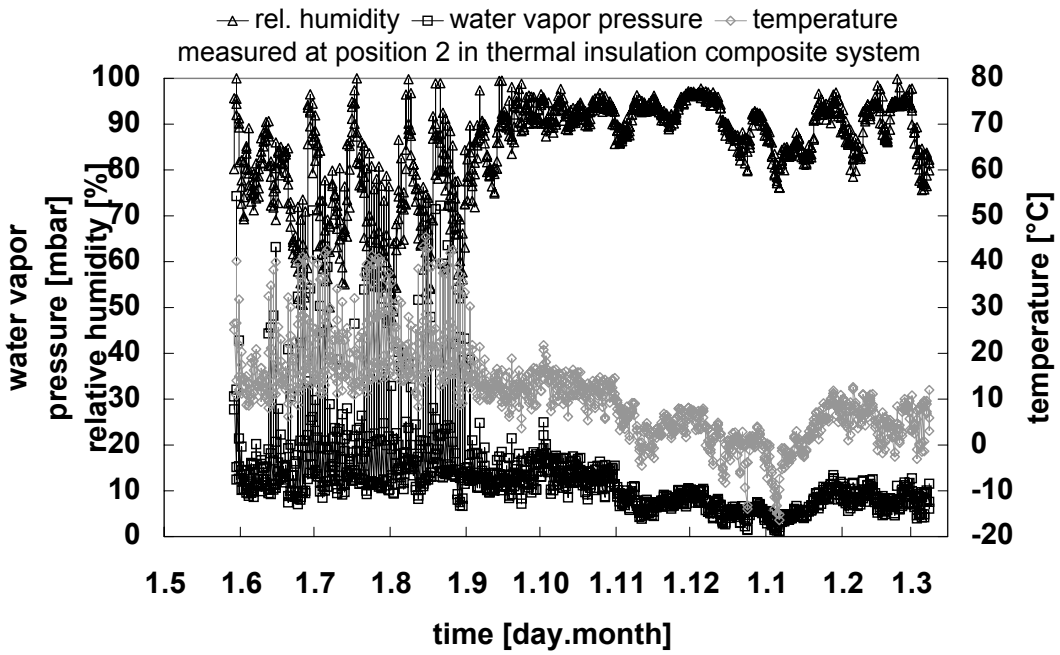

Figure 82: Temperature, relative humidity and water vapour pressure measured at position 2 in the thermal insulation composite system (see Figure 77) as a function of time.

In the summer one may observe large fluctuations in temperature and water vapour pressure. As with a lower sun the façade is structurally shadowed, high temperatures and water vapour pressures no longer occur in September. The relative humidity in general stays above 70% throughout the year. Figure 83 illustrates the histogram associated with Figure 82.

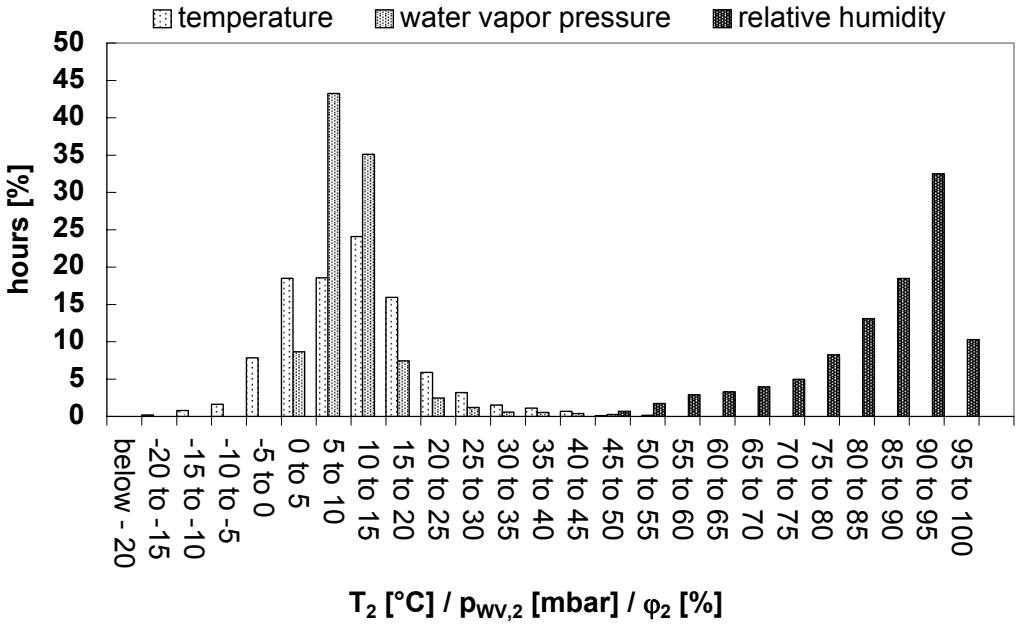

Figure 83: Histogram of the temperature T_2, relative humidity φ_2 and water vapour pressure $p_{wv,2}$ measured in the thermal insulation composite system at position 2 (see Figure 77).

In comparison with the balustrade element, the relative humidity is considerably higher here. High temperatures over 40°C did occur rarely. For the main part of the year, as was also the case with the balustrade element, the temperature and water vapour pressure are between 5°C and 15°C and between 0 mbar and 10 mbar, respectively.

The following two figures show the climatic conditions for the wooden construction (see Figure 78) measured at position 2 (see Figure 84) and at position 1 (see Figure 85).

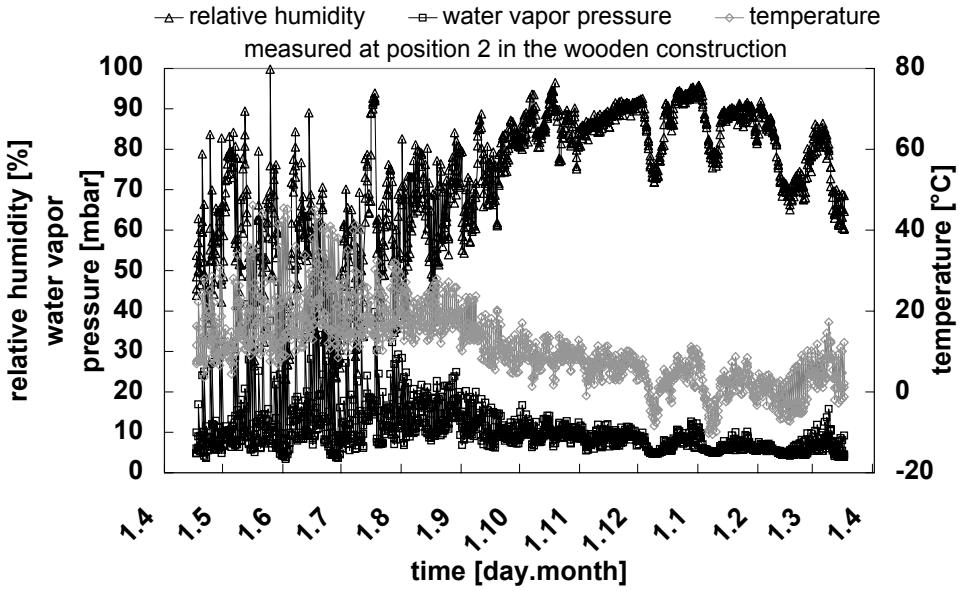

Figure 84: Temperature, relative humidity and water vapour pressure measured at position 2 in the wooden construction (see Figure 78) as a function of time.

In Figure 84 one may observe in the summer, just like in Figure 82, large fluctuations in temperature and water vapour pressure, which no longer occur in September as the façade is structurally shadowed with lower sun. In Figure 85, at the position of sensor 1, the fluctuations in temperature and water vapour pressure are reduced, since the sensor 1 is located between the massive wall and the rear side of the VIP. The relative humidity during summer is higher than in winter time.

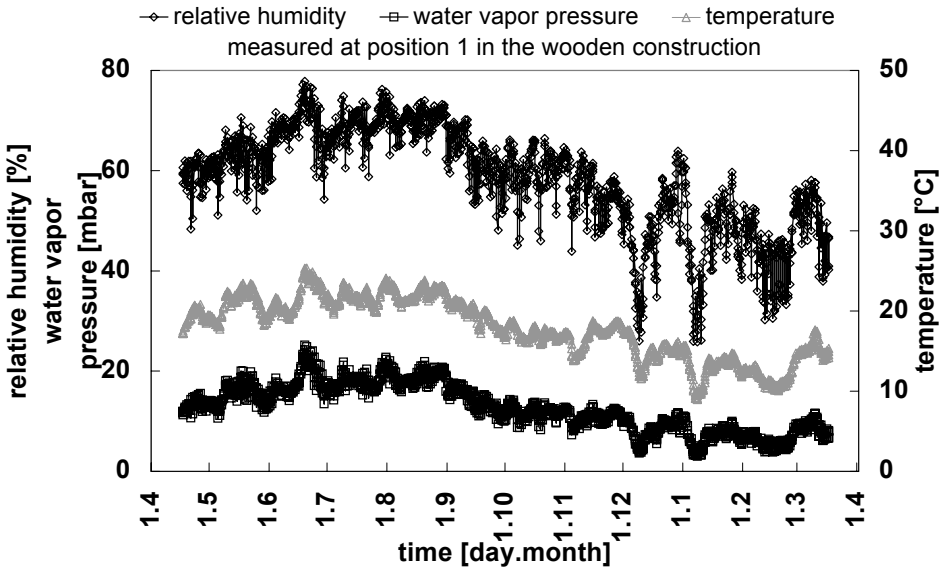

Figure 85: Temperature, relative humidity and water vapour pressure measured at position 1 in the wooden construction (see Figure 78) as a function of time.

Figure 86 shows the histogram of the climatic conditions that occur on the outside of the VIP (at position 2) in the wooden construction.

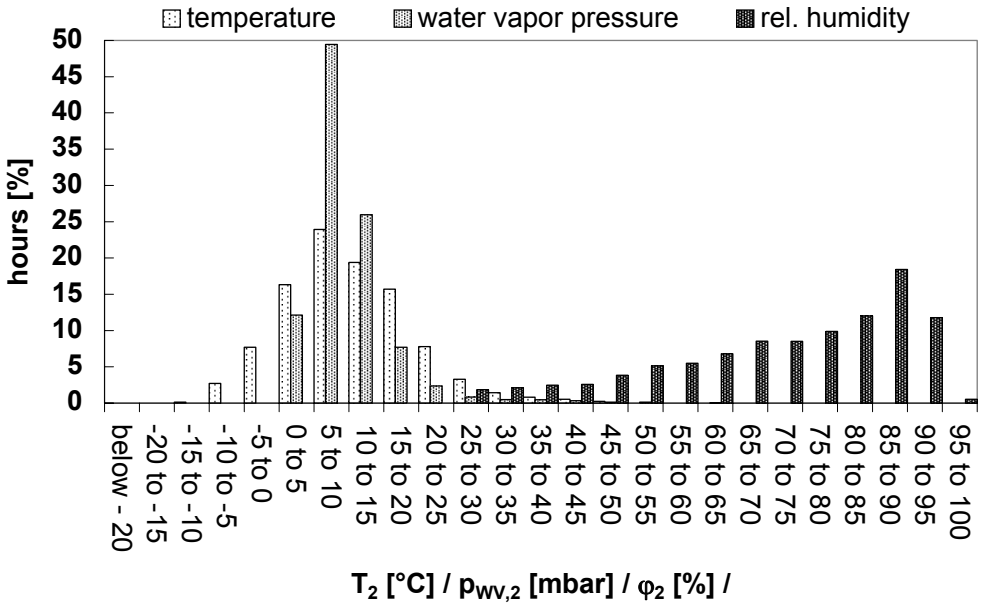

Figure 86: Histogram of the temperature T_2, relative humidity φ_2 and water vapour pressure $p_{wv,2}$ measured in the wooden construction (see Figure 78).

The histogram in Figure 86 is similar to that for the thermal insulation composite system (these constructions were mounted side by side onto the lightweight concrete wall). The relative humidity is somewhat lower. This can be explained by the different sorptive properties of the surface. While, due to its capillary properties, the plaster absorbs some rain, the outside of the wooden construction was painted with a water-repellent layer of lacquer so that the rainwater splashed off.

Table 41 presents the average values of temperature, relative humidity and water vapour pressure at position 1 and 2 of the four construction types within the measurement period.

Table 41: Time mean values for the temperature, relative humidity and water vapour pressure measured derived from sensors 1 and 2 in the four investigated constructions.

	$T_{mean,1}$ [°C]	$T_{mean,2}$ [°C]	$p_{wv,mean,1}$ [mbar]	$p_{wv,mean,2}$ [mbar]	$\varphi_{mean,1}$ [%]	$\varphi_{mean,2}$ [%]
Balustrade element	-	15.2	-	9.5	-	44.2
Thermal insulation composite system	16.8	10.3	13.0	12.1	63.0	84.8
Wooden construction	17.9	10.7	12.7	10.0	58.6	75.3
Internal insulation	20.4	14.5	14.4	15.5	55.1	85.9
Average value	18.4	12.7	13.4	11.8	58.9	72.6

For the balustrade element $T_{mean,2}$ is somewhat higher than for the other constructions. This is due to the black surface and the south orientation. The relative humidity and the water vapour pressure is lowest for the balustrade element, as the system was designed to be nearly vapour-tight. The temperature difference between position 1 and 2 amounts to about 6

to 7 K, the water vapour pressure around the VIP is about 12 mbar and the relative humidity between 60 and 80%. The average values determined from measurements in four different constructions represent typical climatic conditions in building constructions.

4.6.1.3 Measured increase in pressure and water content on the VIP in the wooden construction

A total of 9 VIP of dimensions (36 x 64 x 1.3) cm³ were investigated. Three different laminates were used and three VIP were produced with each laminate type. The laminates were an aluminum laminated foil (AF) with a 8 µm thick aluminum foil laminated on both sides with two polymer films, and two aluminum coated multi-layer films (MF1 and MF2) consisting of laminated polymer foils coated with a 30 – 80 nm thick aluminum layer. The 9 VIP were integrated into the wooden construction. Figure 87 illustrates the pressure and mass increases measured within one year.

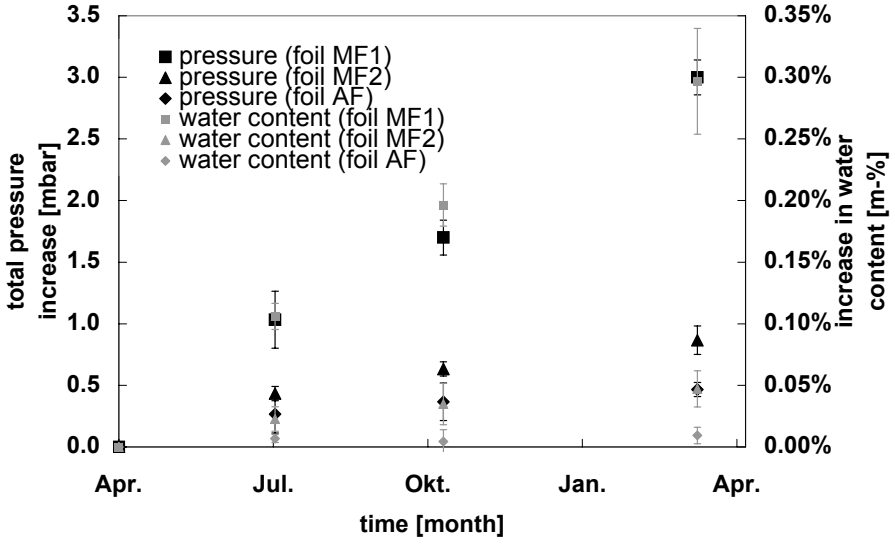

Figure 87: Measured pressure and mass increases on the VIP integrated into the wooden construction; each measurement point represents the average over 3 measurements; the error bars indicate the deviations between the three measurements.

Large pressure and mass increases were measured on the VIP with the film MF1, an Al-coated film of low quality. The pressure increases within the VIP with the film MF2 ranks second, while foil AF leads to the smallest pressure increase. A similar behavior holds for the mass increases.

4.6.1.4 Comparison of prediction and measurements

In chapter 4.5 a transient model was presented, which describes the increase in pressure and water content within the VIP as a function of time taking into account all the fluctuations of the climatic conditions. Regarding built-in VIP the different climatic conditions on the rear- and front-side of the VIP (position 1 and 2) are considered [40].

The permeances for air and water vapour for the laminates AF, MF1 and MF2 depend both on temperature as well as on humidity. While the temperature dependence of the permeances can be described by an Arrhenius relation, the functional dependence on the humidity is unknown and is thus neglected. The activation energies for air $E_{a,air}$, which are

assumed to be the same for surface and perimeter permeances, are given in Table 43. The temperature dependence for water vapour can be neglected for the laminates AF, MF1 and MF2. The performed calculations are based on the perimeter and surface transmission rates given in Table 42, which were determined at 23°C / 75% RH for the laminates AF, MF1 and MF2 [40].

Table 42: Surface and perimeter transmission rates for air and water vapour of the laminate covers AF, MF1 and MF2 [40], which were taken as a basis for the calculations.

	$WVTR_A$ *[g/(m²·d)]*	**ATR_A** *[cm³/(m²·d)]*	**ATR_L** *[cm³/(m²·d)]*
AF	0.0006 ± 0.0004	-	0.0018 ± 0.0003
MF1	0.035 ± 0.002	0.016 ± 0.008	0.0080 ± 0.0018
MF2	0.0086 ± 0.0010	-	0.0039 ± 0.0011

Table 43: Activation energies for air of the laminates AF, MF1 and MF2 [48].

	AF	**MF1**	**MF2**
E_a *[kJ/mol]*	26 ± 2	40 ± 7	28 ± 3

For the model calculation a computer program “VIP-Prog” was written, which allows to calculate the pressure increase and the mass increase with time and climatic conditions.

Figure 88 shows the pressure increases with time that were calculated with the program “VIP-Prog” for the VIP (size: (64 x 34 x 1.3) cm³) with the laminates AF, MF1 and MF2 integrated into the wooden construction (see Figure 78). As climatic conditions the hourly-measured values for temperature and relative humidity as well as the water vapour pressure according to Figure 84 were taken. The calculated air pressure increase could not be directly compared with the measured pressure increase which is the sum of partial pressures of air and water vapour. Therefore the corrected pressure increases ($p_{air} = p_{total} - \varphi(X_W) \cdot p_{wv,saturated}(T)$) are shown in Figure 88. For X_W the measured water content, for $\varphi(X_W)$ the measured sorption isotherm and for T a value of 20°C were assumed.

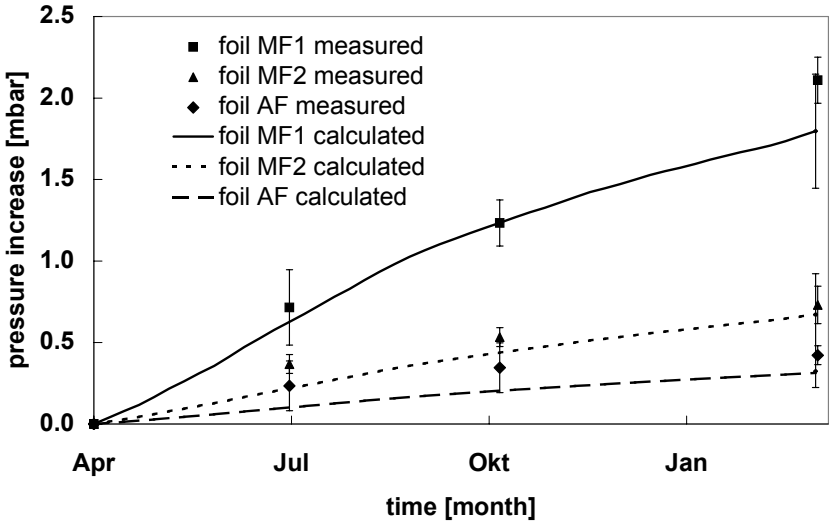

Figure 88: Comparison of measured and calculated air pressure increases as function of time in the wooden construction for the VIP with laminates AF, MF1 and MF2 and with dimensions (64 x 34 x 1.3) cm³. Each measurement point represents the average over 3 measurements; the error bars at the measured points indicate the deviations between the three measurements. The error bars at the end of the calculated lines result from the uncertainties given in Table 42.

It can be seen that the measured data agree well with the calculated dependence. The model calculations with linearly extrapolated pressure increases calculated with equation (36) with a constant air transmission rate at constant climate also are compared. Table 44 gives the pressure increases at the end of the testing period of 334 days, which result from the model calculation and from linear extrapolations of the pressure increase according to equation (36). Two linear extrapolations are given; one with air transmission rates at 23°C (see Table 42) and the other with air transmission rate converted to the annual average temperatures using the Arrhenius relation (see Table 41).

Table 44: Increases in air pressure of the VIP integrated into the wooden construction at the end of the measurement period of 334 days according to the model calculation and according to a linear extrapolation with equation (36) with constant air transmission rates at 23°C (see Table 42) and with air transmission rates corresponding to the average temperature (see Table 41).

	Pressure increase *[mbar]*		
	Foil AF	**Film MF1**	**Film MF2**
Model calculation	0.32	1.8	0.67
Linear extrapolation at 23°C	0.42	2.7	0.91
Linear extrapolation at annual average temperature	0.30	1.6	0.63

The model calculations and the linear extrapolations at average temperatures do agree well. The differences between the model calculation and the linear extrapolation at 23°C indicate the influence of the temperature on the pressure increase. The pressure increases at 23°C are about 30 to 50% larger than the pressure increases at the real ambient temperatures. They can be used as upper estimates. With a reliable knowledge of the average temperature, the pressure increase can be estimated using a linear extrapolation. To determine the climatic conditions on the laminate-cover of the VIP it is not necessary to perform measurements under real built-in conditions. These conditions can be determined using non-

stationary thermal-humidity simulation programs [60], with which the temperature and the humidity inside of building constructions can be calculated in relation to the outside climatic conditions.

4.6.1.5 Model comparison for increase in water content

Figure 89 shows the measured increase in water content as a function of time. Also the calculated values for the VIP with laminates AF, MF1 and MF2 that were integrated into the wooden construction are shown. A clear difference can be seen between measurement and calculations. For the foil AF the mass increases are within the measurement fluctuations. A cause for this deviation is that the model neglects an explicit dependence of the water vapour permeance on temperature and relative humidity. As illustrated in [48] and [40], the water vapour permeance can depend strongly on the humidity. As the relation between the water vapour permeance and humidity is not known a constant permeance is assumed in the model.

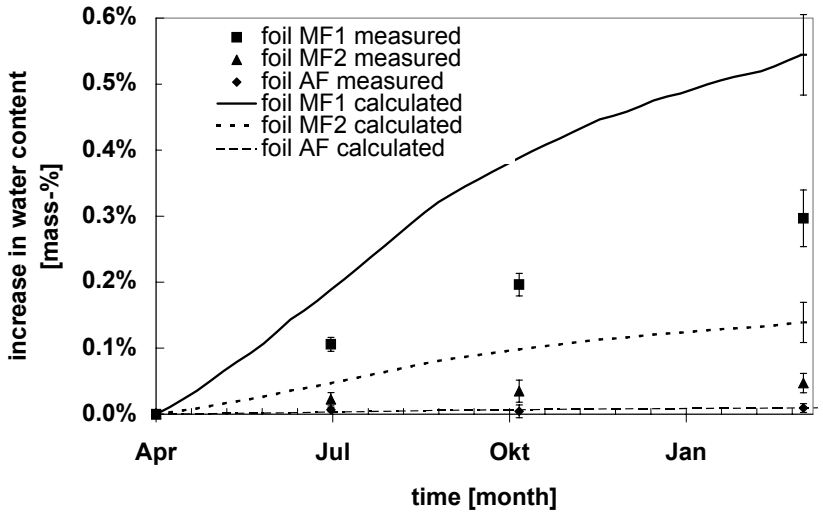

Figure 89: Comparison of the measured and calculated increases in water content as a function of time for the VIP with laminates AF, MF1 and MF2 and dimensions (64 x 34 x 1.3) cm³ integrated into the wooden construction (see Figure 78). Each measurement point represents the average over 3 measurements; the error bars at the measured points indicate the deviations between the three measurements. The marked error bars at the end of the calculated lines results from the uncertainties given in Table 42.

In the model the climate was taken into consideration via the time-dependent water vapour pressures around the VIP. For the linear extrapolation at constant climate (23°C / 75% RH) a water vapour pressure of 21 mbar is assumed. Table 45 shows the measured and calculated water contents at the end of the testing period (334 days).

Table 45: Increase in water content of the VIP in the wooden construction from the model calculation, linear extrapolation and measurement at the end of the testing period of about one year (334 days).

	Increase in water content *[%-mass]*		
	Foil AF	**Film MF1**	**Film MF2**
Linear extrapolation at 23°C / 75% RH	0.02	1.07	0.26
Model calculation	0.01	0.54	0.14
Measurement	0.01	0.30	0.05

The water contents according to the linear extrapolation are several times higher than the measured values. The water contents determined with the model are about half of the values resulting from linear extrapolation, but are still higher than the measured water contents, particularly for VIP with Al-coated films. Therefore, for a reliable prediction, the dependence of the water vapour permeance on temperature and relative humidity must be taken into consideration.

4.6.1.6 Application of the model to predict mass increase over long time periods

If one considers periods of several decades, the mass increase by infusion of water vapour levels off. This happens when the water vapour pressure inside the VIP approaches the mean level of the water vapour pressure on the outside. The equilibrium level of the water content in the VIP thus depends on the climatic conditions. Based on the above model, Figure 90 shows the calculated increase in water content of a VIP with film MF1 and size (64 x 34 x 1.3) cm³ for the three different climatic conditions, that were measured in the balustrade elements, in the thermal insulation composite system and in the wooden construction. The film MF1 was chosen as VIP-cover to get a fast mass increase within the simulated time span.

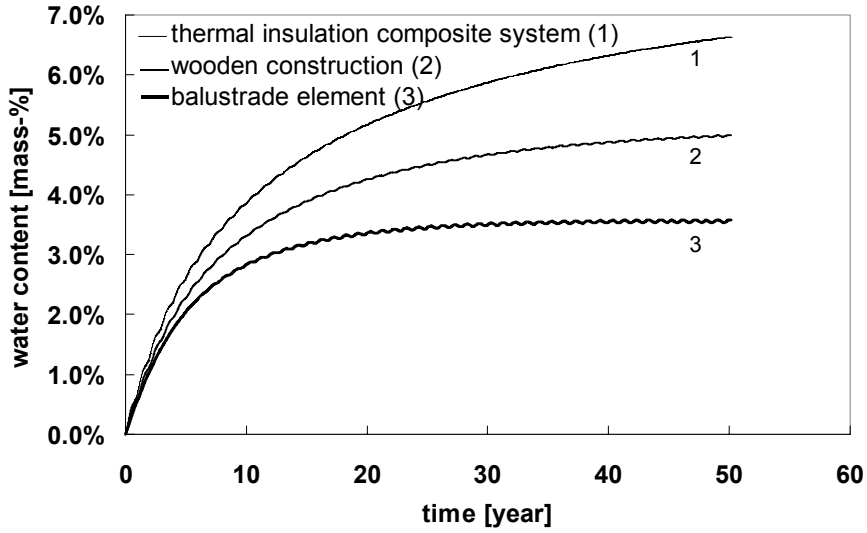

Figure 90: Calculated water content as a function of time of VIP with film MF1 and panel size (64 x 34 x 1.3) cm³ in different constructions as marked (1) thermal insulation composite system, (2) balustrade element and (3) wooden construction, under actual climatic conditions around the VIP.

Depending on the considered constructions, different saturation levels of water content between about 3 and 7%-mass result. The higher the mean humidity measured around the VIP (see Table 41), the higher the saturation level becomes. Taken into account the influence of the water content on the thermal conductivity ($0{,}5 \cdot 10^{-3}$ W/(m·K) per %-mass water content [42]), one expects a humidity-related increase in thermal conductivity between (1.5 and 3.5)$\cdot 10^{-3}$ W/(m·K)after 50 years.

4.6.2 VIP in a flat roof (EMPA)

4.6.2.1 Service life estimation

The procedure of calculating an Arrhenius weighted average temperature (see 4.5.3.2) to estimate the service life of VIP in building applications was applied to a terrace building on a hill side, which is a typical construction in densely populated areas in Switzerland (see Figure 91).

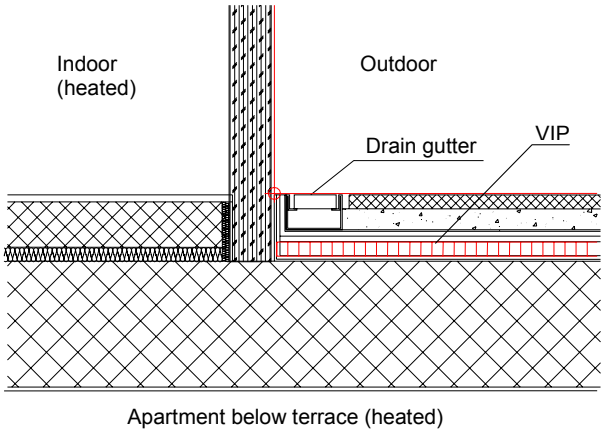

Layer	d [mm]
Concrete plate	20
Crushed gravel	30
Fleece	2
Bituminous water barrier	7
Protective layer	8
VIP	20
Protective layer	5
Water barrier	3
Concrete	180
Interior plaster	5

Figure 91: Cross section and material layers of a walkable terrace with a thin VIP insulation. A solar absorptance of 65% was assumed for the outside surface in the thermal calculation. Underneath are heated rooms of the apartment in the lower storey.

Underneath the VIP insulated accessible flat roof are heated rooms of the apartment below. In spite of potential risks with water penetration few ten thousand square meters of VIPs are installed in this type of roof construction by now. The reason for this trend is that the floor height inside and outside can be made equal, even under the stringent heat resistance requirements for the outside part of terrace roof. Surface temperatures on both sides of the VIP layer were calculated by means of the building simulation tool HELIOS [63]. The program calculates hourly values of temperatures and heat fluxes in a single zone and on the surrounding wall surfaces depending on the indoor temperature control strategy and outdoor climate data such as air and sky temperature, wind speed, and solar irradiance and absorption on outer surfaces.

In the calculation a constant indoor temperature of 22°C was assumed for simplicity. For the outdoor climate the design reference year for Zurich airport (Switzerland) was chosen. The solar absorptance of the outside surface was set to 65%. In Figure 92 temperatures on the two main faces of the 20 mm VIP are shown from the beginning of October until the end of September. On the inside the temperature is quite constant according to the boundary condition, while the temperature on the outside varies between about -18°C up to +44°C. The temperature histogram in 2-degree steps is indicated also in Figure 92.

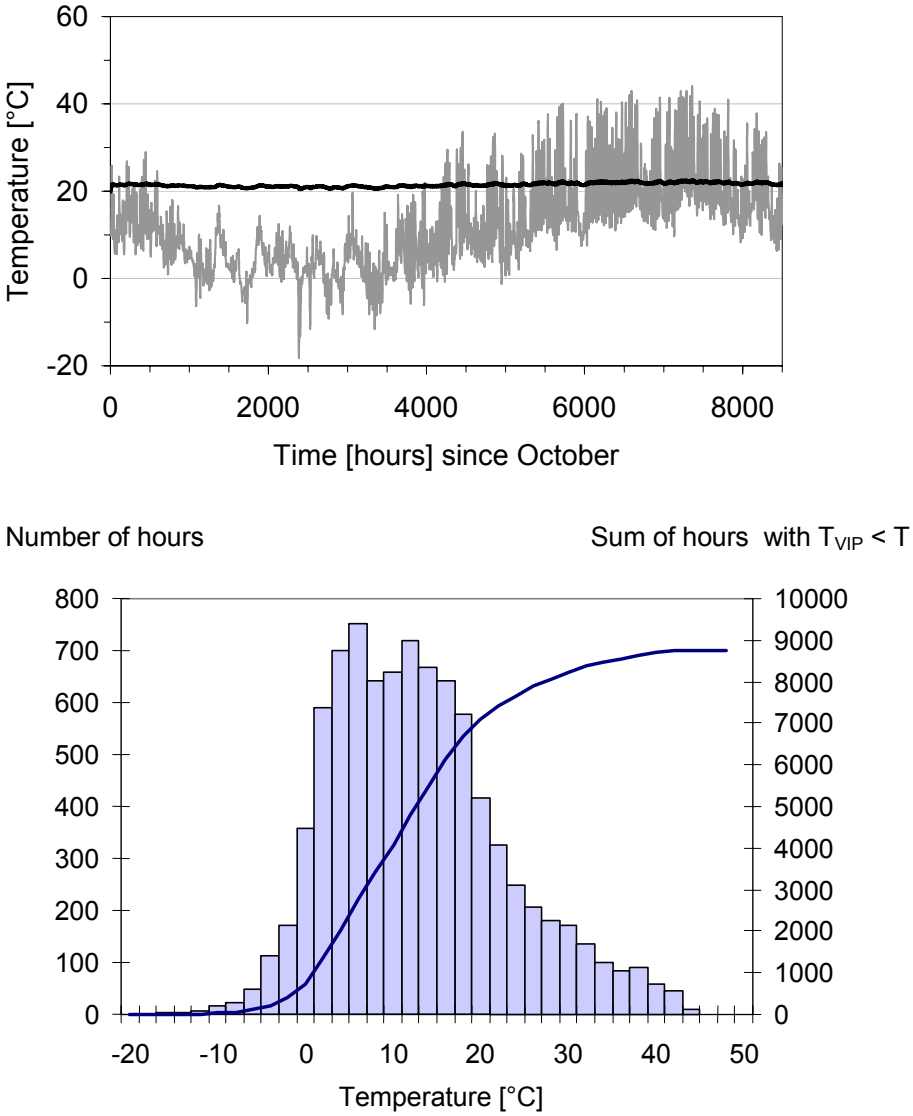

Figure 92: Surface temperatures of a VIP in a terrace insulation application for a Swiss design reference year (Zurich Airport), starting on 1st of October (a), and (cumulative) temperature histogram of hourly temperature values on the outside surface of a VIP in the terrace application (b).

The temperatures and the respective number of hours of occurrence were fed into Equation (39), along with the parameters obtained from the Arrhenius fits. A panel size of 50 x 50 cm^2 was modelled by scaling parameter A according to the size dependent laboratory aging results. The results of the thermal and the aging evaluation are given in Table 46.

Table 46: Results of the thermal and aging calculation for the inside and outside surface of a 20 mm VIP layer (size 50 x 50 cm²) in a terrace construction

		VIP inside	VIP outside
Maximum temperature	*[°C]*	*22.5*	*44.1*
Average temperature	*[°C]*	*21.5*	*11.9*
Effective temperature (Arrhenius)	*[°C]*	*21.5*	*16.0*
Pressure increase rate	*[mbar/yr]*	*2.5*	*1.7*
Moisture accumulation rate	*[%-mass/yr]*	*0.21*	*0.14*

The effective temperature at the inside surface, close to the time average value, is about 21.5°C. On the outside surface, the effective temperature of 16.0°C is clearly higher than the time average of 11.9°C due to the temperature peaks in summertime. Nevertheless, the high-temperature periods are short enough to keep the average stress lower on the outside than on the inside surface. Averaging the results of both sides, the mean pressure increase rate pa is about 2.1 mbar per year, and the initial moisture accumulation rate X_a is 0.18%-mass per year. On a long-term scale saturation effects with respect to moisture accumulation have to be accounted for. Assuming a constant slope of the sorption isotherm ($s \approx 0.08$%-mass per % RH, see Equation (17)) the yearly change of the moisture content may be written

$$\dot{X}_w = \frac{1}{\tau}\left(X_{w,equi} - X_w(t)\right) \tag{40}$$

Xw,equi: equilibrium moisture content (= $s\ \varphi_{amb}$), %-mass
τ: $X_{w,equi} / X_a$ (saturation time constant)
φamb: relative humidity,%

The solution for constant parameters is:

$$X_w(t) = X_{w,equi}\left(1 - exp(-t/\tau)\right) \tag{41}$$

Thus the saturation time constant τ is 35.6 years for the equilibrium moisture content $X_{w,equi}$ of about 6.4%-mass at 80% RH According to Equations (18), (19) and (21) the yearly thermal conductivity increase becomes

$$\Delta\lambda(t) = 0.035 \times 2.1t + 0.50 \times 6.4\left(1 - exp(-t/35.6)\right) \tag{42}$$

in 10^{-3} W/(m·K), and time t is in years (Figure 93). Hence the thermal conductivity will be increased by $4.0 \cdot 10^{-3}$ W/(m·K) after 31.6 years under these rather unfavourable assumptions.

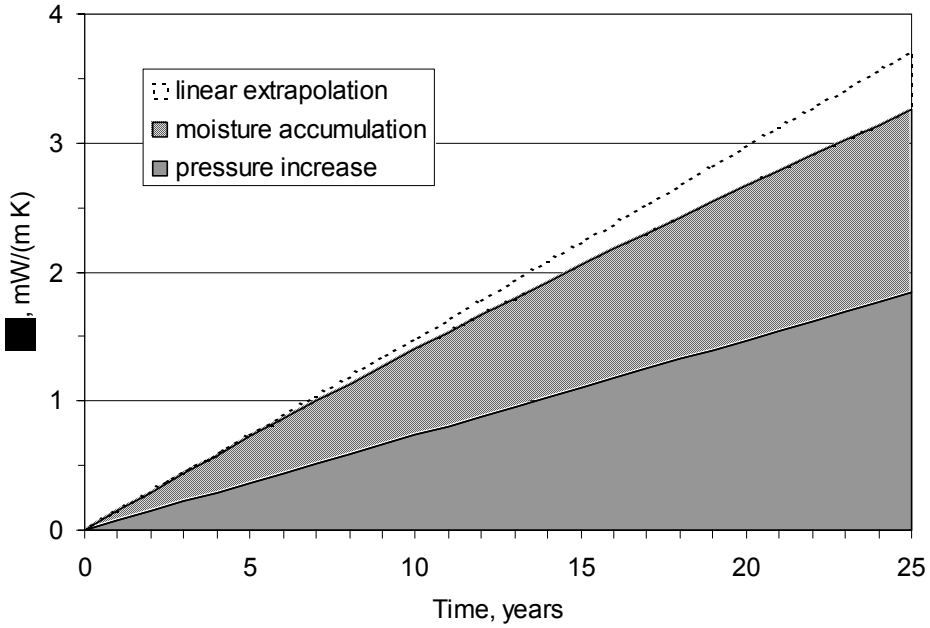

Figure 93: Increase of the thermal conductivity of a VIP terrace insulation due to pressure increase and moisture accumulation.

A similar calculation was made for an external thermal insulation compound system (ETICS) often applied on concrete or masonry walls in Central Europe. Thick mineral wool or polystyrene foam boards are normally used. The standard thermal insulation board was replaced by a 20 mm VIP covered by a 10 mm polystyrene layer on both sides. Of importance for the dynamic behaviour is a sufficient heat buffering capacity of the outside rendering. With a three centimetre mortar layer, the yearly effective temperature – dependent on the wall orientation – does not exceed 15°C for similar boundary conditions as in the terrace calculation (solar absorptance 35%). That is, reasonable service life can be expected also for this application.

In summary it was found that the temperature and moisture loads in proper flat roof and façade applications should not be critical for Swiss climate conditions, as long as temperature peeks are smoothed out by thermal inertia to avoid temperatures above 50 to 60°C.

However, it shall be emphasized that no other aging mechanisms but temperature and humidity are included in this aging considerations. For instance, frequent occurrence of condensation on surfaces or along joints between VIP edges could cause aging effects not covered by the underlying acceleration function. More detailed construction performance calculations will have to include at least two-dimensional heat and moisture transport in order to evaluate condensation risks on VIP surfaces or joints. The relevance of other stresses, e.g. of mechanical and/or chemical origin, and the correlation between laboratory based service life prediction and real world behaviour can be assessed only by comparison of laboratory data with real long term performance data from installed VIP.

4.6.2.2 Monitoring of a VIP insulated flat roof

In order to verify service life models and to assess the importance of additional real life stresses effective on installed VIP a monitoring study of a flat roof with VIP insulation was

started in June 2004. Two square fields with VIP of different size were installed and carefully sealed on an existing inverted roof construction near Zurich

Figure 94: Installation and equipment of a VIP area on a flat roof.

The layer sequence was similar to that in Figure 91. One field was equipped with temperature and humidity sensors on the indoor and the outdoor faces near the centre of the panels and at the cross joints. The other field was not equipped but prepared for repeated opening. As often in Swiss climate there was a little rain shortly before the initial installation, so the protective outer rubber layer was slightly wetted (but cleaned again before installation of the VIP).

Climate conditions and installed sensors are monitored in hourly steps. One area has been opened repeatedly (third time in December 2004) to take out panels for internal pressure and moisture content measurement in the laboratory. First monitoring data are displayed in Figure 95.

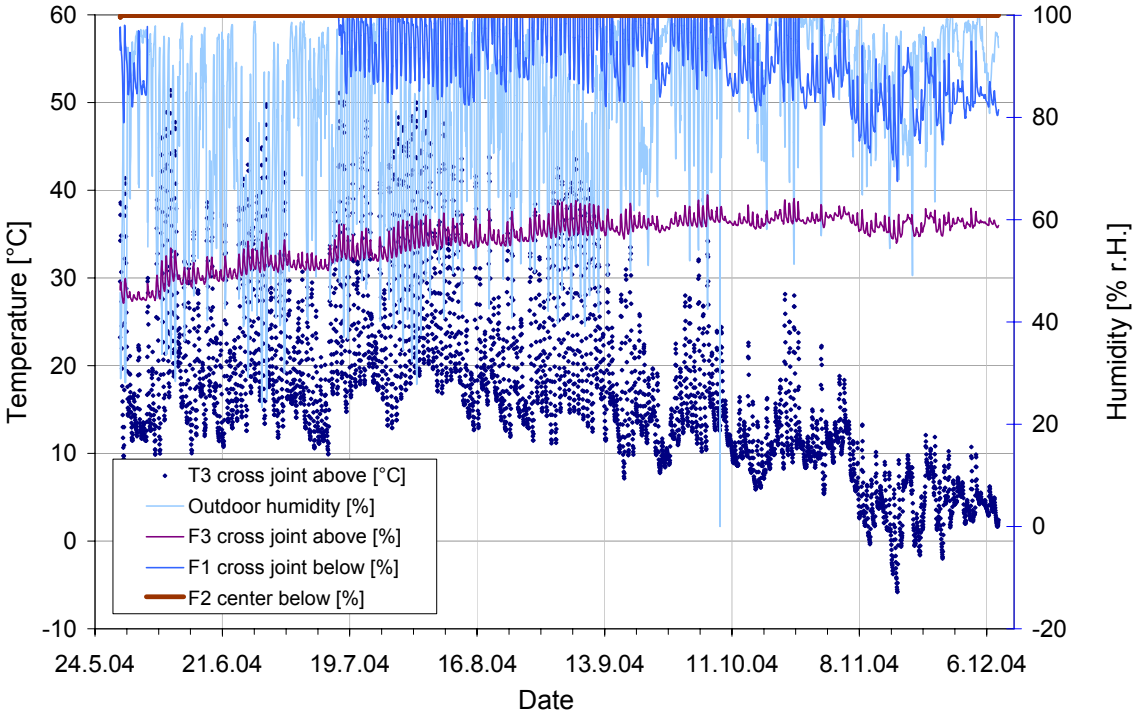

Figure 95: Temperatures and relative humidity measured on VIP surfaces and joints.

The environmental data show that the assumption of a closed cavity applies quite well: the relative humidity is almost constant on both sides of the panel. The humidity on the lower face is fixed to saturation. In fact the interface was found wet when the panel was removed again. This indicates that the conditions during installation are essentially conserved in a sealed construction, although the surfaces have been dried as far as possible. After a significant increase of the internal pressure and moisture content the values have been rather constant between the second and third measurement. For a detailed analysis of the results more data are required.

4.7 Summary "Panel"

The thermal conductivity λcore of a well evacuated dry VIP with a fumed silica core is typically about 0.004 W/(m·K) after production. As the low internal pressure is not in equilibrium with the environment, pressure gradients are present that act as driving forces for the intrusion of atmospheric gas (essentially N_2, O_2 and H_2O). In this context one might distinguish between aging and durability in the following sense: aging is a continuous process of performance degradation due to (normally) slow permeation of atmospheric gas molecules through the imperfect barrier, resulting in a non-reversible pressure increase and moisture accumulation in the hygroscopic VIP core. In contrast, durability is the ability of a VIP to withstand chemical or mechanical impacts that would cause failure of the barrier envelope, thus changing the internal low-pressure state within a short time by severe damage or rupture of the barrier.

Temperature and humidity dependent aging was investigated in detail for a wide range of environmental conditions and different products. It was found that the aging speed depends on a number of parameters such as barrier material, panel dimensions and temperature-

humidity conditions. A weak-point of polymer based high quality barriers is their water vapour permeability that takes place throughout the whole envelope surface. Dry gas permeation is much slower and mainly related to the panel perimeter. If a time span of 25 years and typical environmental conditions (23 to 25°C and ambient vapour pressure) are taken as a basis for the long-term performance (in analogy to European Standards on thermal insulation products) it can be concluded that the pressure increase will be rather linear over the whole period, whereas the moisture content could approach the saturation range (about 4%-mass) within this time period. Moisture equilibrium under normal conditions is basically acceptable, but must be accounted for by a respective increment on the initial thermal conductivity.

Maximum values (approximate) for VIP with actual multi-layer metallized polymer laminate barriers, measured or calculated from laboratory based aging experiments, are given in Table 47. Applying known relations for the pressure and moisture impact on the thermal conductivity, maximum values for the thermal conductivity after 25 years are given in the table as well. These values are thought to be on the safe side in applications with VIP surface temperatures and vapour pressures in the range of ambient or indoor air.

Table 47: Aging characteristics for SiO_2-VIP with polymer based multiple metallized barrier (safe values).

		50 x 50 x 2 cm^3	**100 x 100 x 2 cm^3**
Pressure increase	[mbar/yr]	< 2.0	< 1.0
Moisture accumulation (initial)	[%-mass/yr]	< 0.2	< 0.2
Thermal conductivity λ_{core} (25 yr)	[W/(m·K)]	< 0.008	< 0.007

Service life prediction models based on panel aging data have been developed and partly compared with monitoring data. A preliminary observation is that the calculated pressure increase seems to fit quite well, whereas the measured moisture accumulation is somewhat less than predicted.

Regarding durability the risks for VIP in suitable building applications occur mainly before or during installation. A certain failure rate is present at the production plant, caused by material imperfections or processing errors. This type of failure can be largely avoided by quality control as well as by storing the panels during a specified time under defined conditions and checking them before they are shipped. It can be stated that the number of damaged or defective panels leaving the production plant was substantially reduced in the last few years. The figure is roughly assumed to be less than one percent. More frequent failures occur during transportation and handling of the panels until they are safely installed. Without protection the envelope is highly sensitive to mechanical impact, especially to point loads e.g. by sand grains, bricks or stone fragments, or other sharp objects including tools and corners of other panels. Once installed workmanlike, failure risks are observed to be really low.

5 Quality assurance, product declaration and design values

5.1 General aspects

Quality assurance for a product, i.e. activities to make sure as good as possible that performance characteristics stated for a product are “true”, is essential for various parties involved:

- The manufacturer is responsible that his product fulfils the specification he claims. If the product would fail the specification problems with customers and competitors would frequently cost a lot of money, and the product would not be successful in the market.
- The customer wants to be assured that the product does have the properties he pays for. Otherwise he could buy a cheaper product or he would need a better product.
- Regulatory authorities are demanding “true” product specifications for various reasons such as health, safety, energy conservation and environmental aspects.

One part of a quality management consists of documented rules that define responsibilities, staff requirements and standard procedures to insure quality requirements in the production process (including quality control of raw materials, traceability of the production process, and procedures in case of detection of faulty products). Another part is the definition of relevant product properties, respective test procedures and specification of performance levels that shall be valid for the final product (or eventually a semi-finished product). Furthermore testing conditions and frequencies for the surveillance of those properties are fixed, and the measured values are collected in a suitable database.

For most building products and construction assemblies this second part dealing with technical characterisation and specification of performance levels is covered by standards (e.g. ASTM, EN, and ISO). Standards are favourable since physical quantities, test procedures and conditions are defined in a harmonised way, thus allowing for product comparison and selection of an appropriate product in accordance with performance requirements for a certain application. In the framework of thermal insulation there exists for instance a series of European and International standards on the specification and surveillance of product properties. A so-called “product standard” [64] contains clauses on specification requirements, test methods to be applied, definition of a designation code, and prescriptions on factory production control, evaluation of conformity, and marking and labelling.

It should be noted that the assessment of conformity with an EN thermal insulation product standard is usually based on a certification procedure including an “initial type test” (ITT) partly performed by an accredited (EU notified) independent testing lab. A conformity certificate is then issued by the accredited (EU notified) certification body. In other fields testing and conformity declaration may be within the authority of the manufacturer.

After the initial conformity evaluation quality control is first and last a permanent task for the manufacturer. Regular third party surveillance of essential properties of thermal insulation products such as reaction to fire or thermal resistance is established in some European countries, but this is not an EN conformity requirement and therefore politically questioned for the reason of trade restrictions.

Looking at the duration of about 15 years for European standardisation of conventional thermal insulation products it seems to be a long way to standardisation of VIP in building

applications. An existing ASTM standard on specification of VIP [65] is focused on confined space applications, such as transportation, equipment, and appliances. Within this project it was not possible to do a normative work for VIP. In the following sections EN 13165 for PU is taken as a model for discussion, as many aspects are quite similar.

5.2 Factory production control, test methods

Since there are various types of VIP and production techniques only general considerations are made here. It is clear that essential properties must be checked regularly either on a sample or on each panel shipped by the manufacturer. In the following table properties and test methods are given in accordance with EN 13165 (where relevant for VIP) with some remarks for VIP. The test methods are more or less applicable to VIP without major changes. The testing frequencies are as in the PU standard, i.e. for a large continuous production line. Frequencies for a VIP production line should be defined by the manufacturer. ITT means that the property is determined once during an initial product assessment, or if production parameters are changed that may influence the product characteristics.

Table 48: Factory production control according to EN 13165 (PU rigid foam), with remarks for VIP

Property	Test method	Testing frequency
Thermal resistance, thermal conductivity (initial value)	ISO 8301/8302, EN 12667 (guarded hot plate, heat flow meter or equivalent)	1 per 24 h
Length & width	EN 822	1 per 24 h
Thickness	EN 823	1 per 24 h
Squareness	EN 824	1 per 24 h
Flatness	EN 825	1 per 24 h
Dimensional stability under specified temperature and humidity conditions	EN 1604 (for PU: 48 h at 70°C, 90% RH, 48 h at -20°C)	ITT
Compressive stress at 10% deformation	EN 826	1 per 24 h
Tensile strength perpendicular to faces	EN 1607 (if relevant in applications)	ITT
Compressive creep	EN 1606	ITT
Reaction to fire	c.f. next section	depending on fire class
Accelerated aged value of thermal conductivity	c.f. next section	1 per 2 years

The following properties and test methods are recommended in addition for VIP:

Table 49: Specific properties for quality control of VIP

Property	Test method (e.g.)	Testing frequency
Apparent core density	EN 1602	1 per production lot
Moisture content of the core (before evacuation)	EN ISO 12570	1 per production lot
Internal pressure (before shipping)	Lift-off method or correlated method	1 per production lot (possibly on each panel)
Seal strength	DIN 55529 ASTM F1921-98	1 per production lot
Moisture content increase per year	EN ISO 12570 (standard size)	ITT
Pressure increase per year	Lift-off method or correlated method (standard size)	ITT
Behaviour under point	EN 12430	ITT

Quality control of the barrier material is clearly a task of the barrier manufacturer. The following set of tests is reasonable for polymer based barriers:

Table 50: Possible factory production control for VIP barrier materials

Property	Test method	Testing frequency
Adhesion strength of metallization	e.g. DIN 53357	according to quality control of the barrier manufacturer
Adhesion strength of lamination	e.g. DIN 53357	according to quality control of the barrier manufacturer
Integrity of metallization	Manufacturer specific method	according to quality control of the barrier manufacturer
Water vapour transmission rate	c.f. film section	according to quality control of the barrier manufacturer
Oxygen transmission rate	c.f. film section	according to quality control of the barrier manufacturer

Additionally special procedures may be developed for the test of laminates used for VIP fabrication which also include e.g. mechanical stress during the processing, for instance by producing VIP with a core material that is much more sensitive to the internal gas pressure. These tests may be performed by the VIP manufacturer.

5.3 Product declaration

The data produced for factory production control (either ITT or continuous surveillance) is the basis for product specification. Typically it is a subset of performance values that is of practical interest to the public. The declared “official” values are mostly understood as limit (“better than”) values that are basically valid for the whole production. Thermal insulation standards

contain quite detailed requirements on the set of performance characteristics, classification schemes and rules for product specification and labelling. The latter is shown for the PU EN standard in Table 51. Taking this standard as a basis, declaration requirements for VIP are briefly discussed in the following paragraphs.

Table 51: Mandatory labeling information according to EN 13165 (PU rigid foam)

product name or other identifying characteristic
name or identifying mark and address of the manufacturer or his authorised representative
year of manufacture (the last two digits)
shift or time of production and manufacturing plant or traceability code
reaction to fire class
declared thermal resistance
declared thermal conductivity
nominal thickness
designation code
type of facing, if any
nominal length, nominal width
number of pieces and area in the package, as appropriate

5.3.1 Product name, manufacturer, year, time or traceability code

Although those items seem to be evident the information is often not complete on today's VIP or shipping units. Manufacturers will have to include these details in future.

5.3.2 Reaction to fire

Due to a long history of national fire safety regulations the reaction-to-fire specification turned out to be one of the hardest problems for harmonisation in Europe. Building materials are generally separated into 5 acceptable classes A1 or A2 (not inflammable), B, C, D, and E (acceptable reaction to fire). With SiO_2-VIP the core is certainly in class A, but the polymer barrier material is of course combustible. This is less of a problem for floor or (flat) roof application, but there are more serious restrictions for façade application. Classification questions and testing requirements are currently under discussion on a national level for instance in Germany and Switzerland.

5.3.3 Declared thermal resistance / conductivity

These are key properties for any thermal insulation product. In European thermal insulation product standards the conditions for the declared value are the following:

- valid for 90% of the production
- mean temperature 10°C
- moisture equilibrium at 23°C, 50% RH
- aging effects shall cover a time span of 25 years

Whereas the first two conditions can be adopted to VIP without problems, moisture and dry gas penetration as significant aging mechanisms have to be discussed in more detail.

The definition of a standard environmental condition, whether it is 23°C / 50% RH (EN) or 24°C / 50% RH (ASTM), gives a reasonable measure of the average climatic conditions in European and North American climate as seen in the panel section of this report. 23°C, 80% RH would be definitely on the safe side, but this would not change figures significantly.

Also the determination of a long-term thermal performance value for a fixed time span of 25 years makes sense for building applications. The opposite – i.e. declaration of the life expectancy based on a fixed minimum performance level – may be favourable for technical applications (c.f. ASTM standard).

A more difficult issue is the evaluation of an (accelerated) test procedure that gives a reliable projection of the performance after 25 years at standard conditions. In Germany the following acceleration test for a set of test specimens is proposed with regard to product certification:

- measurement of the initial λ- / R-value
- cycling in changing climate + 80°C / -15°C
- storage for 3 months at 80°C (dry ?)
- measurement of the λ- / R-value
- storage continued for another 3 months at 80°C (dry ?)
- final measurement of the λ- / R-value

An open question is the acceleration factor that may be in the range of 5 to 50 and that depends on the barrier material.

The proposed procedure requires that the core material initially is well dried. Actually no method is described how to prove this on the wrapped material in a VIP. If there is no method or if the core material is not dried, either by problems in the manufacturing process or as the manufacturer did not include a drying step in the process, more different climatic conditions for the storage at elevated temperatures may be necessary to separate the aging effects by the uptake of water vapour and that of permeating “dry” gases.

In Switzerland the projection of a long-term value is based on the determination of the yearly pressure increase and moisture accumulation rate, which is either measured directly or calculated by an Arrhenius relation from measurements at accelerated conditions. However, these results are not used for product specific design values (section 5.4).

The linear edge transmittance Ψedge, in W/K per unit length of the edge, has to be determined and declared as well. This value is used to calculate the format-dependent equivalent thermal conductivity or effective R-value of a VIP (section 5.4).

5.3.4 Nominal thickness

The thickness is a basic property that has to be declared in relation to the thermal conductivity and the thermal resistance. For this reason it should be clarified whether it is the overall thickness or the net thickness of the core.

5.3.5 Designation code

In the designation code additional properties are indicated in a classified scheme. Below is a list of the classified characteristics for PU with comments concerning VIP. More details can be found in EN 13165:

- Thickness tolerances / Ti:
  Less important for VIP because of the small thickness
- Dimensional stability under specified temperature and humidity conditions / DS(TH)i
  Not really investigated within IEA Annex 39, does not seem to give real problems
- Behaviour under load and temperature / DLT(i) %
  Less important for VIP compared to an organic foam core
- Compressive stress or strength / CS(10\Y)i
  Basic performance value that should be declared for load bearing applications
- Compressive creep / CC(i1/i2/y)c
  Admissible permanent load should be declared for load bearing applications, not investigated within IEA Annex 39
- Tensile strength perpendicular to faces / Tri
  Should be declared if relevant in applications (e.g. faced panels in façade applications)
- Flatness after one-sided wetting / FWi
  Not relevant for VIP
- Long term water absorption / WL(T)i
  Not relevant for VIP
- Water vapour transmission / MUi or Zi
  Not relevant for VIP
- Practical sound absorption coefficient / APi
  To be declared if relevant in applications
- Weighted sound absorption coefficient / AWi
  To be declared if relevant in applications

Additional properties that might be relevant for VIP:

- maximum service temperature (no appropriate standard, depending on barrier material)
- resistance to point load (e.g. EN 12430)
- dynamic stiffness (e.g. EN 29052-1) for floor applications

5.3.6 Type of facing

The type of barrier and potential additional (protective) layers.

5.3.7 Nominal length and width

Although the measurement is trivial a precise definition and tolerance limits of those values are of practical importance. It is often unclear whether the declared dimensions are valid for the core or include the wrapped barrier envelope at the end faces.

5.3.8 Number of pieces and area in the package, as appropriate

Similar to conventional products.

5.3.9 Handling and storage instructions

Basic handling and storage instructions should be available at least on each package in order to prevent damage before and during installation. More information on these issues can be found in the IEA Annex 39 STB report.

5.4 Thermal design values

Since there are very different national approval schemes for building products and for thermal design values in particular, just the (preliminary) state of ideas in Germany and Switzerland is briefly summarized here.

In Germany only standardised methods can be used for declaration procedures. Since there is no such procedure to measure internal pressure in the short run, the declaration procedure will probably be based on thermal conductivity measurements. For a general approval the following elements are foreseen:

- Initial type test including determination of an aged λ-/R-value for the bare VIP as described above.
- Further testing, (e.g. dimensional stability, compression behaviour, reaction to fire) based on EN standards as for conventional products.
- Numerical calculation of the linear edge transmittance Ψ_{edge}.
- At least three years of application experience (in-situ).

The thermal design value is not necessarily equal to the declared (aged) λ-/R-value. For conventional products that are under continuous third-party surveillance a safety increment of 5% is put on the declared value in Germany. Without this surveillance the increment is

20%. The procedure how to come to a design value for VIP is not yet defined. In addition to the open question concerning the acceleration factor the aged value will depend significantly on the panel format.

In Switzerland the preliminary procedure includes thermal conductivity and internal pressure measurements (lift-off method). The preliminary rules are as follows:

- Initial type test including thermal conductivity, internal pressure, and determination of the pressure increase rates for at least three temperature levels (depending on the declared maximum service temperature). Requirement: the pressure increase rate at standard conditions 23°C, 50% RH shall be less than 2 mbar per year for a 50 x 50 x 2 cm^3 panel.
- Aged value λ_{core}: a product independent thermal conductivity value λ_{core} of 0.008 W/(m·K) with polymer based barrier and 0.006 W/(m·K) with aluminium foil barrier is assumed for SiO_2-VIP (see comment below).
- Calculation or measurement of the linear edge transmittance Ψ_{edge} valid for the product thickness range and covering material(s) used in applications. More information about Ψ_{edge} can be found in the IEA Annex 39 STB report.
- Design value: an equivalent thermal conductivity $\lambda_{equivalent}$ is attested that can be used for the design of a large area single layer VIP insulation (e.g. floor, flat roof, wall) with negligible constructive thermal bridges:

$$\lambda_{equivalent} = \lambda_{core} + \Psi_{edge} \cdot thickness \cdot \frac{perimeter}{area} \qquad (43)$$

perimeter: *length of perimeter*
area: *area of the panel*

Note: Following the EN round-up rule to 3 decimal places the increment caused by edge transmission becomes 0.001 W/(m·K) for most polymer based barriers and panel formats from 50 x 50 cm^2.

- The U- or R-value of building envelope components like doors, frames, and wall elements must be determined either by measurement or by at least two-dimensional calculation that takes into account all thermal bridge effects (including barrier material).

Comment

A safety increment of 0.004 W/(m·K) is put on the "ideal" initial thermal conductivity value 0.004 W/(m·K) for VIP with metallized polymer barrier. One part is due to the non-negligible moisture accumulation, which may be around 4%-mass in the long term, corresponding to a thermal conductivity increment of about 0.002 W/(m·K). In addition, a dry air pressure increase of 50 mbar is accounted for, roughly corresponding to another 0.002 W/(m·K) increment. Half increments are taken for VIP with metal foil based barrier. These figures are thought to be on the safe side with respect to both pressure increase and moisture accumulation over a time span of 25 years. It should be noted that this is a very preliminary approach. For panel dimensions 100 x 100 x 2 cm^3 or larger a design value λ_{core} of 0.007 W/(m·K) would be adequate as indicated in Table 47. If clearly better barrier quality is proven and proper initial conditions (low pressure, low moisture content) are guaranteed by

the manufacturer, lower (individual) design values will be considered by the Swiss thermal insulation standardisation committee.

5.5 Summary “Quality assurance, product declaration and design values”

Quality assurance and proper declaration of proven product performance data is very important to all parties involved. Requirements for factory production control, test methods and declaration of properties are standardized for conventional thermal insulation products, but not for VIP. Following an EN standard for PU foam insulation suggestions have been made on factory production control of VIP and barrier material as well as on product declaration. The discussion of suitable thermal design values is still at the beginning. Possible or preliminary rules currently under evaluation in Germany and Switzerland have been summarized.

6 Outlook

During this research program vacuum insulation has developed rapidly. At the beginning VIP was hardly known in the building branch and only a few pilot applications were realized. Only little was known concerning key questions as durability, gas tightness of envelope materials, behaviour under humid and hot conditions. Today it can be stated that VIP properties are well known and some important weaknesses have already been eliminated. We now have well documented experiences from the building site which have been implemented by the building industry for their VIP developments. The VIP production has been professionalized and the VIP have been better adapted to the needs of building applications.

Today we see a very broad interest in the VIP technology from the building branch and large number buildings in which VIP have been applied. But the quantitative wide use of vacuum insulation is still hindered by mainly two factors:

- high price
- lacking confidence in VIP technology and their use in building applications

Today cost

The work under the annex has shown that for the design of vacuum insulated constructions one may not use the thermal conductivity of VIP just after production of ~0.004 W/(m·K) but 0.006 to 0.008 W/(m·K). Hereby the already high material cost rise to a level which hinders strongly the mass use. Even when gains by space savings and constructional simplifications are considered, the resulting costs are hardly acceptable for standard insulation applications. Unfortunately today just little advantage is taken of the regained liberty to develop low U-value building parts with new slim designs. VIP is mainly used in special applications where further advantages are obtained. In renovations by the use of VIP, additional expenses can be avoided, as for instance the lengthening of the roof when insulating the façade. Often VIP is used as a problem solver, e.g. for terrace insulation, VIP is here the only possibility to prevent a step between the heated room and the terrace.

That today the rather crucial direct use of unprotected panels has become the common practice on building sites, has its reason probably also in the high VIP prices. Only very innovative producers of prefabricated insulated building parts (sandwich panels, doors, façade systems etc.) do invest in the new technology. Many others hesitate because they assess VIP as too expensive to be used in their products.

Cost reduction potentials

To achieve a distinct higher market share it is absolutely necessary that VIP prices come down. To estimate how and to what extent price reductions are possible, it would be interesting to know the main cost factors for VIP production. Unfortunately we only have limited information on that topic. For example, it is known that the materials (core and envelope materials) represent quite a high portion of the total cost. With the envelope materials, it can be assumed that it is mainly the production quantity which defines the price. However, fumed silica is already a mass product. Physically it seems to be possible to reduce the portion of fumed silica in the board or to replace it with a cheaper material (e.g. organic foam). In particular the latter requires tighter films to maintain a lower pressure in the panel. Such high barrier films are not only needed for VIP with other core materials but also for (building)

applications in more humid / hotter environments. This kind of extreme high barrier film is also developed for other applications (e.g. OLED) which have similar demands. It is therefore quite probable that they will be available soon.

Furthermore the production of VIP is still dominated by expensive manual work. But the portion of the automated production steps has increased in the last years. This development must lead to a price reduction in the near future.

For the next five to ten years, it can be assumed that VIP solutions will remain more expensive than conventional constructions with the same U-value. This is also caused by the fact that conventional insulations are being improved.

Quality assurance

Annex 39 has also contributed to increased confidence in VIP. For instance it was shown that the environment in the main building applications allow a VIP service life of 50 years and more.

Actions are needed in the field of quality assurance. It has to be made sure that the VIP applied in a building do not get damaged during handling and installation processes. Through systematic measurements of the internal pressure of the panels, defective specimens can be tracked down and crucial processes identified. The today available measurement technology is only partially suitable for quality control of the whole process chain. Ongoing developments lead to the conclusion that in the near future a cheaper and more easily applicable measurement device will be available.

Official certification

Another obstacle are missing product approvals for VIP and VIP based systems for buildings.

References

[1] M. Knudsen: *Die molekulare Wärmeleitung der Gase und der Akkommodationskoeffizient*. Annalen der Physik IV. Folge 34, 593--656 (1911).

[2] S.J. Gregg & K.S.W Sing: *Adsorption, Surface Area and Porosity* – Academic Press 1982.

[3] R. Pirard, A. Rigacci, J.C. Marechal, D. Quénard, B. Chevalier, P. Achard, J.P. Pirard: *Characterization of hyperporous polyurethane-based gels by non-intrusive mercury porosimetry.* Polymer 44 (2003) 4881-4887.

[4] K. Kumaran: *Heat, air and moisture transfer in insulated envelope parts*. IEA Final Report Vol.3 Task 3: Material Properties 1996.

[5] A.W. Adamson & A.P. Gast: *Physical Chemistry of Surface* – 6th Ed – 1997 – John Wiley & Sons.

[6] D. Quénard, D. Giraud, F.D. Menneteau, H. Sallée: *Heat transfer in packing of cellular pellets: microstructure and apparent thermal conductivity High Temperatures*. High Pressures 1998, volume 30, pages 709-715, Presented at the 14th European Conference on Thermophysical Properties, September 16-19, 1996 –Lyon – Villeurbanne, France.

[7] A. Rigacci, B. Ladevie, H. Sallée, B. Chevalier, P. Achard, O. Fudym: *Measurements of comparative apparent thermal conductivity of large monolithic silica aerogels for transparent superinsulation applications* - High Temperatures - High Pressures - 2002 Volume 34, issue number 5, pages 549 - 559.

[8] R. Caps, U. Heinemann, M. Ehrmanntraut, J. Fricke: *Evacuated Insulation Panels Filled with Pyrogenic Silica Powders: Properties and Application*, High-Temperatures-High Pressures, volume 33, pages 151-156, 2001.

[9] R. Caps, U. Heinemann, J. Fricke, P. Randel: *Application of Vacuum Insulation in Buildings*. VIA Symposium: Progress in vacuum insulation, June 2000, Vancouver.

[10] E.H. Kennard: *Kinetic theory of gases*. Mc-Graw-Hill, New York and London, (1938) 311-326.

[11] A. Christfreund & al.: *Vacuum based super insulation panels for appliances*. ICI Polyurethane SPI 96 – Las Vegas USA – 20-23 October 1996.

[12] S.Q. Zeng, A. Hunt, R. Greif: *Transport properties of gas in silica aerogel*. Journal of Non-Crystalline Solids 186, 1995 264-270.

[13] R. Caps, J. Fricke. *Thermal Conductivity of Opacified Powder Filler Materials for Vacuum Insulations*. International Journal of Thermophysics, Vol; 21, N°2, 2000.

[14] U. Heinemann, R. Caps, J. Fricke: *Characterization and optimization of filler materials for vacuum super insulations.* Vuoto scienza e tecnologia, Vol. 18, N. 1-2 1999, p. 43-46.

[15] F.A.L. Dullien: *Porous media fluid transport and pore structure*. Ed. Academic Press, 1979, p.254-.

[16] Y. Gueguen, V. Palciauskas: *Introduction à la physique des roches*. Ed. Hermann, 1992, p.118.

[17] I. J. Polmear: *Light Alloys, Metallurgy of Light Metals*. Arnold, London, 1995.

[18] H.-C. Langowski: *Flexible Barrier Materials for Technical Applications*. Fraunhofer Institute for Process Engineering and Packaging, 46th Annual Technical Conference Proceedings of the Society of Vacuum Coaters, 559-565, 2003.

[19] D. Altenpohl: *Aluminium von innen*. Auminium Verlag, 5th Edition Düsseldorf 1994 (in German), english version: Aluminum Viewed from Within, 1981.

[20] C. Krammer. *Aluminium Taschenbuch*. AluminiumVerlag 1998 (in German only).

[21] M. Pourbaix: *Atlas of electrochemical equilibria in aqueous solutions*. Houston - Tex.: NACE; Brussels: Cebelcor, 1974.

[22] H. Dominighaus: *Die Kunststoffe und ihre Eigenschaften*. Springer Verlag, 4 Edition, 1999 (in German), English version: Domininghaus, Hans Plastics for Engineers, Hanser, 1992.

[23] Ch. Krebs; M.A. Avondet: *Langzeitverhalten von Thermoplasten - Alterungsverhalten und Chemikalienbeständigkeit*. Hanser Verlag, München 1999 (in German only).

[24] H. Zweifel (ed.): *Plastics Additives Handbook*. 5th Edition, Hanser Munich 2000.

[25] R. W. Paynter: *XPS studies of the ageing of plasma-treated polymer surfaces*. Surface and Interface Analysis 29 (2000) 56–64.

[26] R. Hippler, S. Pfau, M. Schmidt, K. H. Schoenbach (Eds.): *Low temperature plasma physics: fundamental aspects and applications*. Berlin: Wiley-VCH, 2001.

[27] T. Moller, Gevert, A. Holmstrom: *Examination of a low density polyethylene (LDPE) film after 15 years of service as an air and water vapour barrier*. Polymer Degradation and Stability 73 (2001) 69-74.

[28] W.Q. Meeker, L.A. Escobar: *Statistical Methods for Reliability Data*. John Wiley & Sons Inc., New York, 1998.

[29] European standards for thermal insulating products for building applications, EN 822 – EN 826, EN 1602 – EN 1609, EN 12085 – EN 12091, EN 12429 – EN 12431.

[30] K. Ghazi, R. Bundi, Th. Frank: *Vacuum insulated panels in building applications*. CISBAT proceedings. Lausanne, October 2003.

[31] U. Moosheimer, H.-C. Langowski, A. Melzer: *Permeation Process Through Vacuum Web Coated Films*. Proc. of the 13th International Conference on Vacuum Web Coat-ing, Tucson, 1999. Bakish Material Cooperation, Englewood, p. 102, 1999

[32] U. Moosheimer, H.-C. Langowski: *Permeation of Oxygen and Moisture through Vacuum Web Coated Films*. Proc. of the 42nd Annual Technical Conference, Chicago, 1999. Society of Vacuum Coaters, Albuquerque, p. 408, 1999

[33] DW. Van Krevelen: *Properties of polymers*. Netherlands: Elsevier Science: 1990. Chapter 18.

[34] G. Nisato, P. C. P. Vouten, P. J. Slikkerveer, W. D. Bennett, G. L. Graff, N. Rutherford, L. Wiese: *Evaluating High Performance Diffussion Barriers: the Calcium Test*. Asia Display 2001, p. 1435.

[35] T. G. Kollie et al.: *Instrument for Measurement of Vacuum in Sealed Thin Wall Packets*. US-Patent 5249454, 1993.

[36] R. Caps, J. Hetfleisch, Th. Rettelbach, J. Fricke: *Thermal Conductivity of Spun Glass Fibers as Filler Material for Vacuum Insulations*, Thermal Conductivity 23, 1996, pp. 373-382.

[37] P. Bendergast, B. Malone: *Characterization und Commercialization of INSTILL Vacuum Insulation Core.* Vuoto scienza et tecnologia, 1-2 1999, pp. 77-82

[38] R. De Vos, D. Rosbothom (eds.): *ICI Polyurethanes 94*. Brussels: Communications Systems SA, 1994.

[39] *Verordnung über energiesparenden Wärmeschutz und energiesparende Anlagentechnik bei Gebäuden (Energieinsparverordnung EnEV)*. Federal legal gazette (BGBI Teil 1 Nr. 51), pp. 3085 ff., 2001.

[40] H. Schwab, U. Heinemann, H.-P. Ebert, J. Fricke: *Prediction of service life time for vacuum insulation panels with fumed silica kernels.* Accepted for publication in: Thermal envelope and building science, 2005.

[41] H. Schwab, U. Heinemann, H.-P. Ebert, J. Fricke, *Prediction for the increase in pressure and water content of vacuum insulation panels (VIP) integrated into building constructions using a model calculations*. Accepted for publication in: Thermal envelope and building science, 2005

[42] H. Schwab, U. Heinemann, H.-P. Ebert, J. Fricke: *Dependence of thermal conductivity on water content in vacuum insulation panels with fumed silica kernels*. Accepted for publication in: Thermal envelope and building science, 2005.

[43] H. Schwab, U. Heinemann, H.-P. Ebert, J. Fricke: *Thermal bridges of vacuum insulated building facades*. Accepted for publication in: Thermal envelope and building science, 2005.

[44] A. Fick, Ann. Physik, 94, 59, 1855.

[45] H.-C. Langowski: *Barriereeigenschaften von Folien, Schichten und Verbunden*, IVV (Hrsg.). Verpackungen aus Kunststofffolien. Neue Entwicklungen und Anwendungsfelder. Symposium on FachPack '98. 15. Oktober 1998, mess center Nürnberg. Freising: IVV, 1998.

[46] H. Utz: *Barriereeigenschaften aluminiumbedampfter Kunststofffolien*. Dissertation TU München, 1995.

[47] J. Nentwig: *Kunststoff Folien.* Carl Hanser Verlag , München, 1994.

[48] H. Schwab, U. Heinemann, H.-P. Ebert, J. Fricke: *Permeation of different gases through foils used as envelopes for vacuum insulation panels*. Accepted for publication in: Thermal envelope and building science, 2005.

[49] F. Kreith: *The CRC handbook of Thermal Engineering.* CRC Press LLC, Boca Raton, 2000.

[50] R. Caps: *Strahlungswärmetransport in evakuierten thermischen Isolationen.* Dissertation University Würzburg, 1985.

[51] M.G. Kaganer: *Thermal Insulation in Cryogenic Engineering*. Israel Program für Scietific Translation (IPST Press), 1969.

[52] O. Krischer, W. Kast: *Trocknungstechnik - Band 1*. Die wissenschaftlichen Grundlagen der Trocknungstechnik, 3. edition, Springer Verlag, 1978.

[53] W. F. Cammerer: *Wärme- und Kälteschutz im Bauwesen und in der Industrie.* 5th edition, Springer Verlag, 1995.

[54] J. Fricke, W. L. Borst: *Energie – Ein Lehrbuch der physikalischen Grundlagen*, 2. Edition, R. Oldenburg Verlag, Munich, 1984.

[55] H. Schwab: *Praxiserfahrung mit Vakuumdämmungen*. Conference "Energieeffizienz im Bauwesen", proceedings, Würzburg 2001, p. 25-34.

[56] H. Schwab, J. Wachtel, U. Heinemann, A. Beck, J. Fricke: *Vakuumisolationspaneele unter baupraktischen Bedingungen*. 1. Conference "VIP-Bau", proceedings, Rostock-Warnemünde, 2003, p. 68-76.

[57] S. Brunner, H. Simmler: *Development of Service Life Prediction Models for Vacuum Insulation Panels*. CISBAT Conference Proceedings, Lausanne, 2003.

[58] H. Schwab et al.: *Entwicklung und Anwendung von evakuierten höchsteffizienten Dämmungen für Gebäude (Vakuumdämmung für Gebäude)*. Project-final-report, Homepage ZAE-Bayern: www.zae-bayern.de/a2/deutsch/projekte_vip/d_vakuum_start.html, 2004.

[59] H. Schwab, U. Heinemann, H.-P. Ebert, J. Fricke: *Increase in Pressure and Mass of foil-covered Vacuum Insulation Panels*. Accepted for publication in: Thermal envelope and building science, 2005.

[60] H.M. Künzel: *Verfahren zur ein- und zweidimensionalen Berechnung des gekoppelten Wärme- und Feuchtetransports in Bauteilen mit einfachen Kennwerten*: Doctoral thesis, faculty of "Bauingenieur- und Vermessungswesen" at University Stuttgart, 1994.

[61] P. Lutz, et. al: *Lehrbuch der Bauphysik.* 3rd edition, Teubner Verlag Stuttgart, 1994.

[62] Th. Blombert: *Manual for Heat 2 5.0*. Lund University: Dept. of Building Technology and Building Physics (Homepage. www.buildingphysics.com/heat2.htm), Sweden, 2000.

[63] Th. Frank. *HELIOS-PC Version 1.0.* EMPA Laboratory for Applied Physics in Building, 1992 (Software in German only, update in preparation).

[64] EN 13165: *Thermal insulation products for buildings - Factory made rigid polyurethane foam (PUR) products – Specification*.

[65] ASTM C1484-01: *Standard Specification for Vacuum Insulation Panels*.

Appendix

Film measurements (NRC)

Two types of laminate bags were tested. One type was identified as a single layer metallized film and the other a three layer metallized film. The bags already had seams on three edges. From each type, six circular test specimens were prepared for vapour permeance tests according to ASTM Standard E 96. Three of the six had the seams in tact at the centre of the test specimens. Dry cup measurements were done on all twelve test specimens at two different chamber conditions, approximately 90% and 94% RH. The results from these measurements are listed Table 52 to Table 55. The results show that the seams do not provide any easier path for vapor diffusion in comparison with the laminates themselves. Also, as one would expect, the three layers metallized film offers measurably higher resistance towards vapour diffusion than that offered by the single layer metallized film. But all values in the Tables are about 1 to 3 ng m^{-2} s^{-1} Pa^{-1}.

Table 52: Water vapor permeance (WVP) of the single layer metallized film.

RH in the cup	**RH in the chamber**	**Temperature**	**WVP**
%	*%*	*°C*	*ng m^{-2} s^{-1} Pa^{-1}*
0	89.8 ± 0.5	22.6 ± 0.1	3.26
0	89.8 ± 0.5	22.6 ± 0.1	2.79
0	89.8 ± 0.5	22.6 ± 0.1	2.84
0	89.3 ± 0.5	22.2 ± 0.1	2.28
0	89.3 ± 0.5	22.2 ± 0.1	2.64
0	89.3 ± 0.5	22.2 ± 0.1	2.47

Table 53: Water vapor permeance (WVP) of the single layer metallized film with the seam at the center of the test specimen.

RH in the cup	**RH in the chamber**	**Temperature**	**WVP**
%	*%*	*°C*	*ng m^{-2} s^{-1} Pa^{-1}*
0	89.8 ± 0.5	22.6 ± 0.1	3.32
0	89.8 ± 0.5	22.6 ± 0.1	3.04
0	89.8 ± 0.5	22.6 ± 0.1	3.98
0	89.3 ± 0.5	22.2 ± 0.1	2.72
0	89.3 ± 0.5	22.2 ± 0.1	2.75
0	89.3 ± 0.5	22.2 ± 0.1	3.22

Table 54: Water vapor permeance (WVP) of the three layers metallized film.

RH in the cup %	RH in the chamber %	Temperature ºC	WVP ng m^{-2} s^{-1} Pa^{-1}
0	89.8 ± 0.5	22.6 ± 0.1	0.90
0	89.8 ± 0.5	22.6 ± 0.1	1.02
0	89.8 ± 0.5	22.6 ± 0.1	0.89
0	89.3 ± 0.5	22.2 ± 0.1	0.76
0	89.3 ± 0.5	22.2 ± 0.1	0.66
0	89.3 ± 0.5	22.2 ± 0.1	0.73

Table 55: Water vapor permeance (WVP) of the three layers metallized film with the seam at the center of the test specimen.

RH in the cup %	RH in the chamber %	Temperature ºC	WVP ng m^{-2} s^{-1} Pa^{-1}
0	89.8 ± 0.5	22.6 ± 0.1	1.30
0	89.8 ± 0.5	22.6 ± 0.1	1.54
0	89.8 ± 0.5	22.6 ± 0.1	0.96
0	89.3 ± 0.5	22.2 ± 0.1	1.18
0	89.3 ± 0.5	22.2 ± 0.1	1.39
0	89.3 ± 0.5	22.2 ± 0.1	0.84

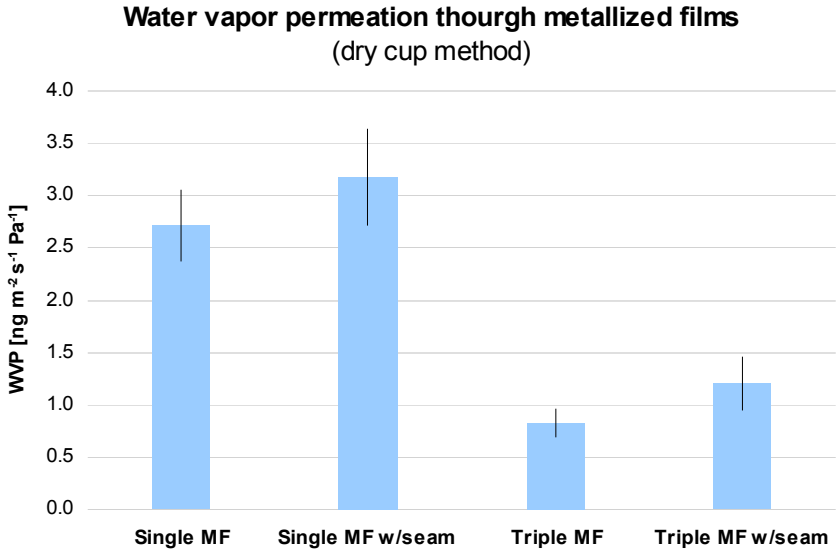

Figure 96: Water vapour permeation through metallized films with and without seam.

Panel measurements (NRC)

Twelve 30 cm x 30 cm x 30 mm VIP were obtained from a manufacturer that has been recommended by the Annex participants. The initial thermal resistances of the panels were determined according to ASTM Standard C 518. Different number of panels was subjected to different environmental loads, as recommended by the Annex participants, and after regular intervals the thermal resistances were repeatedly determined. This was continued for more than a year. The exposures during that time included fixed periods of

- Exposure to standard laboratory conditions
- Exposure to laboratory temperature but high (about 90%) RH
- Exposure to 32 ºC and 90% RH
- Exposure to 5 bar over pressure and
- Exposure to 3 bar over pressure

The core material and laminate were separated from one VIP specimen. The sorption curve for the core specimen was determined according to ASTM Standard C 1498. The water vapour permeance of the envelope was determined according to ASTM Standard E 96.

At the recommendation of the Annex participants, two types of unused laminate bags with seams on three sides (these are the bags that are eventually used to produce the VIP) were acquired. The water vapour permeability was determined according to ASTM Standard E 96 of the laminates with and without the seams.

The results from the test program are reported below.

Preliminary Tests to Confirm the Applicability of ASTM Standard C 518

The ASTM Standard C518 uses Heat Flow Meter (HFM) Apparatus to determine heat transmission characteristics of traditional thermal insulation materials where the measured thermal conductivity is typically between 0.016 and 0.055 W m^{-1} K^{-1}. As seen earlier, the thermal conductivity of a VIP can be as low as 0.004 W m^{-1} K^{-1}. One had to test whether the HFM Apparatus could be used to measure the thermal conductivity and changes in thermal conductivity of VIP. To accomplish this, a fresh test specimen of a VIP with a label claiming a thermal conductivity of 0.004 W m^{-1} K^{-1} from its manufacture was chosen. The thermal conductivity of the panel at four different mean temperatures was determined according to ASTM Standard C518. The results in Table 56 and plotted in confirmed that the ASTM Standard could be used in this investigation. Rather than depending on the absolute value, the incremental change in the thermal conductivity with temperature was used to come this conclusion.

Table 56: The thermal conductivity of a VIP at four mean temperatures.

Mean Specimen Temperature *°C*	Thermal Conductivity *W m^{-1} K^{-1}*
-1.0	0.00434
6.1	0.00443
12.0	0.00454
24.0	0.00485

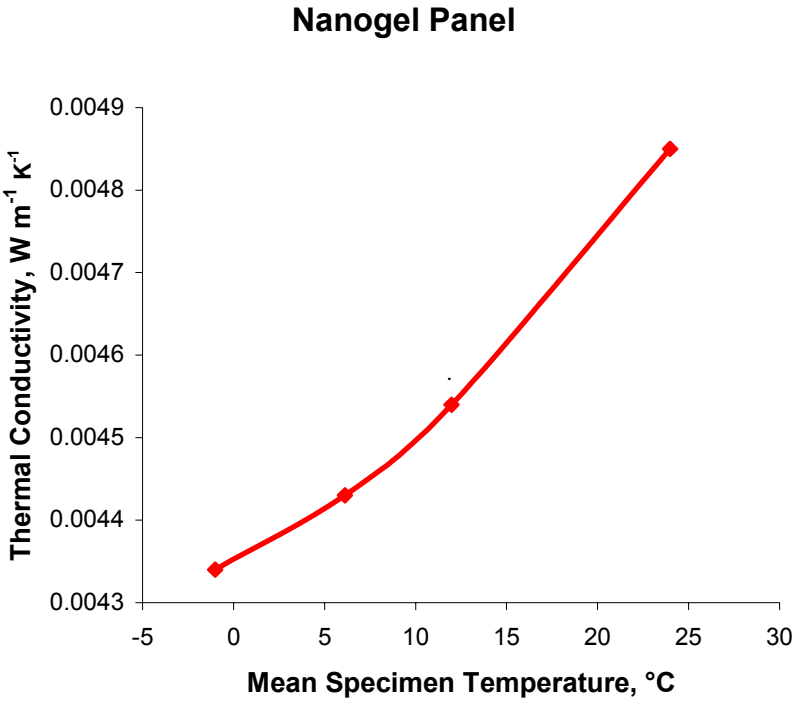

Figure 97: The thermal conductivity of a VIP at several mean specimen temperatures, according to ASTM Standard C 518.

Note:

All subsequent data obtained from C 518 will be expressed as thermal resistivities (reciprocal of thermal conductivities) since we are more interested in the loss of thermal performance with time. For reference, the thermal resistivity of a typical low-density fibrous or open-cell foam insulation will be approximately 25 K m W^{-1} and that of a freshly made high performance cellular polymer insulation will be approximately 55 K m W^{-1}.

Initial Thermal Resistivities of Twelve VIP

The initial thermal resistivities (Standard C518 conditions) of the twelve test specimens, as tested within two weeks of arrival at IRC laboratory are listed in Table 57 and are plotted in Figure 98.

Table 57: Initial Thermal Resistivities of Twelve VIP specimen 1 to 6 with a metallized film, specimen 7 to 12 with an Al-foil.

Specimen Number	Thermal Resistivity $K\ m\ W^{-1}$
1	103
2	252
3	249
4	240
5	244
6	231
7	246
8	256
9	269
10	267
11	265
12	263

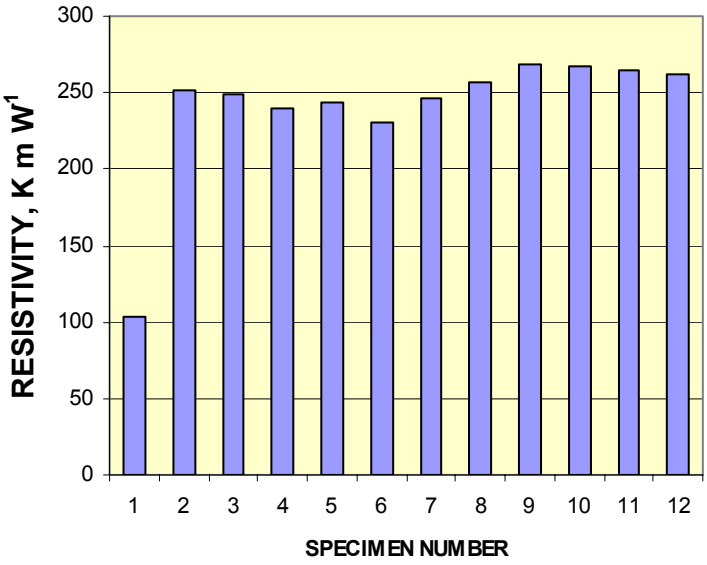

Figure 98: Initial thermal resistivities of twelve VIP; specimen 1 apparently arrived with a defect, but none was visible.

Eleven of the twelve VIP tested had the expected high thermal resistivity. The remaining one had approximately half the thermal resistivity of the others. That was an indication of some defects. Visually nothing was apparent.

Aging behavior

Laboratory Ageing of Specimens 9 and 10

Specimens 9 and 10 were aged in the laboratory, under standard laboratory conditions, (21 ± 1) ºC and approximately 50% RH. The results are listed in Table 58.

Table 58: Ageing of two specimens in the laboratory; numbers in parenthesis indicate the time in days.

Specimen	Thermal Resistivity $K\ m\ W^{-1}$					
9	269 (0)	253 (43)	253 (98)	248 (195)	250 (254)	251 (373)
10	267 (0)	251 (42)	250 (97)	247 (194)	248 (252)	248 (372)

Initially there was a measurable (about 6%) drop in the resistivity of both specimens, but after that the changes were negligible for nearly one year. Within the limits of the precision of the heat flow meter apparatus the resistivity remained the same.

Ageing of Specimen 4 Partially at 90% Relative Humidity

Specimen 4 was aged in a way similar to specimens 9 and 10, except that between 90 days and 190 days, the specimen was exposed to 90% RH at 23 ºC for 60 days. The results are listed in Table 59.

Table 59: Ageing of one specimen in the laboratory; numbers in parenthesis indicate the time in days.

Specimen	Thermal Resistivity $K\ m\ W^{-1}$					
4	240 (0)	227 (53)	226 (90)	222 (189)	223 (264)	221 (377)

Comparison of the data in Table 58 to those in Table 59 suggests that the 60-day exposure to high RH has not affected the ageing pattern of the test specimen in any noticeable way.

Ageing of Specimens 6 and 12 partially at 32 ºC and 90% Relative Humidity

Specimens 6 and 12 were aged similar to specimens 9 and 10 except that between 255 and 290 days they were exposed to 32ºC and 90% RH for 30 days. The results on these specimens are listed in Table 60.

Table 60: Ageing of one specimen in the laboratory; numbers in parenthesis indicate the time in days.

Specimen	Thermal Resistivity $K\ m\ W^{-1}$					
6	231 (0)	218 (55)	215 (92)	214 (255)	212 (292)	210 (377)
12	263 (0)	243 (44)	243 (95)	243 (246)	240 (294)	240 (372)

Comparison of the data in Table 58 and Table 60 reveal that the higher temperature and higher RH together also have no noticeable effect on the pattern of ageing of the specimens.

Ageing of Specimens 3 and 8 partially at 90% Relative Humidity and then partially 32 ºC and 90% Relative Humidity

Specimens 3 and 8 were exposed to 90% RH at laboratory conditions, initially at 30 days followed by another 30 days. Then after about 250 days they were exposed to 32ºC and 90% RH for 30 days. The changes in the thermal resistivity of these specimens are listed in Table 61.

Table 61: Ageing of one specimen in the laboratory; numbers in parenthesis indicate the time in days.

Specimen	**Thermal Resistivity** $K\ m\ W^{-1}$					
3	249 (0)	235 (30)	231 (60)	225 (259)	221 (290)	220 (377)
8	256 (0)	240 (30)	240 (60)	237 (252)	235 (290)	235 (373)

Comparison of the data in Table 61 with those in Table 59 and Table 60 even 90 days of exposure during 1 year to high humidity and out of that 30 days at higher temperature than laboratory temperature has not affected the overall ageing of the specimens.

Ageing of Specimens 2, 5, 7 and 11 at Over-pressures 5 bar and 3 bar

Initially for about 250 days specimens 2, 5 and 11 were aged, like specimens 9 and 10 and specimen 7 was aged identical to specimens 3 and 8. But then they were stacked in a pressure chamber and kept at an over-pressure of 5 bar for 30 days, tested for their resistivity and then subjected to an over-pressure of 3 bar for 15 days. The exposure to 5 bar shrunk all specimens by approximately 6% in all dimensions. But the vacuum was apparently unchanged as indicated by visual inspection. A further exposure to 3 bar over-pressure for 15 days did not alter the physical appearances of the four specimens. The shrinkage affected the resistivity significantly, as shown in Table 62. However there was no significant change in the resistivity due to the second exposure to 3 bar over-pressure. When the specimens were retested after nearly 480 to 490 days of total ageing, the results as shown in Table 62 indicated that the vacuum remained in tact. So the shrinkage probably only collapsed the pore structure, that too partially and more solid particles came together. This may be the reason for the substantial decrease in the resistivity after the exposure to the 5 bar over-pressure.

Table 62: Ageing of four specimens in the laboratory for about 250 days followed by 30 days over-pressure at 5 bar and then 15 days over-pressure at 3 bar; numbers in parenthesis indicate total ageing time in days.

Specimen	**Thermal Resistivity** $K\ m\ W^{-1}$					
2	252 (0)	232 (90)	231 (254)	125 (292)	125 (307)	124 (490)
5	244 (0)	228 (90)	224(252)	139 (289)	136 (304)	138 (486)
7	246 (0)	231 (60)	230 (249)	116 (286)	114 (301)	117 (483)
11	265 (0)	250 (97)	248 (243)	128 (281)	127 (296)	129 (479)

Recently, an experimental facility has been developed at the institute to observe the panels within a vacuum chamber and hence to determine the total gas pressure within the VIP. The pressure within the chamber can be increased or decreased in very fine steps – fraction of a millibar. By doing so, the VIP can be made to inflate when the pressure within chamber is

less than the pressure within the VIP or deflate when the pressure within chamber is more than the pressure within the VIP. Within a very narrow range, in between the inflation and deflation, the envelope appears very fluffy for an observer. The mean pressure corresponding to this range can be regarded as the gas pressures within the VIP. This procedure was used to determine the gas pressures within the 11 VIP that were used for the exposure tests. All 11 specimens were exposed to laboratory environment only after the exposures described before. By the time the pressure measurements were done the VIP were nearly two years old. The results from the measurements are listed in Table 63. Also, included in the Table are the changes in the weights of the panels during the two years.

Table 63: Total gas pressures in the 11 VIP after two years.

Specimen #	**Pressure** *mbar*	**Main exposure**	**Weight increase** *g*
2	9.7	5 Bar overpressure and then 3 bar overpressure	3.66
3	5.6	About 60 days exposed to 90% RH and 23°C and 30 days exposed to 90% RH and 32°C	2.48
4	5.8	About 60 days exposed to 90% RH and 23°C	1.06
5	13.8	5 Bar overpressure and then 3 bar overpressure	2.58
6	13.0	About 30 days exposed to 90% RH and 32°C	1.64
7	16.3	5 Bar overpressure and then 3 bar overpressure	0.93
8	4.2	About 60 days exposed to 90% RH and 23°C and 30 days exposed to 90% RH and 32°C	-0.17*
9	2.3	Throughout kept in the lab environment only	0.03
10	2.4	Throughout kept in the lab environment only	0.06
11	6.0	5 Bar overpressure and then 3 bar overpressure	1.21
12	3.1	About 30 days exposed to 90% RH and 32°C	0.14

**measurement error*

If one considers specimens 9 and 10 as a basis for a comparison among all the 11 specimens, with all the different exposure conditions considered the highest increase in internal pressure is about 14 mbar. The core material being nano-structured, from Figure 4, this increase alone is not enough to observe a substantial decrease in the thermal resistivities of the panels. As speculated earlier, the decrease in the resistivities of specimens 2, 5, 7 and 11 is mainly due to the collapse of the porous structure due to the exposure to the 5 bar overpressure. Specimen 6 that was subjected to higher temperature and high relative humidity showed an increase in the internal pressure by 11 mbar, but the thermal resistivity had not changed significantly.

Specimens 2 to 6 have metallized films and seem to have gained mass due to all exposures. Specimens 7 to 12 have metallic foils and seem to have gained less weight. Laboratory exposure alone and exposure to higher humidity have not increased their weights measurably. Exposure to high pressure has increased their weights by about a gram.

It may be concluded that, exposure to higher temperature and high relative humidity may be one of the exposures that can be recommended for accelerated ageing tests of at least VIP with metallized films. Overpressure also may be considered for both types, but the safe limit shall be determined first to avoid dimensional changes due to the changes in the pour structure of the core material.

A new series of measurements on 20 VIP panels has just started at the Institute. The initial gas pressures of the panels have now been determined, in addition to the initial thermal resistivities. The average gas pressure for the 20 panels is 3.8 mbar with a standard deviation of 1.0 mbar. The average initial thermal resistivity is 240 K m W^{-1} with a standard deviation of 7 K m W^{-1}.

Based on the information available to date from the investigations at the Institute, the following conclusions can be made:

- Environmental loads such as high relative humidity and higher than normal indoor temperatures have no measurable influence on the ageing pattern of the VIP.
- Over-pressure may compact the VIP but do not accelerate the aging by air intrusion. Thus the laminate and seams appear to be very resistant towards the diffusion of air molecules.
- Precipitated silica has large affinity towards water molecules. Therefore at the initial stages of water vapour diffusion majority of the water molecules that traverse the laminates and seams will be adsorbed by the core material and thus will delay any increase in the net pressure inside the VIP.
- The technology used to make the seams prevents additional vapour diffusion paths across the seams.
- The thermal bridges that the edges of VIP can create are significant.
- In future work, it may be necessary to measure the net pressure rather than the thermal resistivity to follow the very slow ageing pattern shown by the VIP.

Mechanical Properties (TU Delft)

At Delft University of Technology three-point and four-point bending tests have been conducted on 20 mm thick fumed silica core based vacuum insulation panels and on sandwich panels made of a the same 20 mm thick vacuum insulation core panels and 4 mm thick mdf or glass facings[6] (Figure 99) . The tests were conducted according to ASTM C 393: *Standard Test Method for Flexural Properties of Flat Sandwich Construction*.

Figure 99: The layout of sandwich panels.

Table 64: Flexural properties of vacuum insulation panels.

	Flexion Modulus VIP	Ultimate Flexural Strength VIP	Deformation at Yielding VIP	Deformation at Fracture VIP
	MPa	*MPa*	*%*	*%*
VIP, intact	63.8 ± 8.6*	0.64 ± 0.11*	1.34 ± 0.38*	-
VIP, no vacuum	38.6 ± 10.7*	0.61 ± 0.04*	0.80 ± 0.16*	-

** uncertainty for a 95% reliability interval*

Table 64 summarizes the measured flexural mechanical properties for single vacuum insulation panels (vacuum insulation panel intact and vacuum insulation panel damaged). As can be seen by comparing the results with the data on fumed silica panels themselves (Chap-

6 The adhesive used to fix the facings on the vacuum insulation is a Polyurethane based glue. All panels have an overhang at both ends of 25 mm and the distance between the load points of the four-point bending apparatus are 150 mm for the 150x350 mm^2 and 300 mm for the 150x550 mm^2 and 150x750 mm^2 panels. The radius of the load points was 10 mm. The vacuum insulation panels consist of a fumed silica core with a laminated metallized polymer high barrier film.

ter 2), vacuum insulation panels have a Young's modulus higher than the single fumed silica core material itself. This, however, is not so astonishing, because the core is restricted in its movement by a low gas pressure, i.e. vacuum, and a high barrier envelope. The value for the Young's modulus, however, is rather low compared to for example steel, aluminium, glass or the high barrier envelope, which have moduli of 210'000, 70'000, 70'000 and approximately 2'000 MPa respectively. Vacuum insulation panels are therefore preferably applied in situations in which no big flexural loads act upon the panels.

Table 64 also shows that damaged vacuum insulation panels are less stiff than undamaged panels, whereas the ultimate flexural strength of both panels is more-or-less equal. This indicates that the pressure difference caused by the vacuum on one side has a significant influence on the Young's modulus but not on the strength of the panel. For practical purposes in the case of a perpendicular to surface loaded panel, thus, a loss of vacuum will

increase the deflection of the panel with a factor 2, but will not cause the panel to fail directly. So, additional safety precautions are not required, unless indirect failure due to slipping out of its grooves is imminent. This, however, could actually be the case only if vacuum insulation panels are applied without a protecting and load bearing facing on both sides, which is only a theoretical situation.

Table 65: Flexural properties of sandwich panels with vacuum insulation panels as core material and different facings. The ultimate fracture strength is the normal stress at which the facing fails.

	Flexion Modulus VIP	**Shear Modulus**	**Ultimate Flexural Strength Panel**	**Deformation at Fracture Panel**
	MPa	*MPa*	*MPa*	*%*
Mdf facing VIP, intact	83.1	27.3	4.3 ± 0.6*	12.2 ± 4.5*
Mdf facing VIP, no vacuum	34.0	12.9	3.9 ± 0.5*	12.3 ± 0.6*
Glass facing VIP, intact	86.2	62.9	4.1 ± 1.6*	1.2 ± 0.3*
Glass facing VIP, no vacuum	36.9	31.3	4.1 ± 0.5*	1.5 ± 0.3*

** uncertainty for a 95% reliability interval*

For application of vacuum insulation panels as part of construction (façade) elements, it is important to know the mechanical (flexural) behaviour of such sandwich panels. Flexion tests on sandwich panels have therefore been conducted at Delft University of Technology as well. The results of these tests for sandwich panels with a vacuum insulation panel core for different facings are presented in Table 65. As can be seen from comparing the data in Table 64 and Table 65, the values for the Young's modulus of the vacuum insulation panel obtained from in-panel measurements are more-or-less equal to the values obtained from single panel measurements, although the modulus of elasticity for undamaged panels obtained from in-panel measurements (Table 65) are slightly higher. This effect, if significant, might be a result of better load diffusion due to the panel facings. Although the vacuum insulation panels themselves seem to be rather flexible, the entire flexural stiffness of a sandwich panel is dominated by the Young's modulus and the area moment of inertia of the facings. A sandwich panel is therefore stiffer than a single vacuum insulation panel. This effect is responsi-

ble for the differences in deformation at fracture between sandwich panels with mdf and glass facings. So, despite their low value for the modulus of elasticity, vacuum insulation panels can be applied in sandwich panels, as long as the distance between both facings is enough to have sufficient flexural stiffness.

The measured data are representative for panel dimensions of 350 x 150 mm^2. At this time it is uncertain whether the data can be used for structural calculations on panels of different dimensions or not, because the influence of the high barrier envelope and the vacuum on the mechanical behaviour on a microscopic level has not yet been fully investigated.